UTILIZATION OF WET-HANDLED AND DRY-HANDLED COAL BOTTOM ASHES IN PORTLAND CEMENT BASED COMPOSITES

A THESIS SUBMITTED TO
THE GRADUATE SCHOOL OF NATURAL AND APPLIED SCIENCES
OF
MIDDLE EAST TECHNICAL UNIVERSITY

BY

SERA TİRKEŞ

IN PARTIAL FULFILLMENT OF THE REQUIREMENTS
FOR
THE DEGREE OF MASTER OF SCIENCE
IN
CIVIL ENGINEERING

SEPTEMBER 2021

Approval of the thesis:

UTILIZATION OF WET-HANDLED AND DRY-HANDLED COAL BOTTOM ASHES IN PORTLAND CEMENT BASED COMPOSITES

submitted by **SERA TİRKEŞ** in partial fulfillment of the requirements for the degree of **Master of Science in Civil Engineering, Middle East Technical University** by,

Prof. Dr. Halil Kalıpçılar
Dean, Graduate School of **Natural and Applied Sciences** _____

Prof. Dr. Ahmet Türer
Head of the Department, **Civil Engineering** _____

Assist. Prof. Dr. Çağla Meral Akgül
Supervisor, **Civil Engineering, METU** _____

Examining Committee Members:

Prof. Dr. Sinan Turhan Erdoğan
Civil Engineering, METU _____

Assist. Prof. Dr. Çağla Meral Akgül
Civil Engineering, METU _____

Assist. Prof. Dr. Güzide Atasoy Özcan
Civil Engineering, METU _____

Assist. Prof. Dr. Özlem Kasap Keskin
Civil Engineering, Muğla Sıtkı Koçman Uni. _____

Assoc.Prof. Dr. Shih-Hsien Yang
Civil Engineering, National Cheng Kung Uni. _____

Date: 07.09.2021

I hereby declare that all information in this document has been obtained and presented in accordance with academic rules and ethical conduct. I also declare that, as required by these rules and conduct, I have fully cited and referenced all material and results that are not original to this work.

Name, Last name: Sera, Tirkeş.

Signature :

ABSTRACT

UTILIZATION OF WET-HANDLED AND DRY-HANDLED COAL BOTTOM ASHES IN PORTLAND CEMENT BASED COMPOSITES

Tirkeş, Sera
Master of Science, Civil Engineering
Supervisor: Assist. Prof. Dr. Çağla Meral Akgül

September 2021, 132 pages

Coal bottom ash (BA) is a coarse, granular, incombustible by-product collected from the bottom of coal-burning furnaces. Traditionally, it has been handled by wet-handling systems (WHS) that use large amounts of water for cooling and conveying BA. WHS relies on established technologies such as impounded hoppers or submerged scraper conveyors. However, the need for water treatment, environmental concerns such as contaminated water, and high operational costs caused a necessary shift from WHS to more sustainable dry-handling systems (DHS) that do not need water and water treatment. Furthermore, returning heat energy to the boiler from the DHS result in lower coal usage. Currently, both handling systems are actively used in thermal power plants. This research focuses on the performance of wet-handled (WH) and dry-handled (DH) BAs in Portland cement-based systems when used as supplementary cementitious material (SCM) or fine aggregate (FA). BAs were collected from two different thermal power units with similar burning systems and operating conditions which burn the same coal. One unit was equipped with WHS and the other with DHS allowing a controlled comparison of the ash handling systems. Both BAs were highly amorphous and had similar chemical compositions; albeit, AHBA was lighter, coarser, more porous, and more grindable.

When ground and used as an SCM or sieved and used as FA, both BAs showed comparable compressive and flexural strengths, heat of hydration, and alkali-silica reaction resistivity. Results show that BAs from both ash-handling systems can be efficiently utilized in Portland cement-based systems.

Keywords: Dry-Handled Bottom Ash, Wet-Handled Bottom Ash, Supplementary Cementitious Material, Fine Aggregate, Sustainability

ÖZ

YAŞ-TAŞINAN VE KURU-TAŞINAN KÖMÜR TABAN KÜLLERİNİN PORTLAND ÇİMENTOSU ESASLI KOMPOZİTLERDE KULLANIMI

Tirkeş, Sera
Yüksek Lisans, İnşaat Mühendisliği
Tez Yöneticisi: Dr. Öğretim Üyesi Çağla Meral Akgül

Eylül 2021, 132 sayfa

Kömür taban külü, kömür yakan fırınların tabanından toplanan kaba, taneli, yanmaz bir yan üründür. Genellikle, taban külünü soğutmak ve taşımak için büyük miktarlarda su kullanan yaş taşıma sistemleri (YTŞ) kullanılmaktadır. YTŞ, su dolu hazneler veya suya batmış konveyörler gibi teknolojilerden oluşmaktadır. Bununla birlikte, su arıtma ihtiyacından, kirli su gibi çevresel kaygılardan ve yüksek işletme maliyetleri gibi sebeplerden dolayı, su ve su arıtma gerektirmeyen ve sürdürülebilir olan kuru taşıma sistemlerine (KTŞ) gerekli bir geçiş yapılmaktadır. Ayrıca, KTŞ'de ısı enerjisinin kazana geri döndürülmesi, daha düşük kömür kullanımı ile sağlanabilmektedir. Mevcut durumda her iki taşıma sistemi de termik santrallerde aktif olarak kullanılmaktadır. Bu çalışmada, çimento ikame malzemesi veya ince agrega olarak kullanıldığında Portland çimentosu esaslı sistemlerde yaş taşınan ve kuru taşınan taban küllerinin performansı araştırılmıştır. Taban külleri, benzer yakma ve çalışma sistemlerine sahip, aynı kömür türü kullanılan iki farklı termik güç ünitesinden toplanmıştır. Ünitelerden biri YTŞ ve diğeri KTŞ ile kurulmuştur böylece kül taşıma sistemlerinden gelen küller kontrollü karşılaştırılabilmiştir. Her iki taban külü de oldukça amorf yapıya ve benzer kimyasal bileşimlere sahip olduğu bulunmuştur. Bunun yanında, kuru taşınan taban külü daha hafif, kaba, gözenekli ve

öğütülebilir olarak bulunmuştur. Öğütülerek çimento ikame malzemesi olarak, elenerek ince agrega olarak veya her ikisi olarak birleşik kullanıldığında, taban külleri benzer basınç ve eğilme dayanımı, hidratasyon ısısı ve alkali-silika reaksiyon direnci göstermişlerdir. Sonuçlar, her iki kül işleme sisteminden gelen taban küllerinin Portland çimento esaslı sistemlerde etkili bir şekilde kullanılabileceğini göstermektedir.

Anahtar Kelimeler: Kuru-Taşınan Taban Külü, Yaş-Taşınan Taban Külü, Çimento İkame Malzemesi, İnce Agrega, Sürdürebilirlik

To my mother…

ACKNOWLEDGMENTS

I want to express my deepest gratitude to my supervisor Assist. Prof. Dr. Çağla Meral Akgül for her guidance, advice, criticism, encouragement, and insight throughout the research. She supported and guided me in all circumstances.

I'm deeply grateful to Eren Enerji - Zonguldak Eren Thermal Power Plant for providing the essential materials and related information for this study.

I want to thank my company, LAVA Engineering family continuous support and motivation through the years.

Finally, I would like to thank my dear family and my valuable friends. I am grateful for every sacrifice that they have made for me. This accomplishment would not have been possible without their invaluable support.

TABLE OF CONTENTS

LIST OF TABLES

TABLES

LIST OF FIGURES

FIGURES

LIST OF ABBREVIATIONS

ACAA: American Coal Ash Association

ASR: Alkali-Silica Reactions

CCP: Coal combustion products

CCR: Coal Combustion Residual

DH: A: Used as aggregate of the dry-handled bottom ash

DH: Dry-handled

DH: P: Used as a binder of the dry-handled bottom ash

ECOBA: European Coal Combustion Products Association

FBA: Furnace bottom ash

FBC: Fluidized Bed Combustion

FGD: Flue Gas Desulfurization

FM: Fineness Modulus

G-DH: Grounded Dry-handled Bottom Ash

G-DHBA: Ground Dry-handled Bottom Ash

G-WH: Grounded Water-Cooled Bottom Ash

G-WHBA: Ground Wet-handled Bottom Ash

IBP: Industrial by-products

LWC: Lightweight concrete

OPC: Ordinary Portland Cement

PC: Portland Cement

P-DH: Paste with dry-handled bottom ash

P-WH: Paste with wet-handled bottom ash

SCM: Supplementary Cementitious Materials

SDA Product: Spray Dry Absorption Product

S-DH: Sieved Dry-handled Bottom Ash

S-DHBA: Sieved Dry-handled Bottom Ash

SSC: Submerged Scraper Conveyor

S-WH: Sieved Wet-handled Bottom Ash

S-WHBA: Sieved Wet-handled Bottom Ash

W/B: Water to cement plus binder materials ratio

WH: A: Used as aggregate of the wet-handled bottom ash

WH: P: Used as a binder of the wet-handled bottom ash

WH: Wet-handled

WHBA: Wet-handled coal bottom ash

CHAPTER 1

INTRODUCTION

1.1 Significance

There is a widespread increase in electricity consumption due to the growing world population and rising energy dependency in daily life. Electricity can be produced from different sources, including fossil fuels (coal, natural gas, and petroleum), nuclear energy, and renewable energy sources (hydro, geothermal, nuclear, oil, solar, and biomass). In 2018, electricity production from coal-based thermal power plants accounted for 38% of worldwide electricity production [1].

Turkey's primary electricity production relies on thermal power plants utilizing mainly coal and natural gas [2]. Figure 1.1 shows Turkey's 2018 electricity production by energy source, with coal-fired thermal power plants supplying 37.2% of the total production.

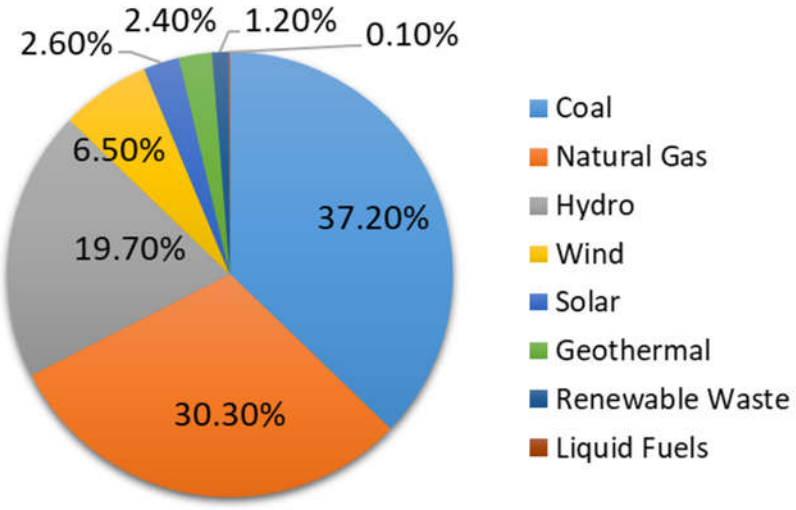

Figure 1.1. Turkey's Electricity Production by source, 2018 [2]

Coal combustion products (CCP) are the solid residues produced when coal is burned to generate electricity. Main CCPs include fly ash, bottom ash, boiler slag, and flue gas desulfurization gypsum. With the worldwide increase in coal consumption, CCPs from coal-fired thermal power plants are increasing intensively ([3], [4], [5], and [6]). The 2016 CCP production for European (EU-15) power plants was reported as 40 million tons [6]. The weight percentages of the produced CCPs are given in Figure 1.2. Fly ash production had the highest rate among all other CCPs at 63.8%. The followings were flue gas desulfurization (FGD) gypsum and bottom ash at 23.6% and 9.0%, respectively. According to American Coal Ash Association [7] 2019 production report, 78.6 million tons of CCP were produced in the USA (Figure 1.3). The top three CCPs were 29.3 million tons of fly ash (~37 %), 22.9 million tons of FGD gypsum (~29 %), and 9.1 million tons of bottom ash. As seen from Figure 1.2 and Figure 1.3, the top three CCPs produced in both Europe and USA were fly ash, FGD Gypsum, and bottom ash, respectively.

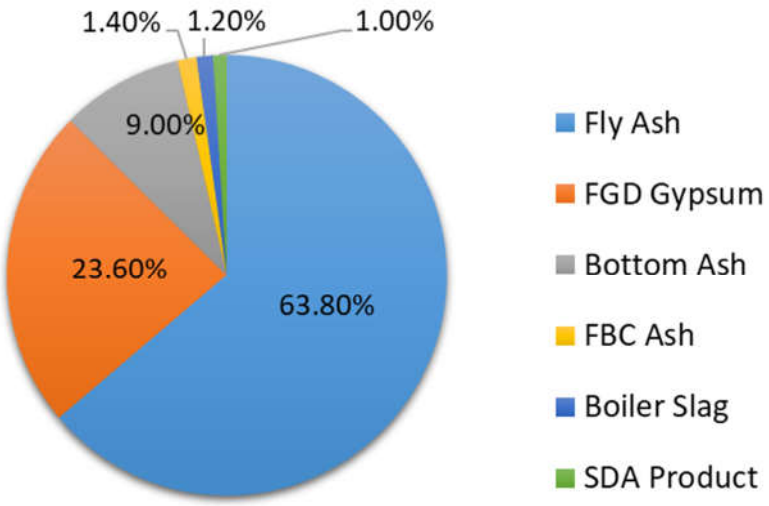

Figure 1.2.The ECOBA Statistics on Production of CCPs in EU 15 Countries in 2016 [6]

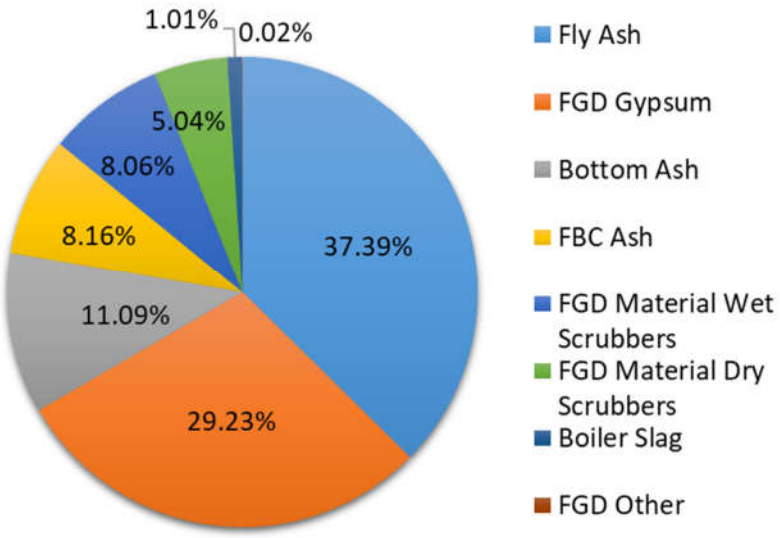

Figure 1.3.The ACAA Statistics on Production of CCPs in 2019 [7]

Coal bottom ashes (BA) are coarse, granular, incombustible by-products collected from the bottom of coal-burning furnaces. In coal-fired power plants, BAs can be handled either with wet or dry bottom ash handling systems. Wet bottom ash handling systems and surface impoundments are currently much more common. Recently, many modern thermal power plants are already evaluating converting to dry bottom ash systems, which are more environmentally friendly and economical. The severe environmental problems such as ash pond (surface impoundment) failure are the main reasons for the change. Further reasons for the shift are summarized in Figure 1.4.

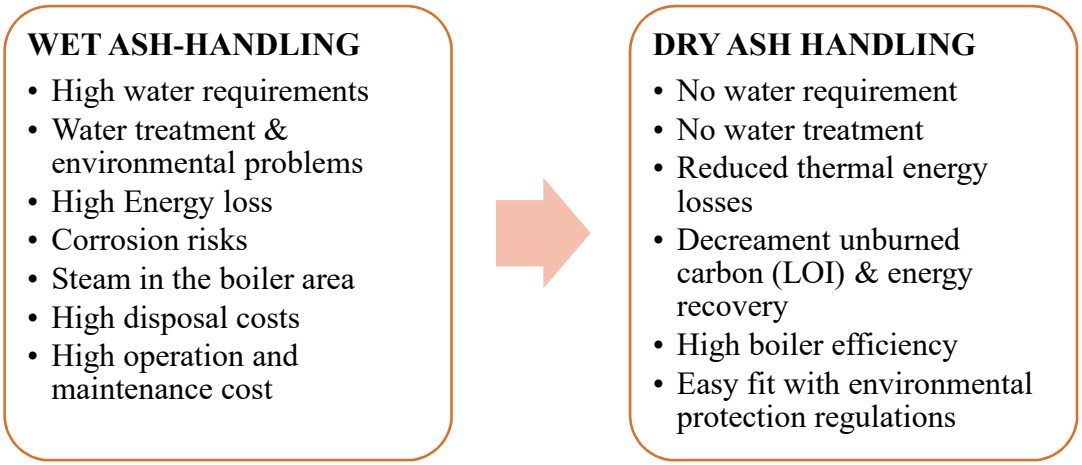

Figure 1.4. Two Ash-Handling Systems Comparison [8]

In this study, the bottom ashes produced in the multi-unit coal thermal power plant was investigated. The wet-handled bottom ash was obtained from the submerged scraper conveyor, and the dry-handled bottom ashes were collected from the DRYCON systems.

Developing and maintaining the world's structures to meet the future needs have industrialized, and developing countries is necessary to grow economically and improve the quality of life. The quality and performance of concrete play a key role for most structures, including commercial, industrial, residential and military structures, dams, power plants, and transportation systems [9].

Natural resources of aggregate, due to high consumption in construction fields, are getting depleted rapidly. Therefore, in the present conditions of inadequate aggregate resources and development in the concrete industry, it becomes crucial and necessary to detect ideal substitute material in durable concrete for aggregate [10]. Therefore, using CCP rather than disposing of them conserves natural resources, reduces greenhouse gas emissions, and saves high costs of construction materials.

Today, coal combustion products are incorporated into a wide range of building materials and engineered composite materials, such as metal alloys and plastics, to

provide strength without adding weight. The utilization of coal ashes in the different aspects of engineering applications is increasing year by year.

Both ACAA and ECOBA have reported the utilization of the coal ashes rates and usage areas. According to ACAA [7] survey report, 52 % of the coal ash produced during 2019 was recycled. More than half of the coal ash produced in the United States was beneficially used rather than disposed of.

Mainly, 31.95% of the bottom ashes was utilized in the blended cement or feed for clinker, structural fills or embankments, blasting grit & roofing granules, CCR (coal combustion residual) pond closure activities, concrete or concrete products or grout, soil modifications/stabilization, road base/sub-base, snow and ice control, waste stabilization/solidification, mineral filler in asphalt, agriculture, oil/gas field services aggregate, and miscellaneous/other.

According to ECOBA [6] EU-15 report, 37% of the bottom ashes were used at the different areas such as reclamation/restoration, non-aerated/ aerated concrete blocks, general engineering fill, disposal, cement raw materials, structural fill, pavement base course, temporary stockpile, bricks and ceramics, subgrade stabilization, and concrete addition.

When selecting construction materials, substitute recycled materials for conventional products to achieve a sustainable design and drastically reduce many environmental impacts. In most cases, these materials cost less, are available locally, and are technically equivalent or superior to original materials.
To conclude, the solutions must be found in the environmentally vital and profitable aspect about the handled storage or usage of the coal combustion by-products. As seen from the data, the new landfills or ash ponds will not be the remedies for our future. The ways of protection of the natural resources must be investigated, and

studies must be performed. The possibility of the usage of the CCPs in the cement industry could be one of the protection ways with this point of view.

1.2 Objective and Scope

In this study, the primary aim is to analyze the mechanical and durability performance of the wet-handled and dry-handled bottom ashes while replacing them with the fine aggregate and ordinary Portland cement in mortar production systems. With the light of this goal, the bottom ashes were obtained from Eren Enerji - Zonguldak Eren Thermal Power Plant.

The mortars were produced by 25 and 50% fine aggregate and cement replacement by volumetric for fine aggregate and by weight for cement replacement. Bottom ash mortars were compared with the control mixtures regarding the design mixtures' fresh, hardened, and durability properties.

1. Raw materials characterization was performed, firstly. Determining the physical and chemical characterization of the bottom ashes was given the concept about the usability of the bottom ashes as a fine aggregate and binder materials.
2. Preparation of mortar and paste samples was the second step. The condition of the bottom ashes was enhanced with sieving, grinding, and drying processes since the as-is usage form of ashes was not chosen in the mortar systems directly.
3. The pastes and mortars were tested in the third step. The heat of hydration test of the pastes was conducted first. Then, the compressive and flexural strength of the mortar's tests were performed. Finally, the durability (alkali-silica reaction resistance) tests were conducted for the mortar specimen.

CHAPTER 2

LITERATURE REVIEW

In this section, the usage of the coal bottom ashes in the cement industry is reviewed and presented in the previous studies. Firstly, the bottom ashes classification is reviewed because, in this thesis study, two types of bottom ashes were investigated. Then the physical and chemical properties of the bottom ashes are tabulated. There is a wide range of physical and chemical properties because the ashes' characteristics depend on too many such ashes, the coal type, the heating and cooling process, etc. The review chapter shows many studies about using the coal bottom ashes' utilization in cement-based systems as a fine aggregate and supplementary cementitious materials, separately. However, limited studies were conducted using CBA both as a fine aggregate and supplementary cementitious material in the one system.

2.1 Coal Bottom Ash

One of the industrial by-products produced from the combustion of coal is coal bottom ashes. In the following sections, the definition and classification of ashes were introduced. Also, different types of CBA's are produced worldwide, physical and chemical properties are presented.

2.1.1 Definition and Formation of Bottom Ash

In coal-fired thermal power plants, pulverized coal burning system is generally preferred. The main reason for this preference is that it is proven technology used for a long time.

The bottom ash and fly ash formation process in thermal power plants where pulverized coal technology is used is summarized in Figure 2.1. Part of the suspended ash agglomerates forms partly larger particles. Particles fall to the bottom of the boiler in solid form or flow as a molten state, depending on the type of boiler and coal.

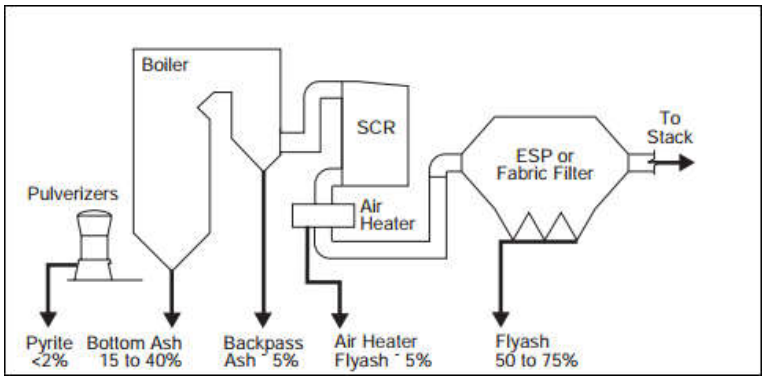

Figure 2.1. Typical Pulverized Coal-Fired Boiler Ash Discharge Locations and Approximate Amounts [11]

The bottom ash water impounded hopper is filled with water to quench the hot ash entering and is stored [11] ; the typical wet bottom ash handling system is shown in Figure 2.2. Coarse and fly ash in wet ash handling are collected by wetting water jets or a hydro-pneumatic system. All the slurry ash is then taken to an ash slurry sump, from which this slurry is pumped into an ash pond for disposal [12].

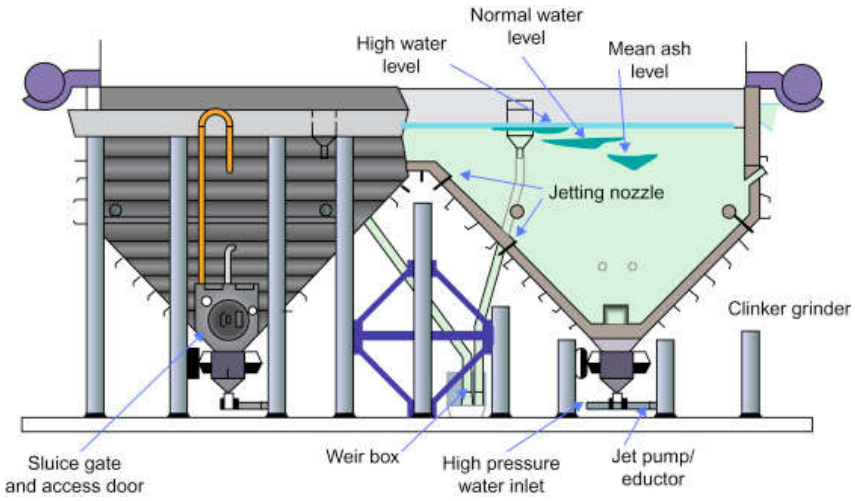

Figure 2.2. Typical Wet- Bottom Ash Hopper Arrangement [9]

The other wet ash-handling system is a submerged scraper conveyor (SSC). The SSC is a heavy-duty dual drag flight chain conveyor. The conveyor is immersed in a water trough below the furnace, which quenches hot bottom ash as it falls from the combustion chamber. The bottom ash is then dewatered as it travels up the inclined section before it discharges. The discharge of the SSC is done with the removable containers or onto a transfer conveyor, which transports the BA to storage for by-product reuse or landfill [8]. The SSC as handling system is presented in Figure 2.3.

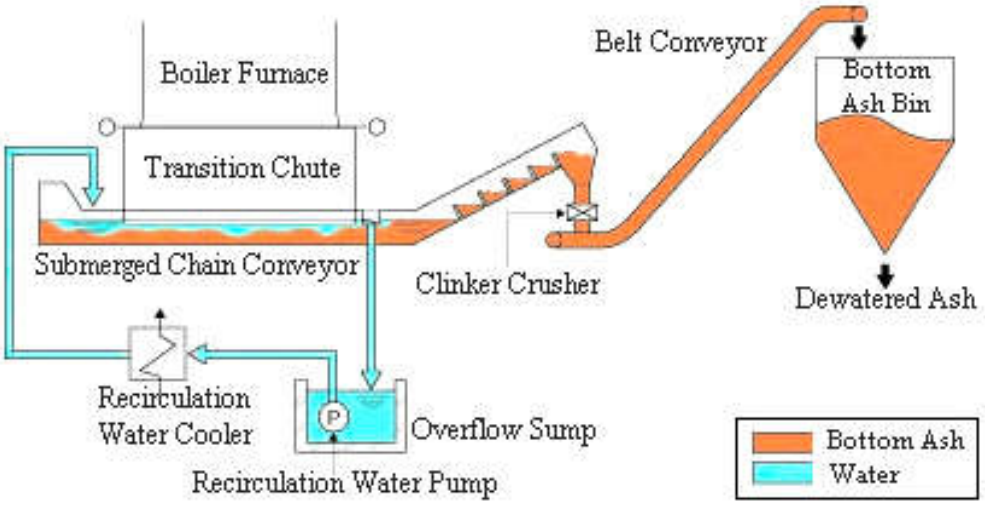

Figure 2.3. Typical SSC system [13]

In a dry ash-handling system, bottom ash and coarse ash are continuously disposed of through a metallic conveyor beneath the boiler and typically transported to a bottom ash silo. This metallic conveyor usually moves very slowly; this is juxtaposed with the flow of cold atmospheric air through the conveyor to the furnace due to the furnace draft. This process allows cooling of bottom ash before its disposal to the silo. Discharge from the bottom ash silo is sent pneumatically to the final bottom ash silo (Figure 2.4) for onward removal through road tankers, trucks, etc. [9]

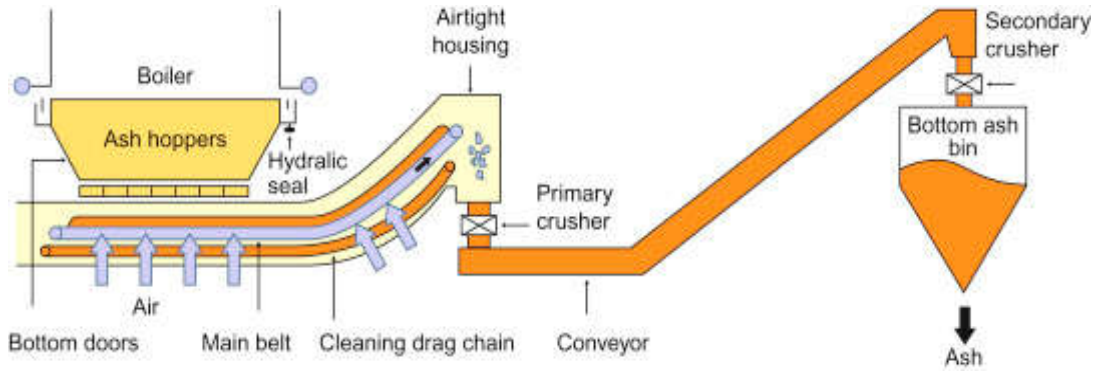

Figure 2.4. Dry- Bottom Ash Hopper Arrangement [9]

The combustion process in pulverized coal-fired furnaces, volatile matters, carbon burns, and coal impurities fuse and remain in suspension. These fused substances solidify when flue gas reaches low-temperature zones to form predominantly spherical particles called fly ash (constitutes a significant component as 75-80% of by-product materials). The remaining matter, which is agglomerated and settled down at the bottom of the furnace, is called bottom ash. These particles are too large for carrying in the gas flow and fall through open grates to an ash hopper at the bottom of the furnace [10]. The pulverized coal-fired furnaces employ either a dry or wet bottom to collect bottom ash [14]. Bottom ash is a dark grey, granular, porous, and predominantly sand-size material that can account for 20–25% of total coal combustion by-products [15].

Thirty years ago, almost all ash from coal-fired power plants was conveyed as slurry and collected in ash ponds, and many of these ponds are still in use today. Today, nearly two-thirds of plants with ash ponds contain dry fly ash systems, while over 90 percent of bottom ash systems remain wet [12].

The combustion of coal in cyclone furnaces occurs by continuous swirling in a high-intensity heat zone. This process fuses fly ash particles into a glassy slag, called boiler slag, which drops to the bottom of the furnace [16] . In the slag or wet bottom boilers, ash collected at the bottom of the furnace is kept in a liquid condition by maintaining the slag well above its fusion temperature. A water-filled pit is positioned below the furnace to receive the molten slag. The resulting product

deposited in water is known as wet boiler slag or bottom slag. It is granular, glassy, and angular in appearance. Dry bottom ash has significantly different characteristics than wet slag. The dry collection procedure yields ash having the formation of fine natural aggregate. In addition, the predominant material is light in color and has a sandpaper-like surface texture.

The classification and definition of the bottom ashes are dependent on their chemical and physical properties also. The source, type, and fineness of the fuel and the operating conditions of the power plant have an essential role in the physical and chemical properties of fly ash and bottom ash [17] ; these properties are covered in the following section.

2.1.2 Physical Properties

Kirthika et al. [18] stated that the color, shape, and appearance of industrial by-products are depended on production and treatment processes. Coal bottom ash particles are irregular, porous, angular, and have a rough surface texture. The particle size ranges are changed from fine gravel to fine sand. Moreover, coal bottom ashes are generally lighter and more brittle compared to fine natural aggregates like sands. Singh and Siddique [19] stated that coal bottom ashes with low specific gravity and a porous texture readily degrade under loading or compaction. The typical physical properties and the origin of the coals of the bottom ashes studied by different researchers are presented in Table 2.1.

The particles of coal bottom ashes are extended from fine sand to gravel, as mentioned before. The properties given in the table above make bottom ashes appealing to be selected as fine aggregate in the mortar and concrete mixture design. The specific gravity of CBA is from 1.39 to 2.47. The range of the fineness modulus of CBA is reported as 1.37 to 3.44. The water absorption of CBA ranged from 5.40 to 32.2, which is a very high range, respectively. According to materials for concrete construction [20], ranges in physical properties of standard weight aggregates are

2.3-2.9, 2.3-3.1, and 0-8% for specific gravity, fineness modulus, and water absorption, respectively. In the literature, researchers are compared different properties of the coal bottom ashes, such as the compacted bulk density, the loose bulk density, the unit weight, the density, and clay lumps and friable particles [21].

Table 2.1 The Typical Physical Properties of BAs from the Previous Studies.

Previous Studies / Physical Properties of Bottom Ash	**Origin Country of the Coal**	**Specific Gravity**	**Water Absorb. (%)**	**Fineness Modulus**
Kim & Lee [22] **Hata! Başvuru kaynağı bulunamadı.**	South-Korea	1.98	5.40	2.80
Naik & Kraus [14]	United-States	1.90	5.60	3.15
Rafieizonooz et al. [23]	Malaysia	1.88	11.61	3.44
Singh & Siddique [24]	India	1.39	31.48	1.37
Bai et al. [25]	Ireland	1.58	32.20	-
Topçu & Bilir [26]	Turkey	1.39	12.10	-
Ghafoori & Bucholc [27]	India	2.47	7.00	2.80
Range of the Properties		1.39 ~ 2.47	5.4 ~ 32.2	1.37 ~ 3.44

2.1.3 Chemical Properties

Chemically, the constitution of coal bottom ashes is differed according to the type of source of coal to incinerate and the process of burning. CBA is composed of silica, iron, and alumina, fundamentally with sparse magnesium, calcium, sulfate, and others [19]. The coal bottom ashes have occurred from three main oxides, which are silicon dioxide (SiO_2), aluminum oxide (Al_2O_3), and ferric oxide (Fe_2O_3). Additionally, Calcium oxide (CaO), magnesium oxide (MgO), sodium oxide

(Na_2O_3), potassium oxide (K_2O), sulfur trioxide (SO_3), and other minor oxides such as P_2O_5 and TO_2 also are contained in lower amounts. Coal bottom ash which generally comes from lignite or sub-bituminous coals has a higher percentage of calcium than that derived from anthracite or bituminous coals. Furthermore, unburn carbon particulars could be existed because of the resulting from incomplete combustion. The specific chemical properties of the coal bottom ashes are shown in Table 2.2.

Table 2.2 The Typical Chemical Properties of BAs from Previous Studies.

Previous Studies/ Chemical Compositions	**SiO_2 (%)**	**Al_2O_3 (%)**	**Fe_2O_3 (%)**	**CaO (%)**	**MgO, Na_2O, K_2O, TiO_2, P_2O_5, SO_3 (%)**	**Origin Country of the Coal**
Yüksel & Genç [28]	57.90	22.60	6.50	2.00	3.99	Turkey
Andrade et al. [29]	56.00	26.70	5.80	0.80	5.49	Brazil
Bai et al. [25]	61.80	17.80	6.97	3.19	5.98	Ireland
Kasemchaisiri & Tangtermsirikul [30]	38.64	21.15	11.96	13.80	5.71	Thailand
Syahrul et al. [31]	54.80	28.50	8.49	4.20	4.29	Malaysia
Ghafoori & Bucholc [27]	41.70	17.10	6.63	22.50	10.52	India
Kumar & Vaddu [32]	46.84	14.36	18.65	7.24	6.40	United-States
Kou & Poon [33]	60.70	18.30	6.56	1.28	8.03	China
Range of the Compositions	**38~62**	**17~29**	**5~19**	**1~22**	**1~5**	-

Range of the $SiO_2+Al_2O_3+Fe_2O_3$	**65 ~ 92**	-

The range of the typical chemical compositions of the bottom ashes are 38-62%, 17 29%, 5-19%, 1-22%, 1-5%, 0-2%, 0-3%, 0-4%, 0-2%, and 0-1% for SiO_2, Al_2O_3, Fe_2O_3, CaO, MgO, Na_2O, K_2O, TiO_2, P_2O_5, and SO_3 respectively. Also, the loss on ignition is reported as 1-7% for the CBA. Additionally, the range of the sum of the SiO_2, Al_2O_3, Fe_2O_3 oxides is considered separately.

The ASTM C618 [34] stated that the fly ashes could be used as pozzolanic materials within the allowable limits. Similar oxides proportions have existed in the coal bottom ashes compositions. Therefore, they could be evaluated as pozzolanic materials also.

As it can be seen from Table 2.2 and stated by Ahamed and Lisak [35], CBA is reported as nonhazardous, which are trace materials such as Hg, As, Cd, and Pb, solid or inert wastes and used widely in construction applications, albeit the absence of legal certainty.

2.2 Use of Bottom Ash in Cement and Concrete Industry

The continuous reduction of natural resources and the environmental hazards of coal ash disposal has reached an alarming proportion. The use of coal ash in concrete manufacture is a necessity than a desire. The use of coal ash in standard strength concrete is a new dimension in a concrete mix design. If applied on a large scale would revolutionize the construction industry by economizing the construction cost and decreasing the ash content [36].

Bai et al. [15] mentioned that using coal bottom ashes in the cement and concrete industry as binder material and aggregate should be one of the best ways to solve the environmental problems caused by CBA in a permanent and environmentally friendly manner.

2.2.1 Usage as a Fine Aggregate

The central part of the waste materials has occurred from Industrial by-products. Therefore, the utilization of these waste materials is researched in many countries. Industrial by-products could be used as fine aggregate individually or partially mixed. One of the industrial products which must be considered is coal bottom ashes as very known. Nevertheless, results reported in the literature are promising regarding the use of bottom ash as a partial or total fine aggregate replacement for natural river sand. There are many numbers of studies that are presented with various aspects.

Bai et al. [25] and Nikbin [21] state that the significant attractive properties of the CBA are the similarity of the particle size and feature with the normal aggregates. Thus, many studies have revealed encouraging results on CBA application as partial or total substitution of fine aggregate in mortar and concrete in recent years. In Figure 2.5, the different industrial by-products, including bottom ashes' particle size distributions, are compared, and the limits are presented. Researchers report these limits that the particle size distribution of IBP usually lies in Zone II and Zone III as per IS 383 [37], which makes it suitable for concrete construction. Based on the rock mineralogy, the fineness modulus varies from 2.5 to 4.2. As it can be seen from Figure 2.5, the bottom ashes are in the desired zones.

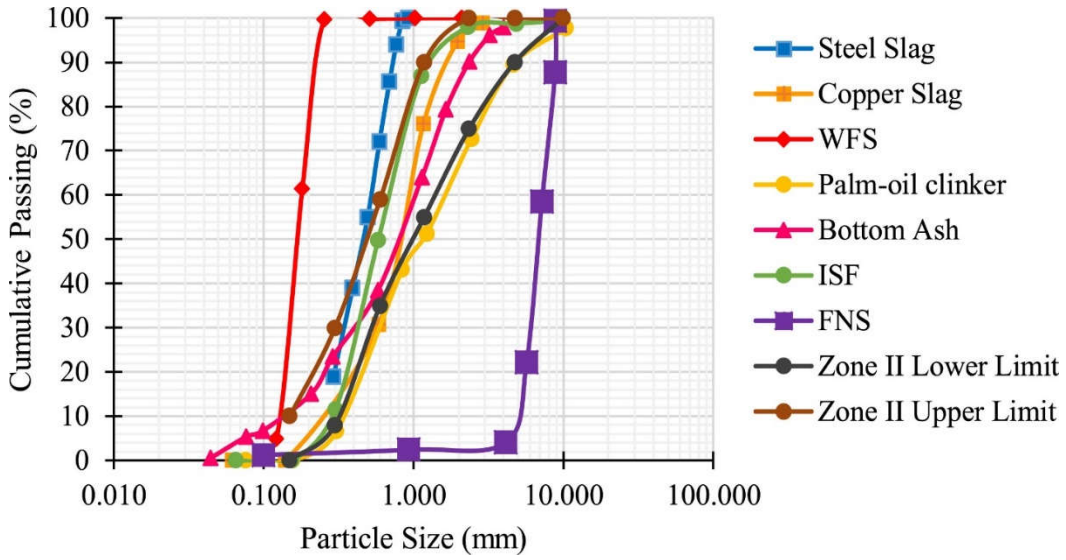

Figure 2.5. Particle Size Distribution of Industrial By-Products [18] (WFS: Waste Foundry Sand, ISF: Imperial Smelting Furnace, FNS: Ferro-Nickel Slag, Zone Limits Refer to IS 383-2016

Additionally, Figure 2.6 is shown a comparison between only natural sand and coal bottom ashes' particle size distribution, and the variation of the sizes was slightly similar

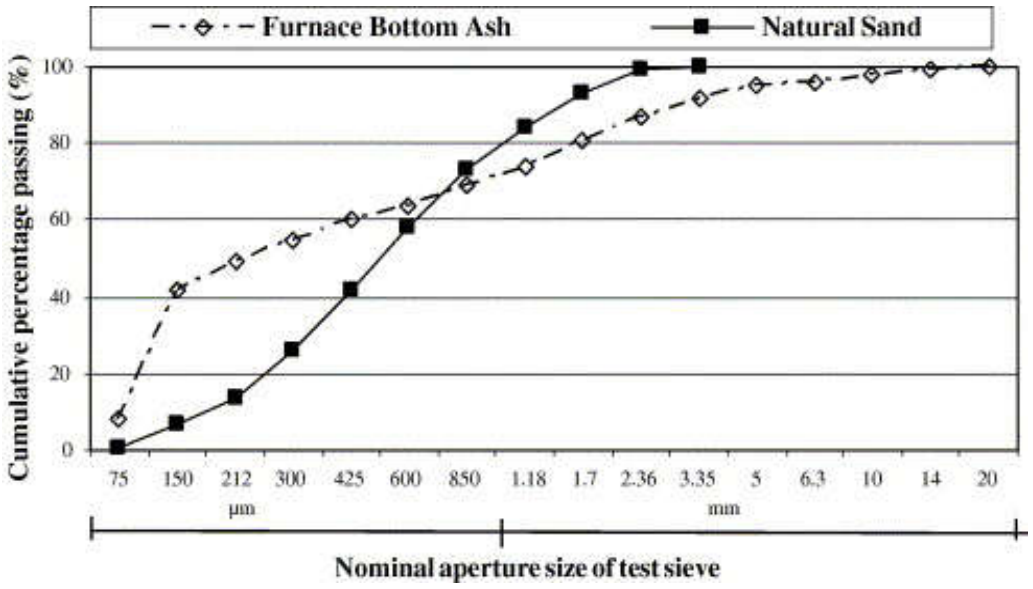

Figure 2.6. Comparison of the Particle Distribution of FBA and Natural Sand [25]

Andrade et al. [29] investigated the different forms of bottom ash mix result in concretes with other properties in the fresh state. Still, the behavioral tendencies are maintained when bottom ash is employed as a replacement for natural aggregates.

Additionally, Singh and Siddique [38] pointed out that coal bottom ash particles have interlocking characteristics. Coal bottom ash is lighter and more brittle as compared to natural river sand. Coal bottom ash with low specific gravity has a porous texture that readily degrades under loading or compaction. Coal bottom ash derived from high-sulfur and low-rank coal is not very absorbent and respectively dense.

On the other hand, generally, the porous structure of the coal bottom ashes makes them use lightweight aggregate. Kim and Lee [22] studied CBA as an aggregate for high-strength, lightweight concrete. Fuel ash, such as fly ash and bottom ash, has many proven advantages as an aggregate and admixture in concrete and is utilized in concrete blocks and road constructions.

Kou and Poon [33] could state the other aspects of the coal bottom ashes, as its particle distribution is similar to that of sand, which makes it attractive to be used as a sand replacement material especially in concrete masonry block production.

2.2.2 Usage as a Supplementary Cementitious Materials

Different researchers have widely reported the uses of supplementary cementing materials, such as fly ash, bottom ash, and natural pozzolan in cement and concrete. The chemical composition of the bottom ashes is generally acceptable range as mention in previous sections.

The usage of fly ashes as a pozzolanic material is more expansive than a usage as bottom ash. Ranganath et al. [39] reported that the bottom ashes from the boilers and the fly ash from the precipitators are mixed and pumped off in the form of slurry to lagoons. Such ash, referred to as ponded ash, some size fractions could be regarded as pozzolanic, and especially the article below 75 mm is about 65% of the ponded ash.

The usage of the bottom ashes as a pozzolanic material could need some treatment for the increased effectiveness. Singh et al. [40] emphasize that the bottom ash particles are coarser in nature, having a large particle size and high porous surface, which offer the high-water requirement and lower compressive strength. However, an attempt has been made to improve the quality of bottom ash for utilization as a pozzolanic material. The grinding operation was performed to reduce the porosity and improve the pozzolanic properties of bottom ash.

There is also pozzolanic potential, although this is low due to the grain size. The low pozzolanic potential of BA is not a limiting factor for its use as a fine aggregate since any positive influence caused by the pozzolanic effect improves the mechanical performance and durability due to calcium hydroxide consumption and formation of calcium silicate hydrate (C–S–H), which can be seen as a positive contribution of the BA [17].

The graining is the crucial point of the improve coal bottom ashes pozzolanic behaviors. The grinding process is also fundamental at this point. Stirred mills are very effective in producing micronized material due to their easy processing, simple construction, high size reduction ratio, low energy consumption, and less wear contamination. Therefore, it has extensively been started to be used in the recent decade in many industries. The grinding process could be non-efficient, but it could be optimized when waste material consideration is done. It can be observed that the particle size distribution is decreased with an increase in grinding duration and Khan and Ganesh [41] is reported a similar result with the grinding process effects shown in Figure 2.7.

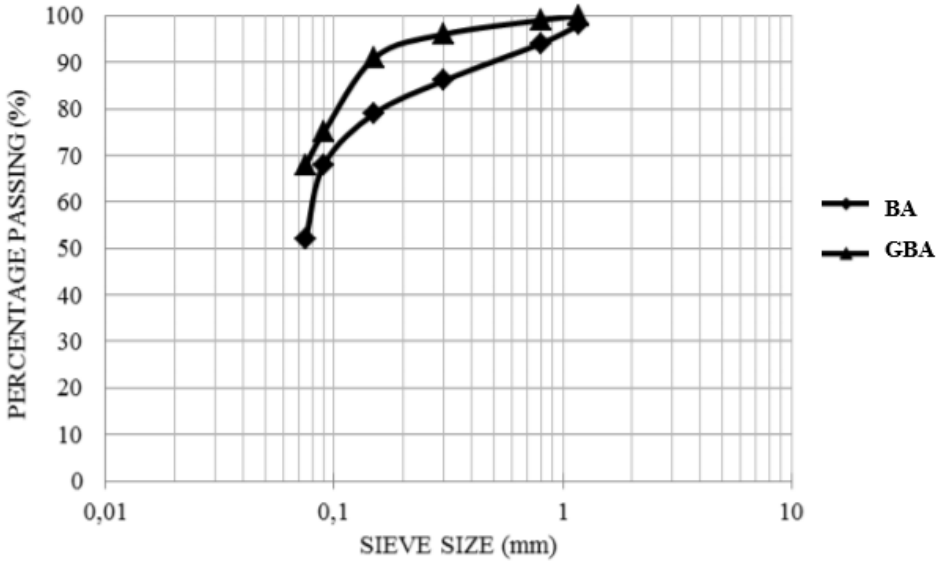

Figure 2.7. Comparison of the PSD as-is Bottom Ash, BA, and Ground Bottom Ash, GBA [41]

2.2.3 Use of Bottom Ash in Civil Engineering Applications

Bottom ash can be beneficially utilized in a variety of manufacturing and construction applications. It is predominantly used for the following applications: Road base and sub-base, structural fill, backfill, drainage media, aggregate for concrete, masonry, and asphalt, and abrasives/traction [10]. The present states of bottom ash management (including boiler slag) in the US and the EU are shown in Figure 2.8. In the case of advanced applications, bottom ash is adopted to introduce unique characteristics such as density, particle shapes, porosity, hydraulic conductivity, thermal resistivity, strength, etc. Advanced applications of bottom ash can be exploited to overcome the limitations of conventional materials in terms of engineering performance, economic efficiency, and even environmental considerations [42].

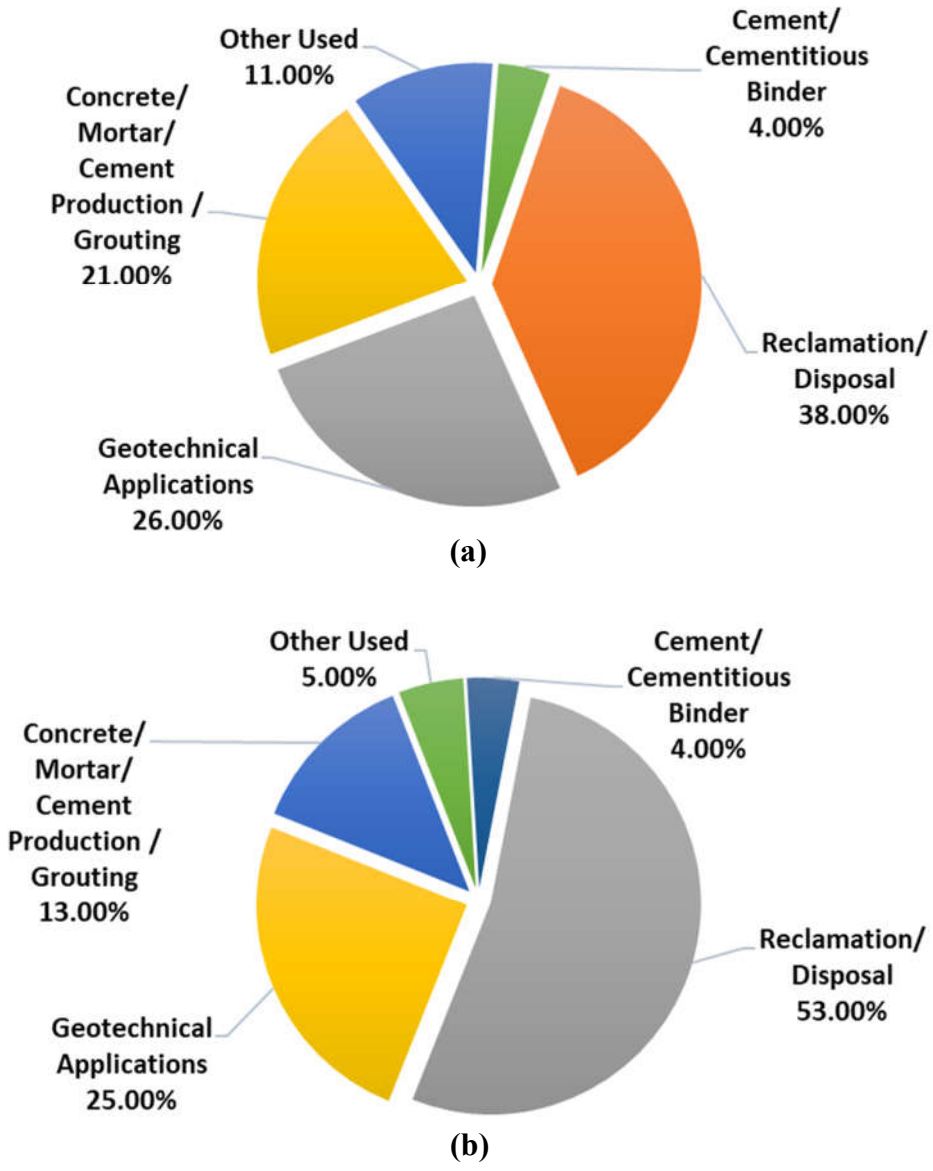

Figure 2.8. Beneficial Utilization and Disposal of Bottom Ash (including Boiler Slag) in (a) EU, (b) US [42]

2.3 Effects of Bottom Ash on Mortar and Concrete Properties

2.3.1 Workability-Water Demand

The previous studies showed that the mortars' or concrete's workability is decreased because of bottom ashes' porous and high-water demand structure, generally. Various studies are presented related to the workability aspects of the different researchers. Topçu and Bilir [26] is studied that the high-water absorption of bottom ashes has led to significantly decreased flow and workability. However, the reduced workability may cause or increase the porosity of the series with the increase in bottom ashes content.

The increase of the bottom ash percentage is caused by the decreasing flowability of the mortar or concrete. This behavior is explained by the porous structure of the bottom ashes compared to the other used natural fine aggregates such as river sands. The bottom ash contains higher porosity, which leads to higher water absorption; consequently, more water is required to cover the bottom ash particle's surface and increase flowability. In contrast, the smaller particle size of the bottom ash compounds the situation, leading to extra water to lubricate the particles. Higher water content is needed for a similar flowability design [43] .

Singh and Siddique [19] performed slump tests and compaction tests to measure the effect of the bottom ashes on the workability of concrete mixtures. The slump values of bottom ash concrete mixtures decreased with the increase in levels of sand replacement by coal bottom ash. The water absorption of coal bottom ash is higher than that of sand. One of the causes of the increment of these parameters is that during the mixing process, the porous particles of coal bottom ash rapidly absorbed more water internally than natural river sand particles, and the availability of free water for lubrication particles was reduced. The other cause is that substituting river sand with coal bottom ash increased the specific surface area of fine aggregate in concrete. The rough texture and complicated shape of particles of coal bottom ash

also played a significant role in increasing the inter-particle friction. The above factors contributed towards lowering the slump and compaction factor values. Therefore, it can be concluded that the decrease in workability of concrete on the use of coal bottom ash is the result of increased specific surface area, complicated shape and texture of particles of coal bottom ash, and absorption of part of water internally by the dry and porous particles of coal bottom ash. The above factors contributed towards lowering the slump and also compaction factor values.

The compaction factor is also one of the workability considerations mentioned in the previous study. The workability measured in terms of compaction factor decreases with the increase of the replacement level of the fine aggregates with the bottom. It can be due to bottom ash's extra fineness as the fine aggregates' replacement level is increased. Thus, an increase in the specific surface due to increased fineness and a greater amount of water needed for the mixed ingredients to get closer packing results in a decrease in the workability of the mix [36].

The coal bottom ashes' porous structure is considered to have caused the increase of the permeability of the mortar or concrete. Therefore, with its porous particle structure and high-water absorption, CBA may act as an internal water reservoir attributed to CBA-like lightweight materials [25].

The slump flow values of fresh concrete were decreased dramatically when 100% of CBA was used. Kim and Lee [44] pointed out that the decrease of the slump flow value could be explained to the following reasons:

1) CBA particles had a more irregular shape and rougher surface than ordinary aggregate particles. The friction between coarser particles is higher than that in using normal aggregate, and this higher friction force prevented the flow characteristics of fresh concrete.
2) The amount of water and cement paste for lubrication between aggregates is decreased because some of the water and cement paste would be drawn into the bottom ash particles. Thus, the water and cement paste are entrapped in craters on the CBA particles during the mixing and curing;

normal contrary aggregates do not have holes. Due to the pores and craters absorbed in the fresh cement paste and the water during the mixing process, some air bubbles, which escaped from the pores of cavities, were entrapped in cement paste, as shown in Figure 2.9.

3) Water absorption on the surface of the bottom ash could be decreased the flow characteristics before the setting of the fresh concrete, an extremely thin water film formed on the interface area between the cement paste and aggregates because of lower water absorption of the surface of the aggregates.

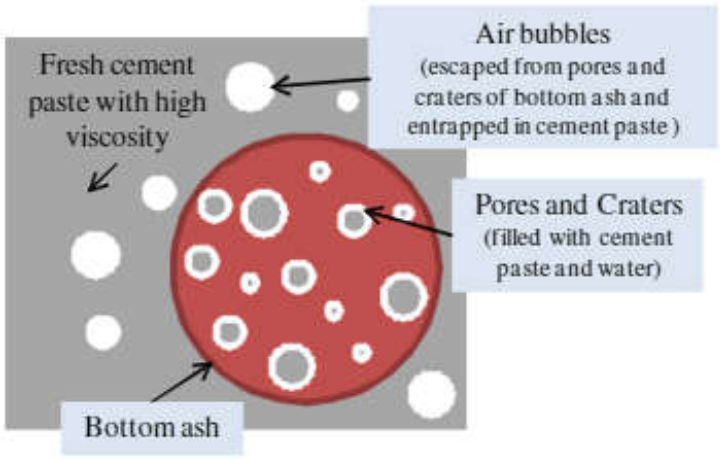

Figure 2.9. Generation of Air Bubbles in Cement Paste [44]

The bleeding could be another factor that is affected to workability. Ghafoori and Bucholc [27] stated that the higher bleeding percentage for the bottom ash mixtures is attributed to the increased demand for mixing water in achieving the required workability.

Cadersa and Auckburally [45] stated that the variation from 20% to 80% of bottom ash replacement decreased workability by 5.56% to 60%, respectively, compared to the control mix. Highly cohesive and sticky mixtures were obtained at 60% and 80% replacement, with low workability. As the replacement of bottom ash was increased,

the amount of cement pastes to coat the bottom ash particles decreased, therefore augmenting friction between the bottom ash particles.

Rafieizonooz et al. [23] are emphasized that in the case of fixed w/c, the workability of concrete reduces with increasing use of CBA as replacement of river sand. The reasons for the decrease in workability are summed as the exact causes of previous studies. These are the use of CBA as fine aggregate enhances the concrete's texture with many more irregular and fine-shaped, porous particles that are usually very rough. Hence, it enhances the interparticle friction, which is responsible for obstructing the flow of fresh concrete.

2.3.2 Heat Evaluation- Isothermal Calorimetry

Isothermal calorimetry is used to estimate the degree of hydration of the mortar mixtures. Immediately after external mixing, the number of glass ampoules was filled with approximately 10 g of mortar. These ampoules were placed in a 23 ± 0.01°C calorimeter within 10 min after water-cement contact. The heat generated by the samples was recorded over desired days. To calculate the degree of hydration of the mixtures, the generated heat was compared to the theoretical heat generated by an equal volume of fully hydrated cement [46].

The temperature increase is a direct result of the heat involved in the cement hydration. The cement hydration reactions are exothermic, and the heat released is dependent on the characteristics of the cement, ambient temperature, and the thermal characteristics of the system. Each event in the hydration process is accompanied by heat evolution.

Andrade et al. [29] is studied that due to the greater cement content, the CRT4 series showed a greater heat evolution, as shown in **Hata! Başvuru kaynağı bulunamadı.**, over time than the reference concrete. Of the two series, greater heat development was also found for series 4, even though the quantity of heat was greater for series 3 in J/g than for the reference sample. The bottom ash content resulted in a greater heat

development for a greater replacement level, except for the 25% and 50% contents of the CRT3 series, where there was an inversion of this tendency, with a greater amount of heat for the 25% content about the 50%

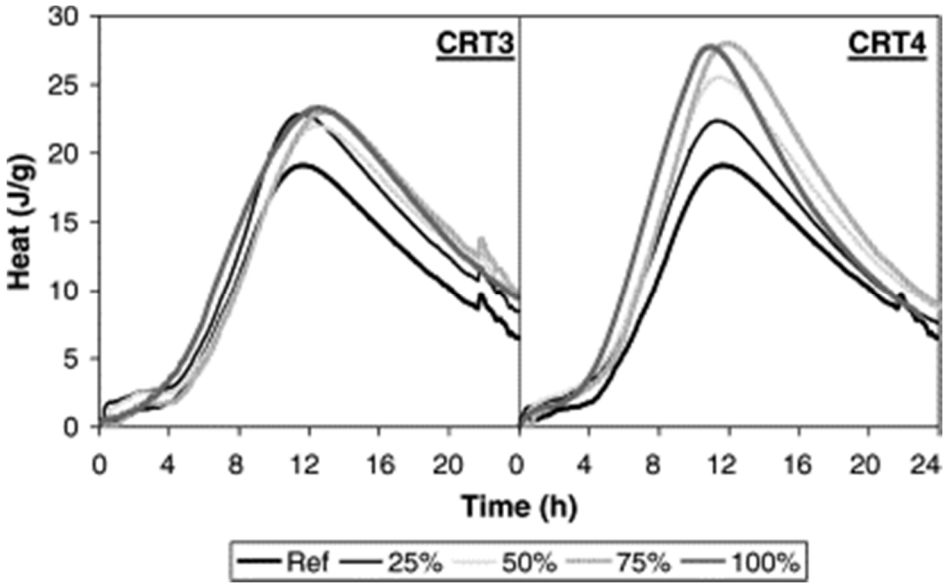

Figure 2.10. Evolution of Heat for Series CRT3, Lower Cement Content, and CRT4, Greater Cement Content [29]

2.3.3 Strength Activity- Compressive and Flexural Strength

The most critical hardened concrete or mortar property is strength evolution. The usage of the bottom ashes is affected the hardened properties in both positive and negative aspects. Generally, the early age strength is reported that the bottom ashes' use decreases the strength. Still, increasing the curing age increases the strength evolution even more significantly than the standard concretes mixes. In the following section, compressive and flexural strength will be investigated.

2.3.3.1 Compressive Strength

The concrete mixes containing bottom ash showed a good strength development pattern with increasing age. Cadersa and Auckburally [45] state that the 7-day strength of the mixes reached about 60-70% of the desired 28-day compressive strength. However, the decrease in compressive strength observed is because of the ash particles' porous surface structure and high absorptivity nature. Therefore, hydration of all cement particles could not have occurred, such that less paste is available for bonding. In addition, as water penetrates through the bottom ash, the expulsion of air bubbles may cause voids between the interface of the cement paste and the coarse aggregates resulting in lower bond strength.

Topçu and Bilir [26] is reported that the replacement level of bottom ash is increased, the gain in compressive strength decreases further. With the decrement in strength up to 10% BA content, there was a slight increase for the 40% ratio. After then, an approximately linear decrement was seen for BA contents higher than 50% up to 100%. The optimum ratio can be determined as 40% regarding compressive strength for both 7 and 28 days. The general idea about the behavior of compressive strength would be sufficient.

The strength development pattern of bottom ash concrete at all the levels of sand replacement with coal bottom ash is similar to that of control concrete. It is evident from the test results that with increasing curing age, the improvement in compressive strength of bottom ash concrete mixtures is continuous and significant, as can be seen in Figure 2.11. The gain in compressive strength of bottom ash concrete mixtures between the curing age of 28 days and 90 days was more than that of the control concrete mixture. The factors responsible for the decrease in compressive strength of bottom ash concrete mixtures at early curing age can be explained as the replacement of the stronger material with the weaker material, absence of pozzolanic activity by the coal bottom ash, and the increased porosity of concrete [19].

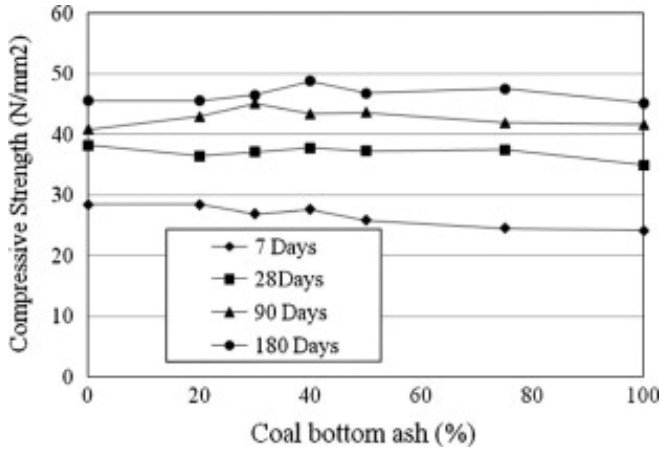

Figure 2.11. Effect of CBA as FA Replacement (vol.%) on Compressive Strength of Concrete [19]

Incorporating BA by up to 40% in silica sand-based matrices does not have a tangible adverse effect on the compression strength of the matrices. At the same time, another replacement reduces the compressive strength. Additional porosity to the matrix leads to a decrease in effective cross-section. Therefore, when the material is under compression, a lateral tension maximizes around the pores and eases a local failure in these areas, and reduces the matrices' strength. On the other hand, a decrease in the water content of the matrix does not necessarily increase the compressive strength. It is due to the dominant role of the porosity of BA compared to that induced by the higher water content. However, reducing the water content weakens the hydration and the cementitious gel formation and, therefore, affects the compressive strength of the matrix. The reduction in compressive strength can also be attributed to the non-proper consolidation of the BA structure, which was partly compensated for using a superplasticizer [43].

The effect of the water-cement ratio is investigated with the Yun et al. [15] studies, and results are found to decrease the compressive strength at both w/c=0.45 and 0.55 at the age of 3 and 7 days. However, at w/c=0.45, the compressive strength of concrete containing 30% and 50% furnace bottom ashes sand was slightly higher than the control at the age of 28 days, and all the concretes containing FBA sand were found to have strength higher than the control at the period of 365 days. In the

case of the w/c=0.55, the compressive strength of all the FBA concretes was lower than that of the control at the age of 28 days. However, at the age of 365 days, the compressive strength of concrete containing 30% and 50% FBA sand was comparable with the control. These results would suggest that there would be a reduction in 28-day compressive strength for most FBA concretes, which might not be a problem later on.

The effect of the water-cement ratio is also Kou, and Poon [33] investigated that generally, the compressive strength of the bottom ash concrete decreased at all the ages with an increase in the furnace bottom ash when used the same water-cement ratio. It is related to the high initial free water content used in the mixes rendered bleeding and poorer interfacial bonding between the aggregates and the cement pastes. When the concrete was designed with a fixed slump range, the compressive strength of the FBA concrete was higher than that of the control. The improved compressive strength should be attributed to the decrease in free W/C because for a given slump of concrete, the high-water absorption properties of FBA would lead to a reduction of free water required to produce target slump value.

Aggarwal et al. [36] state that the bottom ash concrete gains strength at a slower rate in the initial period and acquires strength at a faster rate beyond 28 days due to the pozzolanic action of bottom ash. Also, at an early age, bottom ash reacts slowly with calcium hydroxide liberated during hydration of cement and does not contribute significantly to the densification of the concrete matrix at earlier ages. The early age mechanical property reduced for bottom ash concrete compared to control mix without BA, but strength improved 56 days of curing because of the pozzolanic reaction [41].

The C-S-H gel is not as monolithic and compact as in the control concrete mixture. Rafieizonooz et al. [23] are pointed out that the formation of an imprecise C-S-H gel and a higher percentage of voids in bottom ash concrete mixtures might have affected their compressive strength at early curing age. At the curing period of 91 d and 180 d, the fine spread of C-S-H gel and formation of extra C-S-H gel due to consumption

of portlandite by pozzolanic action of coal bottom ash resulted in higher compressive strength of bottom ash concrete mixtures. At 180 d curing age, the concrete mixtures gained the same compressive strength as control concrete.

2.3.3.2 Flexural Strength

The flexural strength of concrete almost linearly decreased as the replacement ratio of the coal bottom was increased. The fracture section of concrete with bottom ash aggregates shows a flatter surface than concrete with normal aggregates. This means that the cracks propagated through bottom ash particles, as shown in Figure 2.12. At the same time, the normal aggregates were hard to penetrate, and consequently, the direction of crack propagation was changed by the existence of normal aggregates. Therefore, the flexural strength of concrete was decreased when bottom ash aggregates were applied [44].

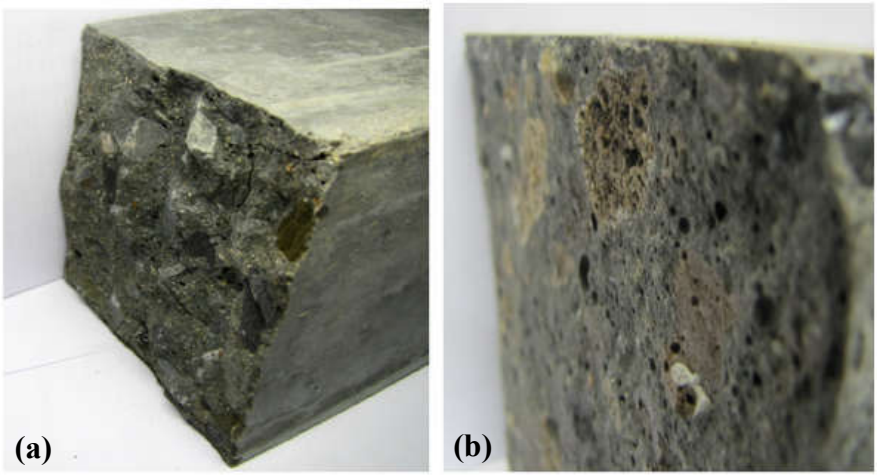

Figure 2.12. Fracture Sections of High-Strength Concrete with Normal (a) and Bottom Ash (b) Aggregates [44]

Cadersa and Auckburally [45] report similar results about crack occurrence in mortar or concrete. Generally, a decrease in flexural strength with an increase in bottom ash replacement. The high porosity of the bottom ash contributed to the rise in the interfacial transition zone and prevented the total hydration of cement particles. The interface zone increased at a higher replacement level of bottom ash, increasing the

risk of micro-crack propagation and interface fractures under stress. Flexural strength is therefore reduced. Moreover, bottom ash being a porous material, the paste becomes weak and porous upon its use as sand replacement. Since the volume of pores in concrete is increased, flexural strength decreases.

Ghafoori and Bucholc [27] stated that if the paste quality improved, the flexural strength of the bottom ash concretes approached that of the control mixes. When 50% of the natural sand was replaced by bottom ash, the average flexural strength fell below the control samples by about 4 %. The use of a low dosage superplasticizer produced a structural concrete superior to that of the reference mixtures.

Furthermore, another study is reported that the flexural strength is affected to more extent than compressive strength with the increase in bottom ash concrete (Figure 2.13). The M1 mixture was prepared as a control, and the other four mixtures were replaced with sand with different percentages. (M2:20%, M3:30%, M4:40% and M5:50%).

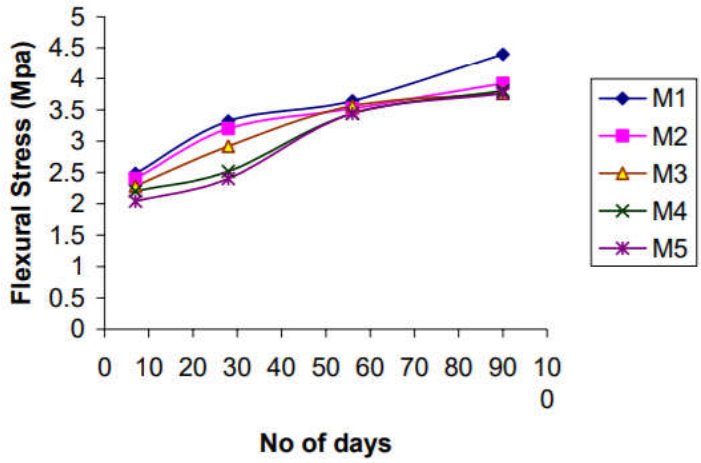

Figure 2.13. Effect of Bottom Ashes on the Flexural Strength [36]

The bottom ash concrete gains flexural strength with the comparable age but less than that of plain concrete. Aggarwal et al. [36] believed this to be due to poor interlocking between the aggregates, as bottom ash particles are spherical.

The pozzolanic reactions of the bottom ashes are also affected with the flexural strength as compressive strength. The lower early age flexural strength is explained by Rafieizonooz et al. [23] is that the delay in hydration and slow pozzolanic activity of CBA at the early curing period. At the later (90 d and 180 d) curing period, the fine spread of C-S-H gel and formation of extra C-S-H gel due to consumption of portlandite by pozzolanic action of CBA resulted in higher flexural strength of bottom ash concrete mixtures.

2.3.4 Durability- Alkali-Silica Reaction

Alkali silica reaction has occurred between alkali oxides, the constituents of cement, and aggregate that includes reactive silica forms. As a result, ASR causes expansion and has two simple phases. In the first phase, through a reaction of alkalis and reactive silica, ASR gel products occur. In the second phase, ASR gels combine with the moisture of the media, and expansion takes place. As time elapses, expansion causes cracks and deformation in the concrete [47]. ASR is a serious durability problem. It is taken from three to even more than twenty-five years to develop in concrete structures depending on the main factors such as the reactivity level of the aggregates used, the moisture and temperature conditions, and the alkali content in concrete [48].

Mineral admixtures are finely divided siliceous materials that are added to concrete during mixing in relatively large amounts. Industrial by-products are the primary source of mineral admixtures. Silica fume, fly ash, ground granulated blast furnace slag, and metakaolin in the concrete mix at appropriate proportions to react with calcium hydroxide to reduce the alkalinity of the cementitious system. The increased amount of C–S–H gels in the composite due to the reaction between calcium hydroxide and pozzolanic mineral additives in the blended cement compositions decreased the ASR gel formation of cement-based composite materials. The pozzolanic reaction and reduced equivalent alkali content of the blended cement increased the durability of the concrete against ASR [49] .

Abbas et al. [50] reported that expansion results show decreasing ASR expansion for mixtures incorporating CBA. For instance, specimens incorporating 10% CBA had an expansion of 0.17% and 0.22% at 14 and 28 days, respectively, which is still higher than the allowable limit of ASTM C1260 [51] (Figure 2.14). Specimens incorporating 20% CBA incurred an expansion of 0.19% at 28 days, less than the ASTM limit. Expansion at 28 days was 0.17% for specimens made with 40% CBA. This reduction in expansion can be attributed to the pozzolanic reaction of CBA.

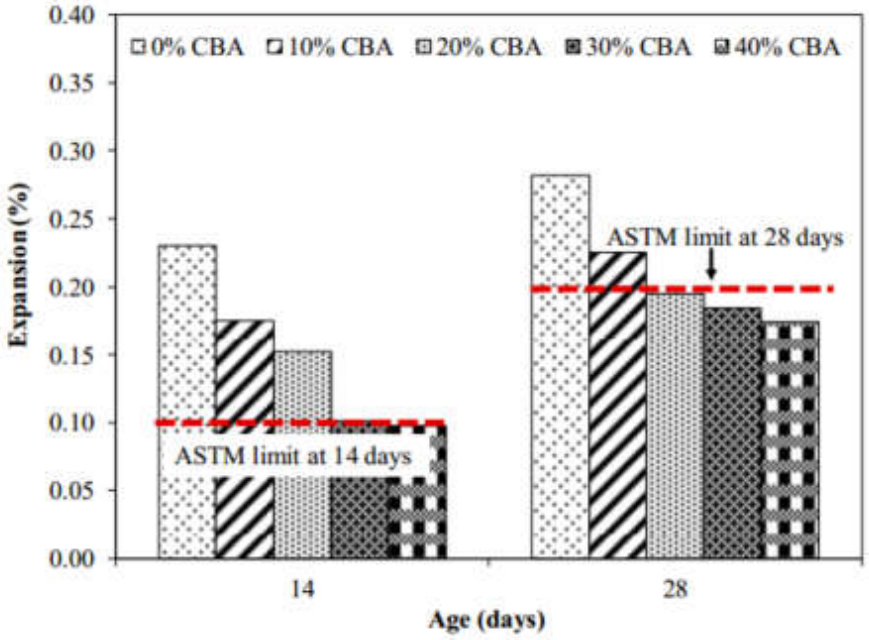

Figure 2.14. Expansion Results and ASTM Limits for Mixture with Various Proportions of CBA [50]

CHAPTER 3

MATERIALS AND EXPERIMENTAL PROCEDURE

The physical and chemical properties of the materials used and the origin of the bottom ashes was studied. Furthermore, the experimental procedures which were followed during the tests are presented in this chapter in detail. The X-ray fluorescence spectroscopy (XRF) test results of the bottom ashes were provided by the Eren Enerji Zonguldak thermal power plant. The scanning electron microscopy (SEM) and mercury intrusion porosimetry (MIP) tests were performed at METU Central Laboratory. The rest of all experiments were conducted in the Materials of Construction Laboratory of the Department of Civil Engineering, METU.

3.1 Bottom Ashes

Bottom ashes were delivered from Eren Enerji - Zonguldak Eren Thermal Power Plant. ZETES (Zonguldak Eren Thermal Power Plant), located within the Çatalağzı municipality of Zonguldak province in Turkey, has a total installed power of 2790 MW. Daily coal consumption (when all units are in operation) is approximately 23,000 tons. Monthly consumption is around 700,000 tons. In the power plant area, there are power plant units with the following characteristics;

- One power plant unit with fluid bed technology with 160 MW installed power, ZETES 1
- 2 x 615 MWe Super Critical Pulverized Coal, ZETES 2
- 2 x 700 MWe Super Critical Pulverized Coal, ZETES 3

Eren Thermal Power Plant is a multi-unit coal thermal power plant, and bottom ashes were obtained from there. The two different types of ash-handling systems are settled there; one of them is dry ash-handling systems, and the other one is wet ash handling

systems. Dry-handled bottom ash was collected in dry condition since the cooling process is done with air ZETES 3. Wet-handled bottom ash was collected in wet condition since the conveyor was filled with water. The hot ash particles were directly dropped into the water-filled conveyor and cooled with water (submerged scraper conveyor, SSC) which is ZETES 2. In the power plants, dry ash-handling systems units are generally used. The temperature of both boilers of ZETES 2 and ZETES 3 is 1300^{o} C -1400^{o} C. The source of the coal is mostly Colombia and, to a lesser extent South Africa. Both unit plants' average hourly coal combustion is 230 tons/hour, and the average ash production for ZETES 2 is 6 tons/hour and 4 tons/ hour for ZETES 3. The dry-handled bottom ash (DHBA) and wet-handled bottom ash (WHBA) are shown in Figure 3.1, respectively.

Figure 3.1. Dry-Handled Bottom Ash & Wet-Handled Bottom Ash, Respectively

3.2 Cement

The used Portland cement type was CEM-I 42,5 R that BAŞTAŞ Cement Factory provided. The CEM-I 42,5 R Portland cement was used with prepared mixes for compressive and flexural strength and alkali-silica reaction mortar bars. This cement, which is an ordinary type, has no extra alkaline characteristics.

3.3 Fine Aggregates

The fine aggregates were used in the control mortar and the test mortars. Two types of fine aggregates were used. The first one was crushed stone sand which mainly included calcareous, and the second one was river sand which was reactive sand. The second one was used in the alkali-silica reaction test only; the regular sand was used for the rest of the experiments. The aggregates (Figure 3.2) were provided from the Materials of Construction Laboratory of the Department of Civil Engineering, METU. Additionally, the water was used as tap water in the laboratory.

Figure 3.2. Sand and the Reactive River Sand, Respectively

3.4 Characterization of the Raw Materials

The properties of chemical structure (XRF), mineralogical structure (XRD), morphological structure (SEM), particle size distributions, specific gravities, water absorption capacities, densities of the materials for the use of bottom ashes as fine aggregates and supplementary cementitious material in mortar were investigated.

3.4.1 X-Ray Florescence (XRF)

Especially to usage as a binder material, the composition should be included in a certain amount of silicon dioxide (SiO_2), aluminum oxide (Al_2O_3), and ferric oxide (Fe_2O_3). The Eren-Enerji Thermal Power Plant analyzed the chemical compositions of the DHBA and WHBA. The compositions occurred from SiO_2 and Al_2O_3 mainly

and included Fe_2O_3, K_2O, CaO, MgO, TiO_2, Na_2O, SO_3, P_2O_5, MnO, and Cl (Table 3.1). The bottom ashes were composed from mainly 58.59% / 62.53% SiO_2, 22.27% / 20.04% Al_2O_3, 8.33% / 8.48% Fe_2O_3, 4.58% / 1.79% CaO, 2.17% / 2.66% K_2O for DHBA/ WHBA, respectively.

According to ASTM C618 [34], the sum of the SiO_2+Al_2O_3+Fe_2O_3 amount should be a minimum of 70% of the materials used as supplementary material. In addition, there were no trace elements in the bottom ashes; thus, it could be used as a fine aggregate without any treatment.

Table 3.1 Chemical Compositions of DHBA and WHBA.

Oxides	**Result (%)**	
	DHBA	**WHBA**
SiO_2	**58.59**	**62.53**
Al_2O_3	**22.27**	**20.04**
Fe_2O_3	**8.33**	**8.48**
K_2O	2.17	2.66
CaO	**4.58**	**1.79**
MgO	1.64	1.63
TiO_2	1.00	0.95
Na_2O	0.84	0.86
SO_3	0.12	0.85
P_2O_5	0.37	0.10
MnO	0.08	0.08
Cl	0.02	0.01
SiO_2+Al_2O_3+Fe_2O_3	**89.19**	**91.05**

3.4.2 X-Ray Diffraction (XRD)

The mineralogical properties of the DHBA and WHBA were investigated by X-Ray Diffraction (XRD) method. The XRD measurements of the bottom ashes were conducted on the XRD device located at the laboratory. The XRD analysis results were finalized using High score Plus software and available literature on the existing measurements.

The mineralogical properties such as the bottom ash's glassy or crystalline structure are essential for the grindability investigation. The fineness and the amorphous structure of the bottom ash are the most desired properties for usage as supplementary cementitious material. The XRD measurements were conducted on 180 minutes of ground bottom ashes samples. The main peaks of the dry-handled bottom ashes were found as quartz and anorthite (Figure 3.3). Quartz and sillimanite were the main peaks for the wet-handled bottom ash, as shown in Figure 3.3. WHBA was found more amorphous than DHBA.

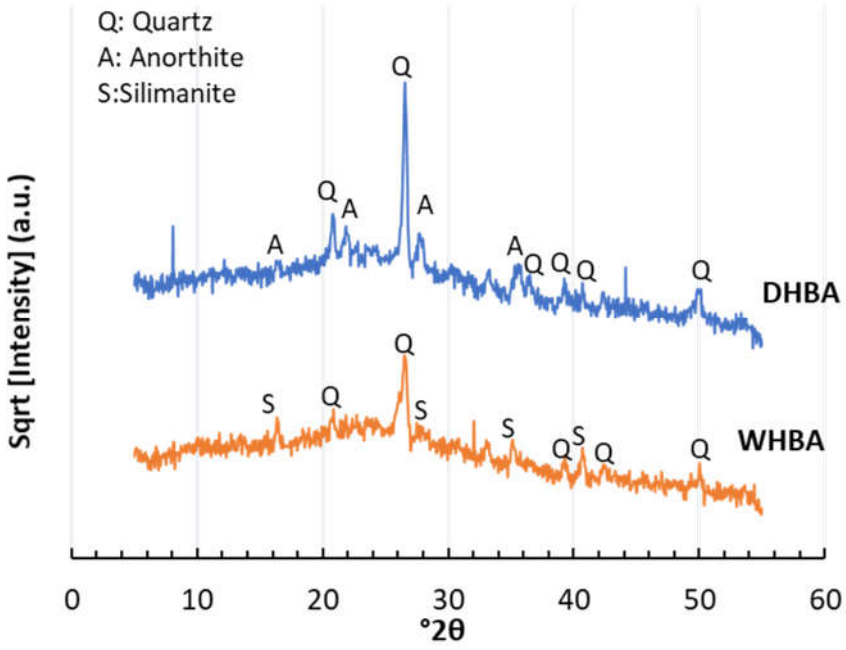

Figure 3.3. XRD Pattern of DHBA and WHBA Ashes

3.4.3 SEM Micrographs

The morphological properties of the DHBA and WHBA were examined by the SEM device. The methodology of the SEM testing was explained with the following steps; specimens are placed on carbon tapes which are put on metal holders, and then, the samples are coated with the gold-palladium mixture as a conductive layer. The desired zoom-in and zoom-out screenshots are taken. The bottom ashes samples were taken their as-is condition as shown in Figure 3.4. The coarser one's sizes were in the range of 2-10 mm.

Figure 3.4. The SEM Test Samples S-WHBA and S-DHBA

Two samples are investigated for both types of BAs that are named WHBA-1 and WHBA-2, and DHBA-1 and DHBA-2. The SEM micrographs were taken with different magnifications such as 1000×, 2500×, 5000×and 10000×. The bottom ashes' porous structure and rough surface could be seen clearly in Figure 3.6, **Hata! Başvuru kaynağı bulunamadı.**, Figure 3.7 and Figure 3.8 for the dry-handled bottom ashes and wet-handled bottom ashes, respectively. The structures explained the reason for the high-water demand and workability issues. The bottom ashes microstructures were found mainly porous and glassy. DHBA samples had a highly porous and glassy matrix. WHBA samples were also glassy; but, they were less porous than DHBA. Furthermore, the average pore size for WHBA samples was smaller than that of DHBA samples.

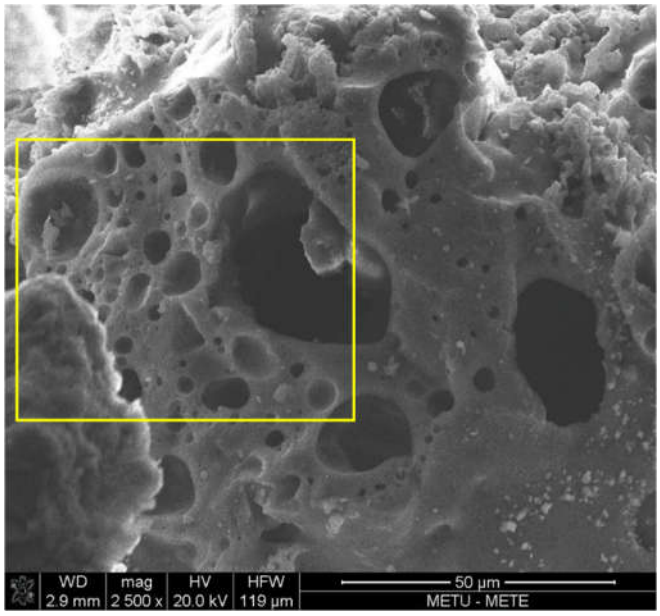
WD
2.9 mm
mag
2 500 x
HV
20.0 kV
HFW
119 µm
50 µm
METU - METE

(a)

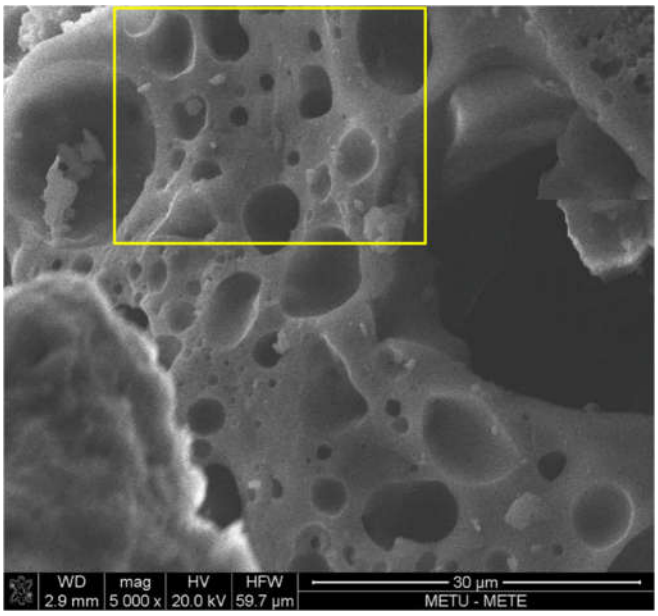
WD
2.9 mm
mag
5 000 x
HV
20.0 kV
HFW
59.7 µm
30 µm
METU - METE

(b)

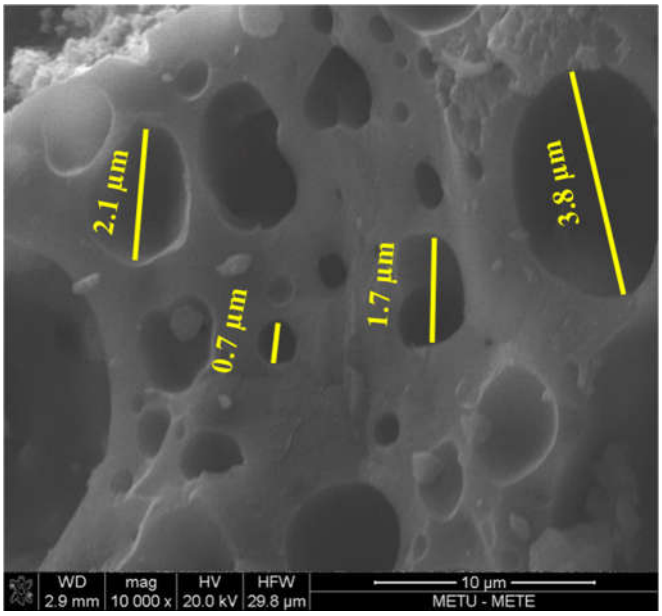

(c)

Figure 3.5. SEM Micrographs of DHBA-1: (a) 2.5k×, (b) 5k×, and (c)10k×

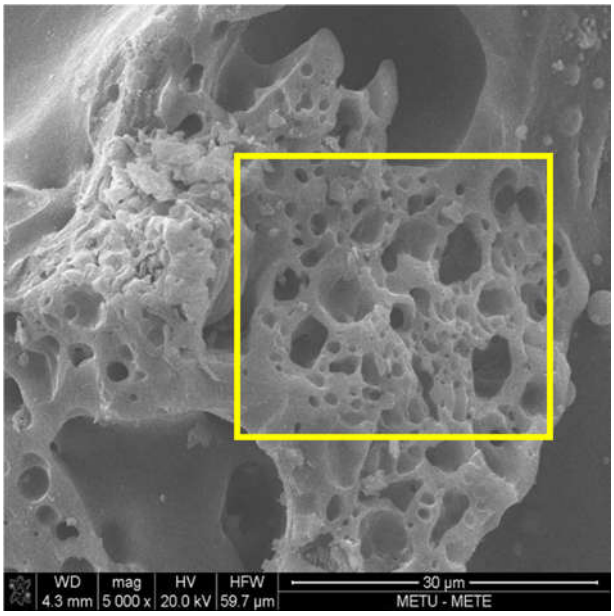

(a)

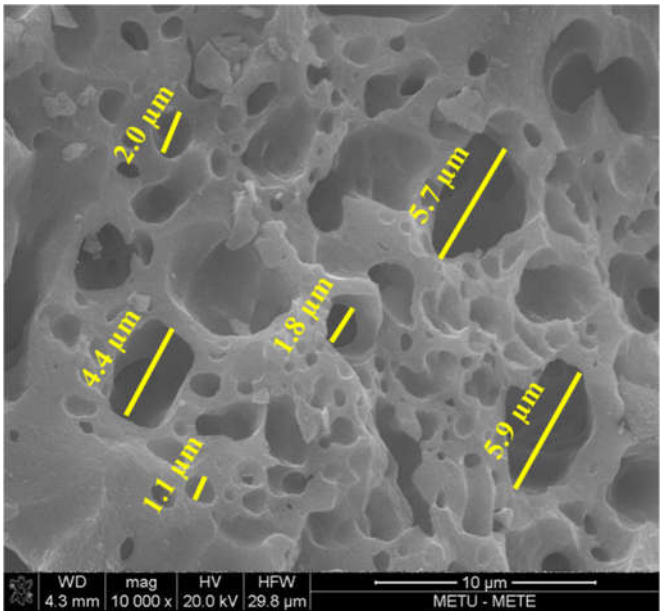

(b)

Figure 3.6. SEM Micrographs of DHBA-2: (a) 5k×, and (b) 10k×

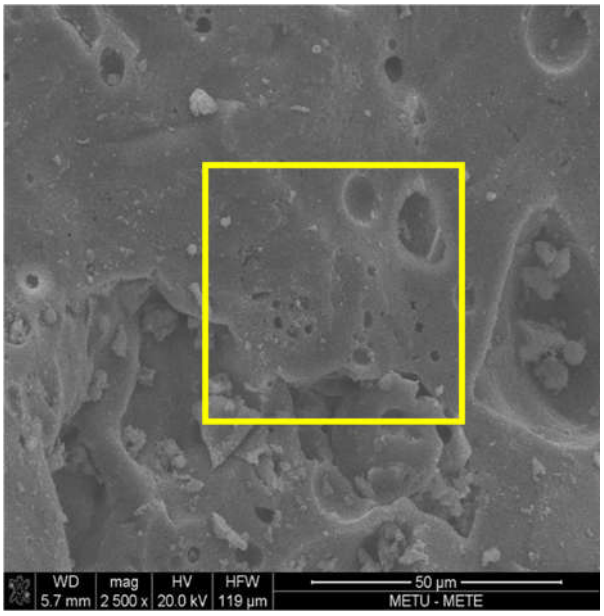

(a)

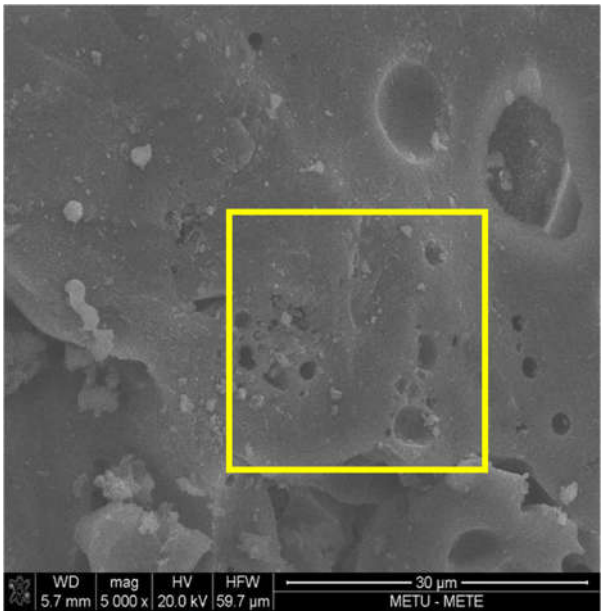

(b)

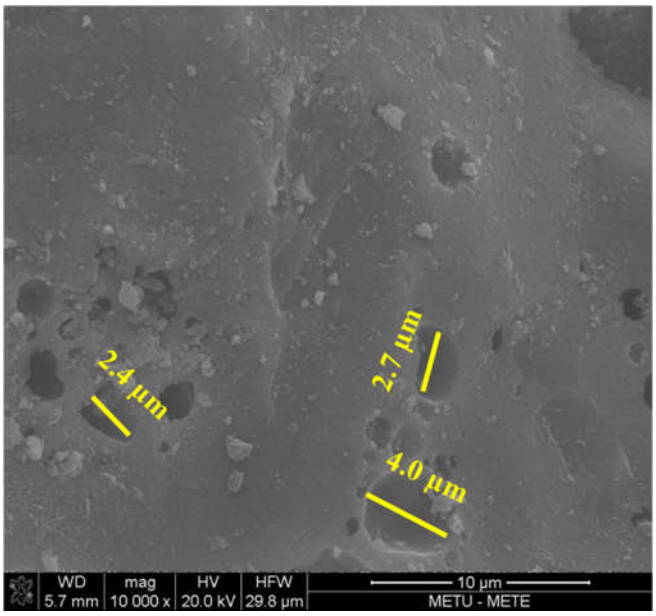

(c)

Figure 3.7. SEM Micrographs of WHBA-1: (a) 2.5k×, (b) 5k×, and (c) 10k×

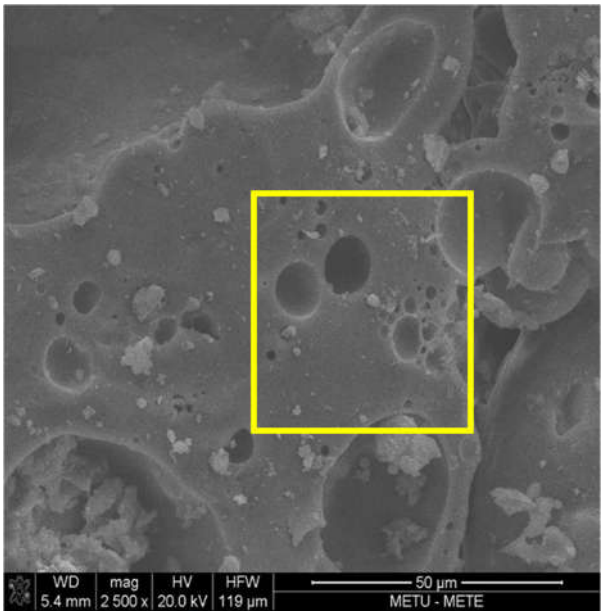

(a)

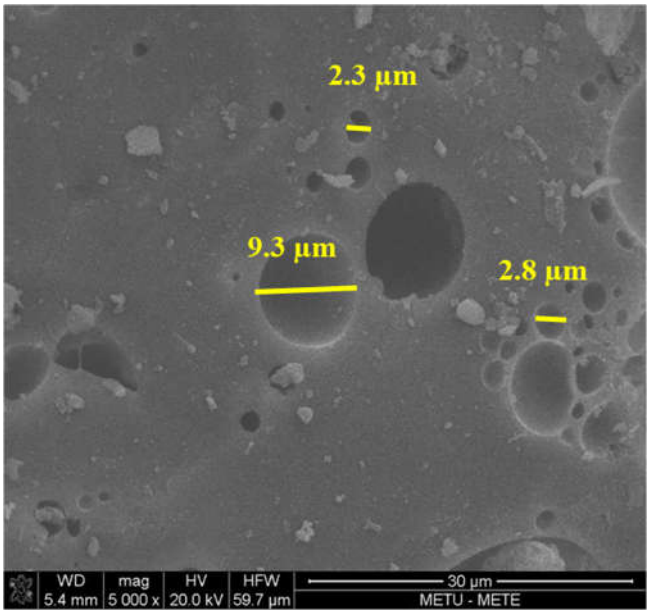

(b)

Figure 3.8. SEM Micrographs of WHBA-2: (a) 2.5k×, and (b) 5k×

Additionally, elemental identification of the samples was made with energy-dispersive x-ray spectroscopy (EDX). As expected, the elemental distribution was

found as Si, Al, Fe, K, Ca, Mg, and Ti. The oxides were normalized according to elements and given in Table 3.2. These results were found nearly similar to the XRF results.

Table 3.2 Elemental Distributions of the BAs Samples Normalized with Oxides

	WHBA-coarse	**WHBA-dust**	**DHBA-coarse**	**DHBA-dust**
SiO_2	0.59	0.52	0.66	0.62
Al_2O_3	0.27	0.21	0.21	0.27
Fe_2O_3	0.03	0.04	0.08	0.04
K_2O	0.02	0.01	0.01	0.03
CaO	0.05	0.15	0.02	0.01
MgO	0.02	0.07	-	0.02
TiO_2	0.02	0.01	0.02	0.01

3.4.4 Specific Gravity and Water Absorption Capacity

The water absorption (WA) capacity is found higher respectively than other fine aggregates in the literature, generally [25], [24]. Therefore, the water absorption capacity is the significant parameter of the bottom ashes and must be considered sensitively. The water absorption capacity affects water-cement ratios and also the workability of the pastes. The water absorption capacities and specific gravities were found according to ASTM C128 [52], all used fine aggregates such as DHBA, WHBA, sand, and river sand. According to water absorption capacities, the required free water demand was found for each mix also.

The specific gravity (SG) of the samples was calculated with the following steps in the specification. Firstly, all types of fine aggregate were oven at 110^{o}C for 24 hours before the experiment. Then, samples were submerged into the water and waited in the water for another 24-hours. After all these preparations to get the surface saturated properties, the cone test was done to fine wet particles. The cone test was performed until found the desired SSD condition was. After that, the fine aggregate was added into the mold with 25 drops of the tamper with the two layers. Lastly, the mold was lifted vertically. In the case of fine aggregates were retained cone shape,

the test was repeated; otherwise, the test was not conducted in the slight slumping case. The slight slumping state was meant that the desired moisture conditions were reached, and the sample was used for the rest of the test. After all these, the pycnometer was filled with water to its limits and measured.

Then the about 500 g SSD condition specimen was placed into the pycnometer and measured. Finally, the pycnometer was filled with water within the SSD condition samples and was measured. For finding the samples' oven-dried mass, the pycnometer was poured into the proper tank, the sample was dried into the oven in 24 hours, and specimens were measured at the end.

The specific gravities and water absorption of the DHBA, WHBA, sand, and reactive (river) sand results are given in Table 3.3. The results were found as an average of the two samples for each type of material. The calculation of the specific gravity and water absorption of the sample was conducted, as indicated in the specification. WHBA was found heavier than DHBA, and the DHBA had more water absorption capacity than WHBA.

Table 3.3 SGs and the WA Capacities of the Raw Materials

Specific Gravity and Water Absorption				
Property	**DHBA**	**WHBA**	**Sand**	**Reactive Sand**
Specific gravity – App.	1.88	1.92	2.72	2.67
Specific gravity - OD	1.41	1.72	2.56	2.33
Specific gravity - SSD	1.66	1.82	2.62	2.46
Water absorption (wt. %)	14.31	4.04	2.35	5.49

3.4.5 Mercury Intrusion Porosimetry (MIP)

Mercury intrusion porosimetry (MIP) is a widely used technique for characterizing the distribution of pore sizes in cement-based materials. The MIP measurement relies on the principle that the intrusion volume of mercury into a porous material depends

on the applied pressure. During the intrusion, the applied pressure is assumed to be in equilibrium with the surface tension of mercury in pores [53] . In this study, the as-is coarse particles of the bottom ashes were analyzed in METU Central Laboratory. In the device, coarse materials can measure macro-mesopore diameters between 200 microns and 0.0036 microns. At the low pressure (up to 50 psi), 200-4 microns can be measured. The differential particle size distribution of the BAs is presented in Figure 3.9. The dominant pore diameter size range was 30-200 μm and 15-25 μm for the DHBA and WHBA, respectively. Additionally, Figure 3.10 shows that DHBA had larger pores than WHBA. It can be concluded that the DHBA was found more porous than WHBA.

In Table 3.4, the real (without pores only solid) & apparent (with pores and solid) densities and total pore volume of the bottom ashes. The densities were calculated with helium pycnometer analysis. WHBA was found denser than DHBA as found in the method of ASTM C128 [52].

Table 3.4 MIP measurements of the DHBA and WHBA at low pressure.

	DHBA	**WHBA**
Real Density (g/cm^3)	1.92	2.34
Apparent Density (g/ cm^3)	0.66	1.32
Total Porosity (%)	65.84	43.77

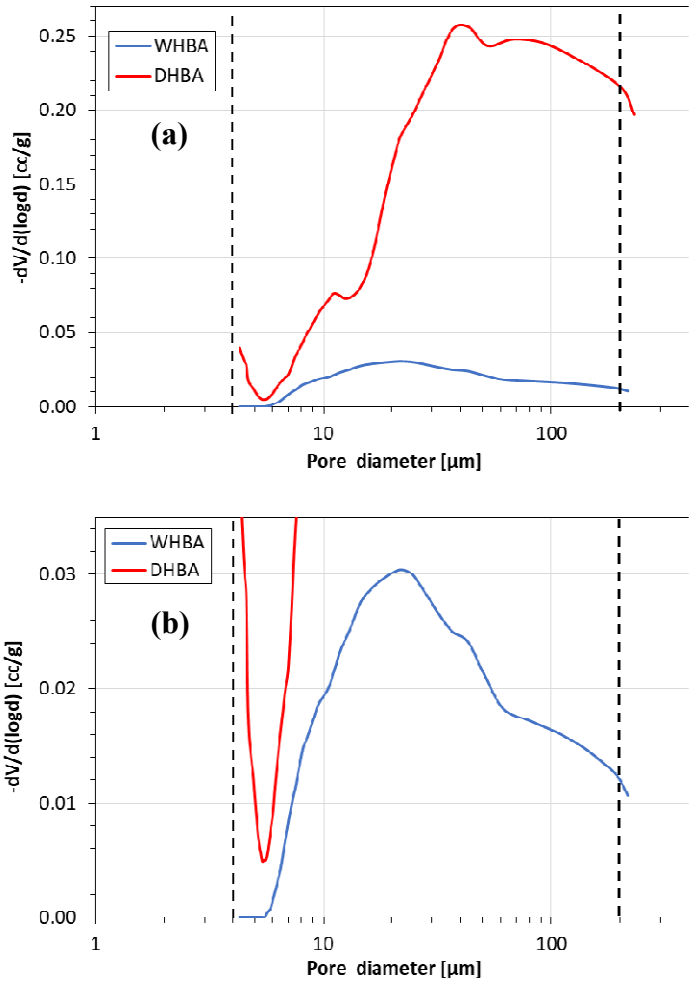

Figure 3.9. PSD of DHBA (a) and WHBA (b) by MIP (4 µm ≤ d ≤ 200 µm)

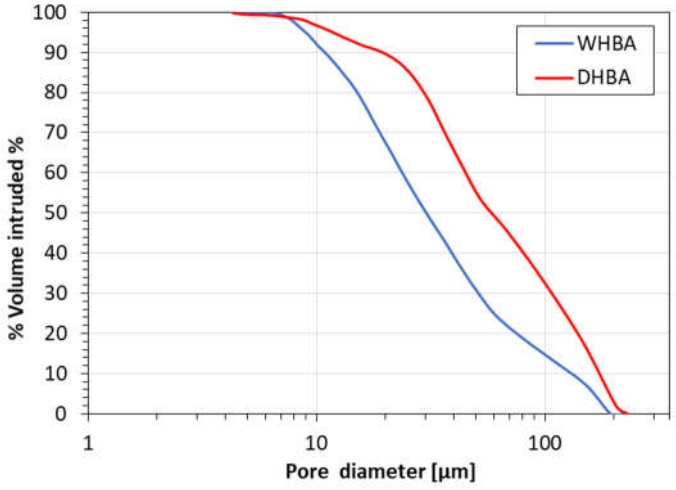

Figure 3.10. Volume vs. Pore Diameter Distributions of BAs

3.4.6 Particle Size Distribution and Fineness Modulus

The different sizes of the bottom ashes have occurred while drop down to the dry or wet boiler hopper of the bottom ashes, as shown in Figure 3.11. Therefore, the particle sizes and shapes of the bottom ashes were investigated to be proper for usage as a fine aggregate.

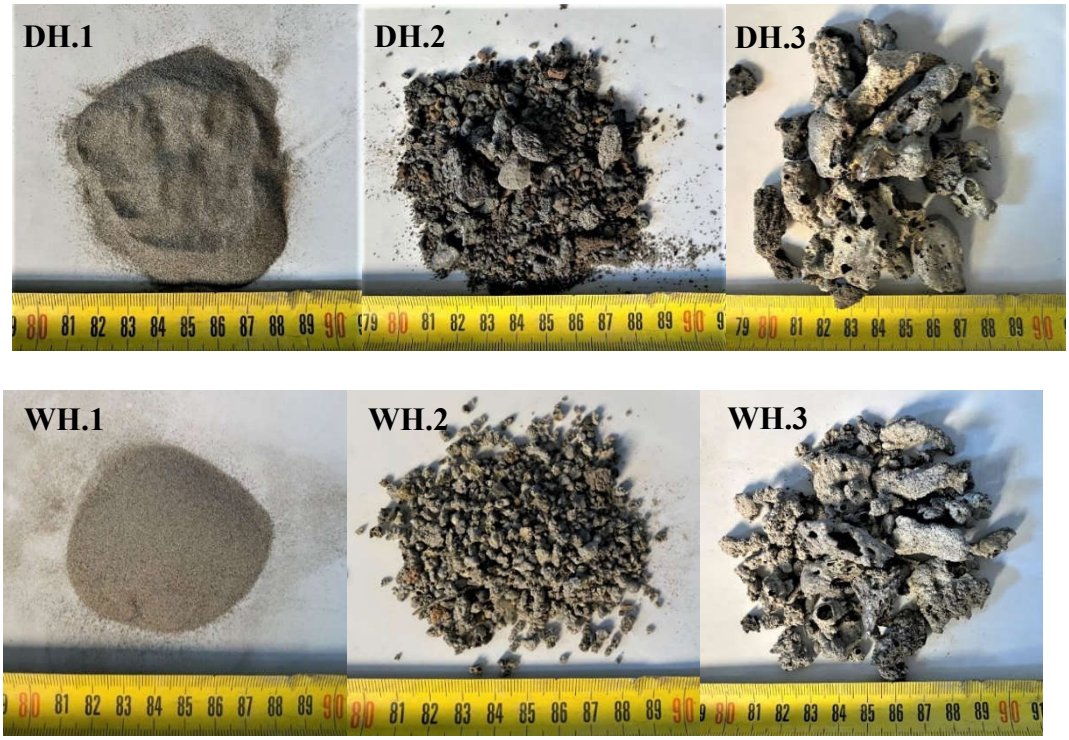

Figure 3.11. Different Size of DHBA (DH.1, DH.2 and DH.3) and WHBA (WH.1, WH.2 and WH.3) as-is Conditions

The as-is particle size distribution of the DHBA and WHBA was performed oven-dried samples according to ASTM C 136 [54]. The four samples (~ 1000 g each) of two types of bottom ashes were sieved, and the average particle size distributions (PSD) of these four samples were calculated. The fine aggregates' PSD of the bottom ashes and the upper & lower limit [55] is presented with a graph in Figure 3.12. The PSD of the bottom ashes was found coarser than standard fine aggregates.

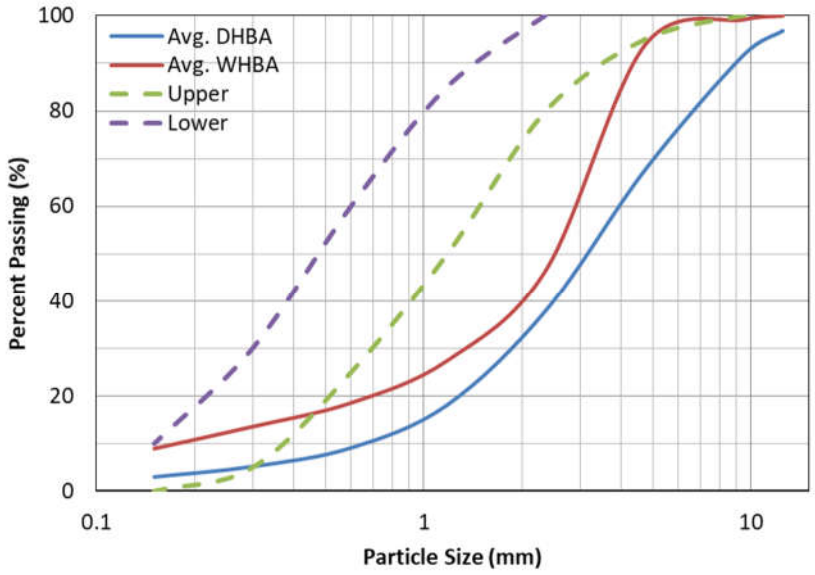

Figure 3.12. PSD of the as-is DHBA and WHBA (Upper and Lower Limit Zones [55])

The fineness modulus (FM) of each four bottom ash samples was also calculated as stated in ASTM C136 [54]. Each cumulative percentage retained of the aggregate which passed standard sieves was sum up and divided by 100. In ASTM C33 [55], the FM limits were indicated in 2.3 - 3.1%. In Table 3.5 and Table 3.6, the FM of the samples was presented. The fineness modulus was found more than the upper limit for dry-handled bottom ashes but in the limits for wet-handled bottom ashes.

Table 3.5 Fineness Modulus of the Dry-Handled Bottom Ash

	Cumulative Percentage Retained (wt. %)			
Sieve #	**DHBA-1**	**DHBA-2**	**DHBA-3**	**DHBA-4**
4.75-mm (No. 4)	24.5	30.1	42.8	31.7
2.36-mm (No.8)	52.9	56.7	76.2	62.4
1.18-mm (No. 16)	75.2	76.5	93.3	82.7
600-µm (No.30)	87.2	86.7	98.1	91.8
300-µm (No. 50)	92.8	92.3	99.1	95.3
150-µm (No. 100)	96.0	95.7	99.4	97.1
Total (%)	428.5	438.0	508.8	461.0
FM (%)	4.3	4.4	5.1	4.6
Avg. FM (%)	**4.6 (> 3.1%)**			

Table 3.6 Fineness Modulus of the Wet-Handled Bottom Ash

	Cumulative Percentage Retained (wt. %)			
Sieve #	**WHBA-1**	**WHBA-2**	**WHBA-3**	**WHBA-4**
4.75-mm (No. 4)	3.4	5.7	6.3	8.7
2.36-mm (No.8)	18.5	26.5	25.9	32.9
1.18-mm (No. 16)	38.0	50.2	48.6	56.7
600-µm (No.30)	49.4	61.0	60.1	67.1
300-µm (No. 50)	59.2	69.4	69.0	74.3
150-µm (No. 100)	72.2	79.0	79.0	82.7
Total (%)	240.6	291.8	288.9	322.4
FM (%)	2.4	2.9	2.9	3.2
Avg. FM (%)	**2.9 (< 3.1%)**			

3.4.7 Chemical and Physical Properties of the Portland Cement

The Portland Cement CEM I 42,5 R properties are assumed it's standard directly, and the calculations and tests were conducted according to presented values which are the content of the cement PC clinker (95%) +limestone (5%) + gypsum (5%). The specific surface area of the cement is in the range between 3300-3900 cm^2/g, and density is 3.00 - 3.15 g / cm^3.

3.5 Experimental Procedure

The experiments were done on to paste (cement/binder + water) and mortar (cement/binder + water + fine aggregate) mixes. The flow table test was conducted just before casting the fresh mortars into the molds. The isothermal calorimetry test proceeded to the fresh pastes during 4- days. The compressive and flexural strength tests were performed for the hardened mortars. The experiments were conducted on the 7th, 28th, and 90th day of the mortars. The alkali-silica reaction test proceeded during the 45- days with the 3-day intervals at the first two weeks, and after the 15-days, additional two readings were done. The summary of the tested and followed specifications was given below in

Table 3.7

The experimental procedure was conducted with three significant steps in this study. The steps were summarized like that;

i. Preparation of materials
ii. Preparation of pastes and mortars
iii. Testing of the specimens

Table 3.7 Experiments and Applied Standards

The Experiments	Age	The Standards
Experiments on Pastes		
Isothermal Calorimetry Test	First 4 days	ASTM C 1702 [56]
Experiments on Mortars		
Flow Table	Pre-Casting	ASTM C 1437 [57]
Compressive & Flexural Strength	Days 7, 28 & 90	ASTM C 349 [58] & ASTM C348 [59]
Alkali-Silica Reactions	During 45 days	ASTM C 1260 [51]

3.5.1 Mix Designs

For this study, 17 different mix designs were prepared. The first one is a control mix for the comparison of the others. According to TS EN 196-1 [60] standard, the initial mix designs were prepared with a fixed initial w/b ratio, 0.5. The control mix was prepared with 1350-gram sand, 450-g cement, and 225-g water. The mix designs incorporating BA were separated into three main parts:

- Replacement of the sand with CBA as fine aggregate
- Replacement of the cement with CBA as supplementary cementitious materials
- Combined replacement

The mixes with CBA were prepared with the 25/50% volumetric replacement of the fine aggregate (in oven-dry condition) and 25/50% weight replacement of the cement. Table 3.8 lists the mix design proportions chosen in this study. Even though adding aggregates in SSD condition is customary, in this study, the utilized fine aggregates were oven-dried to better control the volumetric replacements of the aggregates as one of the bottom ashes arrived too dry, whereas the other one was soaked. Considering their varying water absorption capacities (sand: 2.35, dry-handled bottom ash: 14.31%, and wet-handled bottom ash: 4.04%), this resulted in very harsh mixes. Therefore, additional water was added to obtain desired flow values increasing the w/b ratios.

Table 3.8 Mix Design Ratios of the DHBA and WHBA Mortar Specimens.

Mixes Codes	Aggregate Replacement (*)			Binder Replacement (+)		
	Sand	S-DH	S-WH	PC	G-DH	G-WH
Control	100	-	-	100	-	-
Part 1: Partial replacement of fine aggregate with CBA						
DH: A25	75	25	-	100	-	-
DH: A50	50	50	-	100	-	-
WH: A25	75	-	25	100	-	-
WH: A50	50	-	50	100	-	-
Part 2: Usage of CBA as an SCM						
DH: P25	100	-	-	75	25	-
DH: P50	100	-	-	75	-	25
WH: P25	100	-	-	50	50	-
WH: P50	100	-	-	50	-	50
Part 3: Combined usage						
DH: A25-P25	75	25	-	75	25	-
DH: A50-P25	50	50	-	75	25	-
WH: A25-P25	75	-	25	75	-	25
WH: A50-P25	50	-	50	75	-	25
DH: A25-P50	75	25	-	50	50	-
DH: A50-P50	50	50	-	50	50	-
WH: A25-P50	75	-	25	50	-	50
WH: A50-P50	50	-	50	50	-	50

(*) Aggregates are replaced in oven-dry condition by volume.
(+) Binders are replaced by weight.
DH:(X) (Y)=Dry-handled Bottom Ash (Usage Purpose) (Replacement portions)
WH:(X) (Y)=Wet-handled Bottom Ash (Usage Purpose) (Replacement portions)
S-DH/WH: Sieved Bottom Ashes
G-DH/WH: Ground Bottom Ashes

3.5.2 Preparation of Materials for Experiments

The bottom ashes preparation procedures were handled into two parts: for the usage as a fine aggregate and SCM usage. The detailed procedures are explained in the following sections. Afterward, the initial trials for the pre-soaking were done before the casting of the mortars.

3.5.2.1 Preparation Procedure for Usage as a Fine Aggregate

The usage as a fine aggregate, bottom ashes, and sands was sieved from No: 4 sieves. Thus, the coarser particles than 4.75 mm were separated from the bulk materials. After that, the DHBA and WHBA were divided, each passing size according to standard sizes such as No: 8, No: 16, No: 30, and No: 50 separately. The separated condition of the different particle sizes of the ashes is shown in Figure 3.13. The particle distribution of all fine aggregates was arranged according to ASTM C1260 [51]. The identical particle size distributions were used in the alkali-silica reactions and compressive-flexural strength experiments. Therefore, any problems caused by different particle size distributions were eliminated.

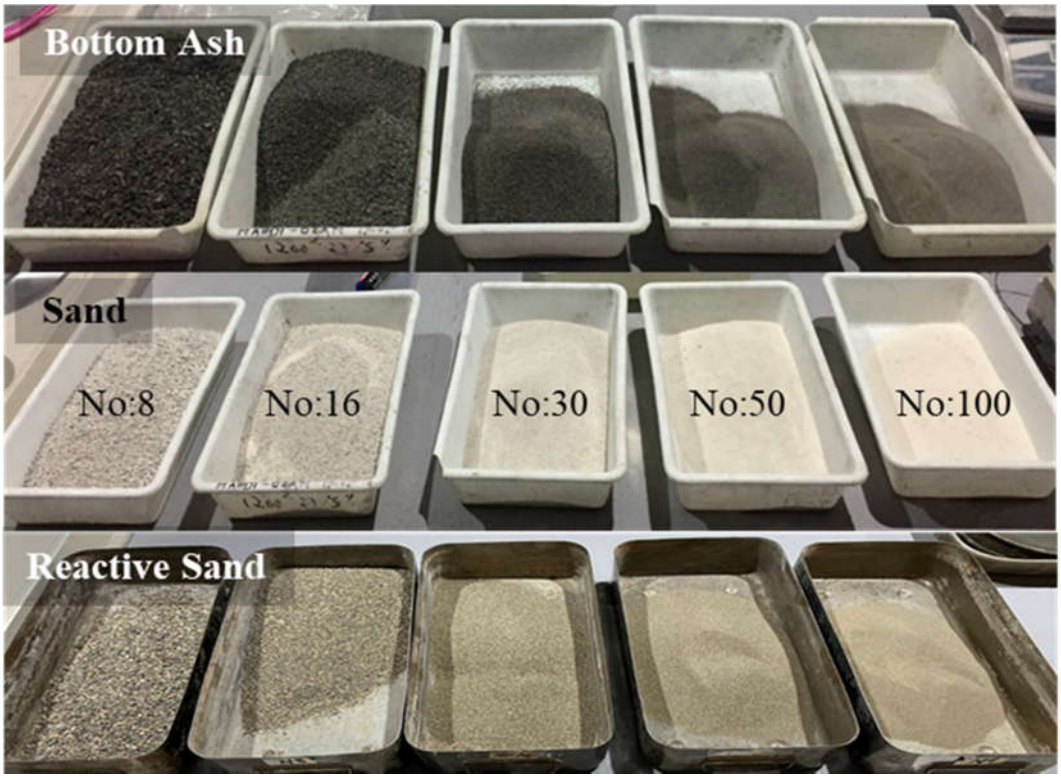

Figure 3.13. PSD Separations of FA as BAs, Sand, and Reactive Sand.

3.5.2.2 The Preparation Procedure for Usage as a Supplementary Cementitious Materials (SCM)

The most critical parameters for utilizing the DHBA and WHBA as an SCM were the grindability of the samples. The finesse and the amorphous structure of the bottom ashes were the most important properties for the usage as pozzolanic materials. As mention before, the XRD results gave an idea about the crystalline structure of the bottom ashes. The non-ground bottom ashes could not be used as an SCM; therefore, the grinding must be handled to obtain a specific surface. The grinding process was conducted until it reached the reference fineness of Portland cement, the specific surface area as 3300 cm^2/g.

3.5.2.2.1 Grinding Process of the Bottom Ashes

The grinding process used a laboratory-type ball mill of 450 mm in length and 400 mm in diameter with 30 revolutions per minute rotational speed. The metal balls were significant for this process since, if there were many balls rather than need, the materials could not move properly, and vice versa, if there were a few balls in the machine, the materials could not be a grind. The selected metal balls and types are shown in Figure 3.14 and given in Table 3.9.

Figure 3.14. Spherical and Cylpebs Ball Mill

Table 3.9 Sizes of the Grinding Machine Balls

Spherical Balls (Diameter)	**Dimensions (mm)**	**# of Pcs**
1	55	17
2	50	50
3	45	21
4	40	165
Cylpebs (Diameter x length)	**Dimensions (mm)**	**# of Pcs**
1	20 x 20	163
2	15 x 15	89
3	10 x10	85

Periodical samples were taken during grinding as 15, 30, 60, 120, 180, 210, and 240 minutes for the bottom ashes. The 5000 g of each bottom ashes poured into the machine, and at the end of each time interval, specimens were collected from the device and packaged as 100-200 g for the density and the specific surface area test. The ground samples are presented in Figure 3.15.

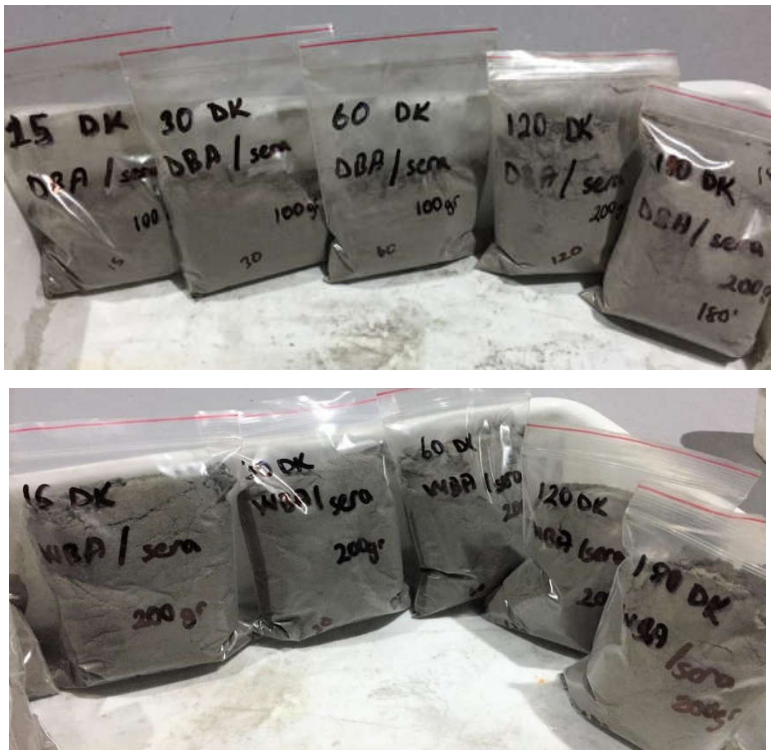

Figure 3.15. BAs Samples of Each Grinding Process Intervals

3.5.2.2.2 The Density of the Ground Bottom Ashes

The densities of each grinding level sample were calculated according to ASTM C188 [61] . The pieces were very fine particles; because of that, the Le Chatelier test was chosen. The procedure of the Le Chatelier test was performed very sensitively because the glasses were very thin, and the tube was thin to the movement of the particles in the flask. The five samples (15, 30, 60, 120, and 180 minutes ground samples) for DCBA and the seven samples (15, 30, 60, 120, 180, 210, and 240 minutes grinding samples) for WHBA were tested.

The procedure of the test was applied as stated at the ASTM C188 [61]. Firstly, the Le Chatelier Flask was filled with the kerosene to the 0 -mL mark at 23^{o}C. Then, the flask with kerosene was weighted. Thus, the first reading was recorded at 23^{o}C temperature. Secondly, the bottom ashes were introduced into the flask. The amount of the DHBA was about 50 grams, and the WHBA was 45 grams. While presenting the ashes, the tapping and the rolling of the tube were performed very gently, avoiding the loss of the raw materials and the kerosene and avoiding ashes sticking to the neck of the flask. Then, the stopper was placed at the top of the flask and whirled horizontally to free entrapped air escape from the liquid. Finally, the flasks were placed at the constant moisture room at 23^{o}C, and the final reading was performed 24-hours after. In this way, the temperature differences of the first and last readings were prevented. The densities were calculated at the end of each time interval, and the results are presented in Table 3.10. It can be seen from the tables when the grinding process was continued, the bottom ashes densities were increased. The grinding of the bottom ashes has enhanced the microstructure and decreased the porosity of the bottom ashes. The better microstructure was to improve the bottom ashes pozzolanic properties. The same results were found by Cheriaf et al. [62].

Table 3.10 Densities of the Dry-handled Bottom Ashes

Grinding Time [Min.]	**Sample**	**ρ [g/cm^3]**	**Sample**	**ρ [g/cm^3]**
15	G-DH15	2.56	G-WH15	2.22
30	G-DH30	2.60	G-WH30	2.31
60	G-DH60	2.63	G-WH60	2.42
120	G-DH120	2.69	G-WH120	2.51
180	G-DH180	2.76	G-WH180	2.53
210	-	-	G-WH210	2.60
240	-	-	G-WH240	2.65

3.5.2.2.3 Specific Surface Area of the Ground Bottom Ashes

The specific surface area was found according to ASTM C204 [63] with Blaine air-permeability apparatus. According to this test, the samples' relative fineness is found, and it must be considered. The relative fineness is found to reference material. Therefore, the calibration must be done before conducting the Blaine test, and the results could be changed for reference materials. The technician calibrated the laboratory Blaine test machine, and also the movement of the test liquid and the balance between air were checked. The calibration parameters and the equations were indicated on the test apparatus in the laboratory as stated in the ASTM C204 [63].

Firstly, the mass of ashes was calculated for twelve specimens according to the standard using densities founded before. The masses were placed between filter papers and the perforated disk and pressed with the plunger. The calculated masses of the samples are presented in Table 3.11.

Table 3.11 The Used Masses of the PC and BAs in Blaine Test.

	Masses [g]		
Sample	**DHBA**	**WHBA**	**PC**
	-	-	2.88
Grinding Time [min]			
15	2.34	2.03	-
30	2.38	2.11	-
60	2.41	2.21	-
120	2.46	2.30	-
180	2.53	2.31	-
210	-	2.38	-
240	-	2.42	-

The liquid into the tube and the air valve were arranged according to standard. The liquid was moved to the indicated point in the apparatus without any bubbles in it. After all these arrangements, the air was allowed into the tube, and the passing time of the movement of the liquid was measured. Finally, the specific surface area was calculated according to these passing times.

According to indicated equations the each SSA was calculated as shown in Table 3.12. The time duration, density, temperature, porosity, and viscosity values were input variables of the equations (indicated as blue in Table 3.12). The output variables were sample weight and the specific surface of the samples (shown as red in Table 3.12). The WHBA sample, which was ground for 15 min. was given as an example. The other Blaine test results were presented in the Appendix-B section.

Table 3.12 Calculation Sample of the SSA of G-WH15

Reference Material			**Example (G-WH15)**	
Time duration (s)	74		Time duration (s)	**2.34**
Density (g/cm^3)	3.150		Density (g/cm^3)	**2.217**
Temperature (^{o}C)	25		Temperature (^{o}C)	**25**
Porosity	0.486		Porosity	**0.50**
b	0.90		b	**0.90**
Specific surface (cm^2/g)	3420		Specific surface (cm^2/g)	**932.37**
Viscosity (µPa.s)	18.32		Viscosity (µPa.s)	**18.32**
W (g) =	**2.03**			

The Blaine test was conducted for the used cement, and its surface area value was used as a reference point of the bottom ashes. The graph of the specific surface area versus grinding time was drawn, and the 3300 g/cm^{2,} which was the reference cement surface area, was chosen to determine the bottom ashes grinding time. The graph is seen in Figure 3.16. The DHBA has reached the desired specific surface area in 180 minutes of grinding, and the WHBA was achieved in 240 minutes at the same specific surface area (SSA). The different grindability times are probably because of the amorphous structure of the ashes.

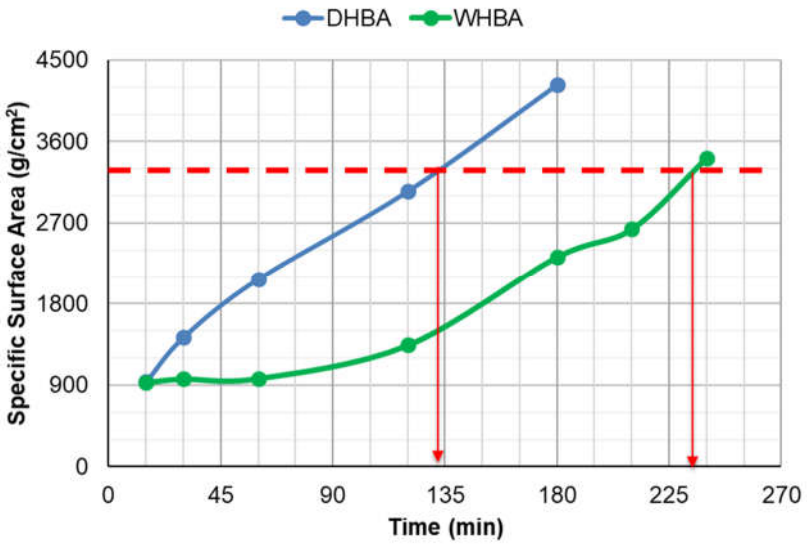

Figure 3.16. SSA vs. Grinding Time Graph of the both DHBA & WHBA

At the end of each grinding time interval, densities of the bottom ashes were calculated. The chosen densities of the bottom ashes were determined according to the same specific area of the cement. The densities that coincided with the 3300 gr/cm^2 specific surface area were founded as 2.72 g/cm^3 for DHBA and 2.64 g/cm^3 for WHBA.

3.6 Pre-Soaking of Bottom Ash

The impact of pre-soaking was investigated on WH: A50-P50 to enhance the mechanical performance of the mixes that utilize BA ash FA. This proportion was selected because it had the highest W/B at 0.65. The mixing procedure was performed on in following steps:

- WHBA was to be used as fine aggregate and half of the mixed water was poured into a container, and the container lid was closed
- WHBA was soaked 24 hours
- After 24 hours, the pre-soaked WHBA and the remaining mix water was used in the mix as usual

With the pre-soaked WHBA, desired flow for the mortar mix was not achieved. Therefore, extra water was added to the mix to reach the desired flow, increasing the overall W/B ratio. Obtained compressive strengths are shown in Figure 3.17 and Table 3.13. Even the results were not satisfied with applying the pre-soak treatment of the bottom ashes the oven-dry condition of the aggregates were used in the experiments.

Table 3.13 PS-WH: A50-P50 Mixture' Strength, Flow, and w/b Results

Mix	WHBA Condition	28-day Compressive Strength	Flow	W/B
WH: A50-P50	Oven-dry	20.04	105	0.65
PS-WH: A50-P50	Pre-soaked	11.54	105	0.71

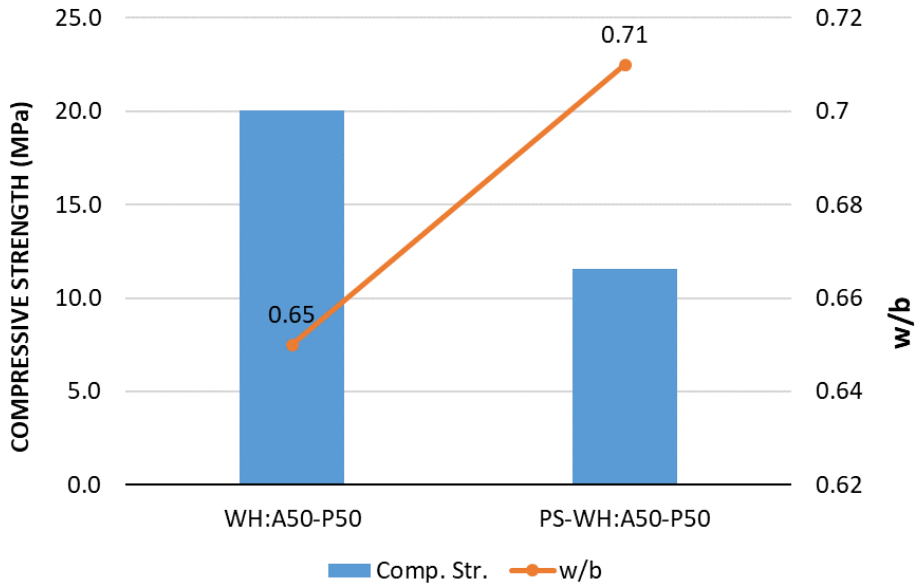

Figure 3.17 Comparison of the WH: A50-P50 Mixture and Pre-Soaking

3.6.1.1 Preparations of the Materials for Casting

The preparations of the materials according to usage purposes were handled as mentioned above. The next step was preparing the DHBA and WBCA for the casting into the molds for the ASR test and compressive-flexural strength tests. The following statements were indicated the preparation steps;

1) Fine aggregate and sieved bottom ashes were oven-dried
2) Additional water to bring aggregates to the SSD condition was calculated.
3) The Portland cement was sieved from the No: 200 sieves before casting to eliminate lumps.

3.6.2 Testing of Specimens on Paste

3.6.2.1 Isothermal Calorimetry

The process of the hydration of ordinary Portland cement is commonly subdivided into several periods (Figure 3.18). These periods are called: (I) the initial stage: immediately within the first few minutes of mixing cement with water, the aluminate reacts with water and sulphate, forming a gel-like material (ettringite) surrounding the cement grains. This reaction releases a significant amount of heat and is represented by the first peak of the hydration process; (II) the dormancy stage: there is a dormant stage for about two to four hours after mixing in which the aluminate reaction is controlled by the amount of ettringite gel surrounding the cement grains due to limiting the access of water to the cement grains, which controls the rate of the aluminate reaction, and thus little heat is released; (III) the acceleration stage: after super-saturation of the pore solution with calcium ions mainly from dissolving main cement minerals which are alite (impure tricalcium silicate (C_3S)) and belite (impure dicalcium silicate (C_2S)), fibre-like calcium silicate hydrate (C-S-H) gel and crystalline calcium hydroxide (CH) start to form with significant heat evolution. The acceleration stage is represented by the second peak of hydration; (IV) the deceleration stage: interaction of C-S-H gel and crystalline C-H with remaining water and undissolved cement grains slows down the alite (impure C_3S) reaction, thus reducing the heat of hydration. The amount of sulphate starts to deplete, and accordingly, the remaining aluminate reacts with ettringite to form monosulphate. The formation of monosulphate generates little heat, which may be associated with the third hydration peak; (V) the slow continued reaction stage: belite (impure C_2S) dissolves and releases calcium ions very slowly and starts to produce C-S-H and CH after several days. However, as long as alite and belite remain in the cement system and there is enough water available in the system, the silicates will continue to hydrate [64].

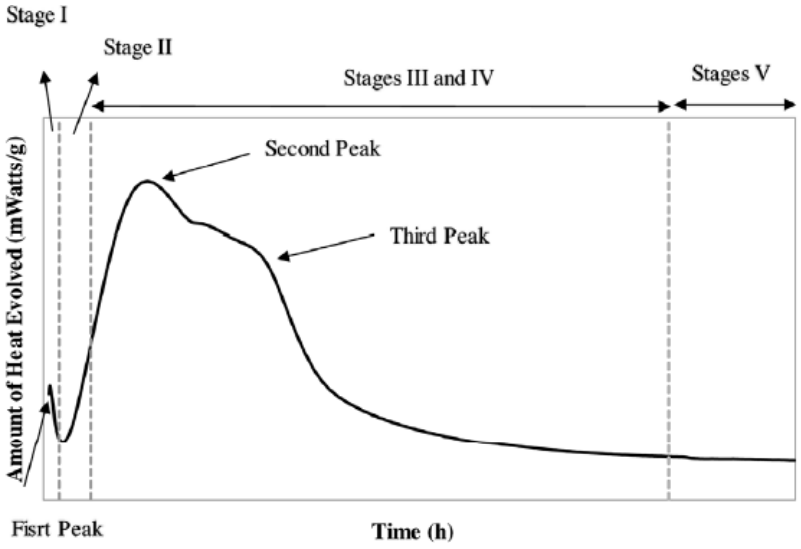

Figure 3.18 Common Cement Heat Evolution Curve [65]

The pastes were tested to measure the heat releases of the hydration process of the binder elements. The binder element (cement + DHBA or WHBA) and the water were only used for the paste. The specimens were prepared according to ASTM C1702 [56]. The cement, bottom ashes, and water were calculated concerning reference sand mass and temperature.

The masses of the samples were calculated according to the preservation of the heat energy, whose formula is Q= m c dt. The specific heat capacities were indicated in the standard and presented in Table 3.14.

Table 3.14 Specific Heat Capacities [56]

Specific Heat Capacity, [J/g. K]	
Reference Sand	0.75
PC	0.75
DHBA	0.80
WHBA	0.80
Water	4.18

The five specimens were prepared and put into the ampules. One of them was designed as a control. The rest of them were 25% and 50% replacement of the cement

with DHBA and WHBA. Since the mass of the sample was relatively small, mixing was performed manually by stirring the cement, bottom ashes, and water with a metal stick. The ampules were put into the calorimetry machine, and the heat evaluations were measured for five days. The test machine gave the results, and these results were reported for comparisons.

3.6.3 Testing of Specimens on Mortar

The flow table, compression-flexural strength, alkali-silica reactions have been conducted on the prepared specimen as mentioned above. The procedures of the experiments are explained in the following sections.

3.6.3.1 Flow Table

According to ASTM C1437 [57], the fresh mortars were tested to find the mortars' flow level. The flow values were determined before casting the mortars. The flow table apparatus and flow mold apparatus conform to the requirements of ASTM C230 [66]. The flow mold was located at the center of the clean and wiped flow table. The mortar was layered into the mold approximately 25 mm in thickness and tamped 20 times afterward; the rest was then filled with the mortar and tamped 20 times more. Thus, the mortar was placed uniformly into the mold. The top of the mold was plane and cleaned the surface of the flow table, especially water was eliminated if there were existing on the flow table.

The mold was lifted and dropped on the table 25 times in 15 seconds immediately. These processes were done quickly to prevent gaining a set of mortar. The DHBA and WHBA have a very high-water absorption capacity than cement and other used fine aggregates. Therefore, the water demand was very high, and mixing water must be added to provide the desired flow. The w/b ratios were changed, but the flow values were maintained in the limits. The limit diameter of the mortars measured between 20.5-21 cm for the proper casting.

3.6.3.2 Compression and Flexural Strength

The mixes were prepared with the partial replacement as fine aggregate and SCM with the 25% and 50%. The packages were prepared for the binder element and fine aggregates for easy mixing procedures. The mix design and mixing of the mortars were done according to TS EN 196 [60].

A medium planetary mixer was used for 4 minutes following procedure: (1) add water and cement or cement + binder in a bowl; (2) mix them for 30 seconds at low speed; (3) add fine aggregates that were sand or sand + bottom ashes at along 30 seconds ; (4) mix them for 30 seconds at high speed; (5) stop the mixer for 75 seconds but at the first 15 seconds scrape to the bowl; (6) mix for 60 s at high speed. The prism molds 40x40x160 were oiled before casting mortars; thus, the de-molding process was done without damaging the specimens. The mortars were cast into the prism's molds immediately. The mortars were poured with two layers. The first layer was placed and compacted 60 times, and the same procedures were conducted for the second layer; thus, the specimen was distributed into the mold uniformly. After casting, the mortar finishing was performed at the top surface of the mold, and the stretch film has wrapped the mold to prevent the water escape from the mortars. The one standard 3-gang mold with mortars is presented in Figure 3.19.

Figure 3.19 Standard Three-Gang Molds

The mortars were cured into the mold during 24 hours in the laboratory at 24ºC and the constant humidity. The casting procedure was repeated three times for the testing each curing period, such as the 7^{th}, 28^{th}, and 90^{th} days. After demolding, each specimen was placed into the water tanks at the curing room at 24ºC and the constant humidity. The water addition into the tanks was done; therefore, sufficient water could be provided during curing.

The specimens were tested according to ASTM C348 [59] and ASTM C349 [58]. As stated in the standard, the flexural strength test was done firstly, and then the compressive strength test was handled using portions of prisms broken in flexure. For each specimen, results were reported separately according to mix designs and curing periods.

3.6.3.3 Alkali-Silica Reactions

The mortars were prepared with the river sand with 25% and 50% of the same replacement ratios. Mainly, for the ASR test, the particle size distribution of the fine aggregates was used the same as indicated in the standard ASTM C 1260 [51]; thus, one of the possible effects of the expansion parameters was prevented. The proportioning of the mortar was prepared as 440-gram cement + binder and 990-gram reactive sand + bottom ashes and water, which was provided the 0.47 by mass w/c ratio. According to TS EN 196 [60], the mixing of the mortars was done similarly to the compressive-flexural test. According to ASTM C490/C490M [67], the apparatus of the alkali-silica reactions was selected, which were molds and measurement of length changes.

In the next step, the mortars were cast into the molds. Because of the slender specimens, the molds were prepared before the casting, such as replacing the thin acetate paper in the mold. The mold had 25 x 25 x 285mm dimensions, and also pins were added at the ends of specimen bars. The molding procedure was conducted for each mix design. The equal two-layer were performed while casting, and each layer

was compacted. For each mix design, three mortar bar samples were cast. The molds were wrapped with plastic film to prevent water loss. During the 24-hours, the specimen was cured in the laboratory at 24°C and constant humidity.

Although precaution was taken, some of the specimens were broken while demolding. The samples were put into the water tanks again at the curing room at 24°C, and the constant humidity during 24 hours and the initial measurement was done. Afterward, the water tanks were placed into the oven, which is 80°C, and one day later, the zero readings were measured. Finally, specimens were put into the NaOH solution, which was at 80°C (Figure 3.20). The NaOH solution was prepared as stated in the standard ASTM C 1260 [51].

Figure 3.20 Oven Curing at 80°C with NaOH Solution of The Specimens

The displacement of the bars was measured at the 3, 6, 9, 12, 15, 30, and 45 days passed. The displacement values were calculated from the pins with a length comparator. The results were reported for each day and each different mix specimen.

CHAPTER 4

RESULT AND DISCUSSION

This chapter presents and discusses the experimental results on the dry-handled and wet-handled bottom ashes as fine aggregate and supplementary cementitious material in cement-based composite systems.

4.1 Isothermal Calorimetry

The data measured was the rate of heat, which after being normalized by the solid weight and calibrated, was expressed in J/h/g. The value was then reported as the cumulative heat, which was the integral of the rate with time.

Table 4.1 The Masses for the Heat Evaluation Test

Masses (g)	Cement	G-DH	G-WH	Water	Solid	w/b
Control	6.26	-	-	3.13	6.26	0.5
G-DH25	4.65	1.55	-	3.10	6.20	0.5
G-WH25	4.65	-	1.55	3.10	6.20	0.5
G-DH50	3.10	3.10	-	3.10	6.20	0.5
G-WH50	3.10	-	3.10	3.10	6.20	0.5

The specific heat capacities were indicated in the standard, and the reference sand mass was calculated as 23.7 grams at the reference temperature of 23ºC. The conservation of the heat energy principle was taken as a basis. The calculated masses which were used for the pastes are given in Table 4.1. The water-cement ratio of the pastes was chosen as 0.5 as indicated in the standard (the sufficient value of w/c > 0.4). The rate of heat flow (Watts) was normalized by the solid's weight, which included cement and ground bottom ashes, and the unit turned to J/s/ gram of solid

and cement. The normalized cumulative heat was also found, and its unit was taken as joules as required.

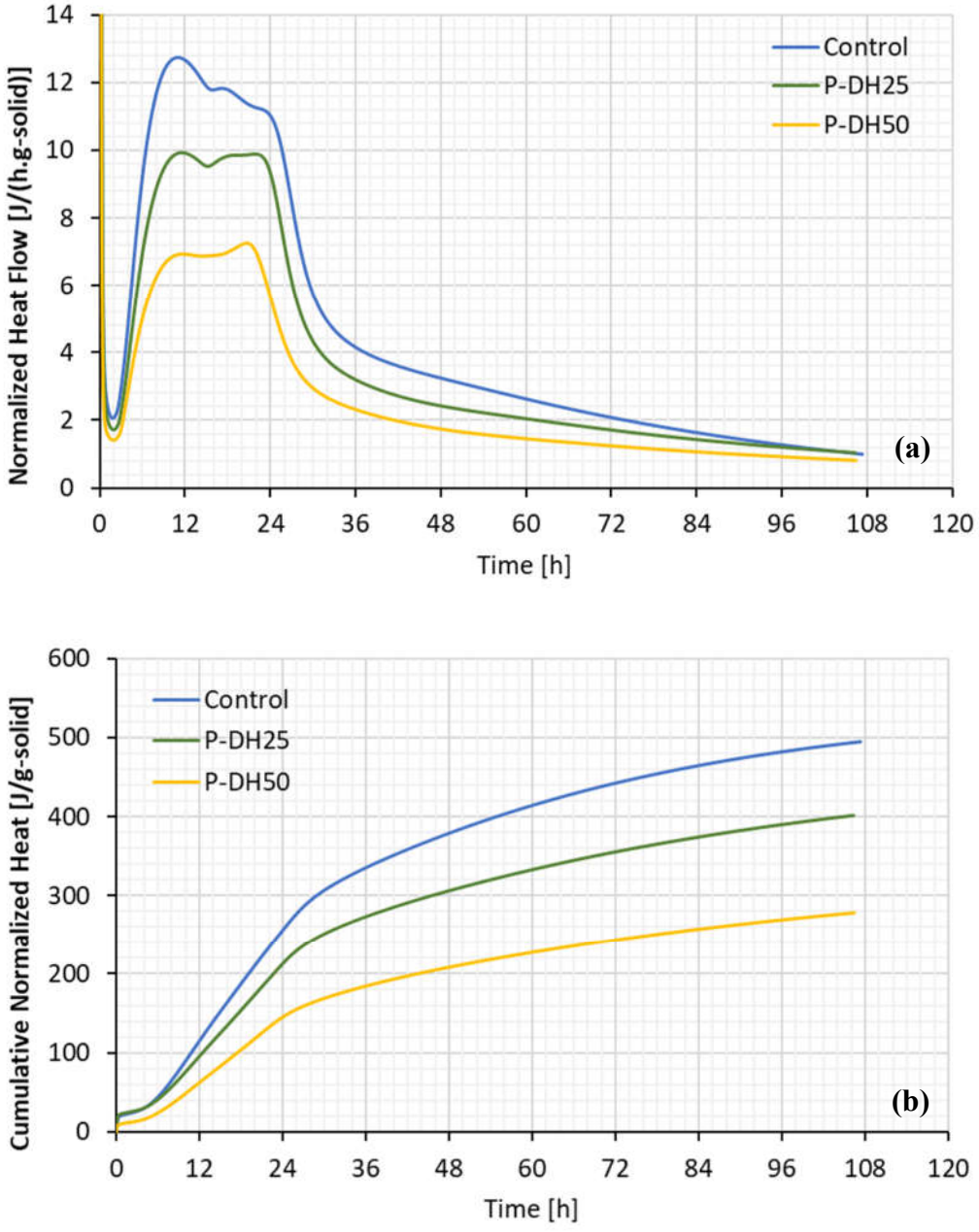

Figure 4.1 Hydration Heat of Control and P-DH25 & P-DH50 Pastes (a) Hydration Heat Evolution Rate, (b) Cumulative Hydration Heat / Solid

The hydration heat and the rate of heat evolution of cement only and the bottom ash powders with cement are illustrated in Figure 4.1 and Figure 4.2. The hydration

normalized heat flow was decreased by about 25% (average 13.05 J/s/g-solid) and 47% by incorporating dry-handled bottom ash with 25% (9.93 J/s/g-solid) and 50% (6.91 J/s/g-solid) by volume, respectively. Moreover, the hydration normalized heat flow was decreased by about 22% (average 12.98 J/s/g-solid) and 48% by incorporating dry-handled bottom ash with 25% (10.16 J/s/g-solid) and 50% (6.80 J/s/g-solid) by volume, respectively.

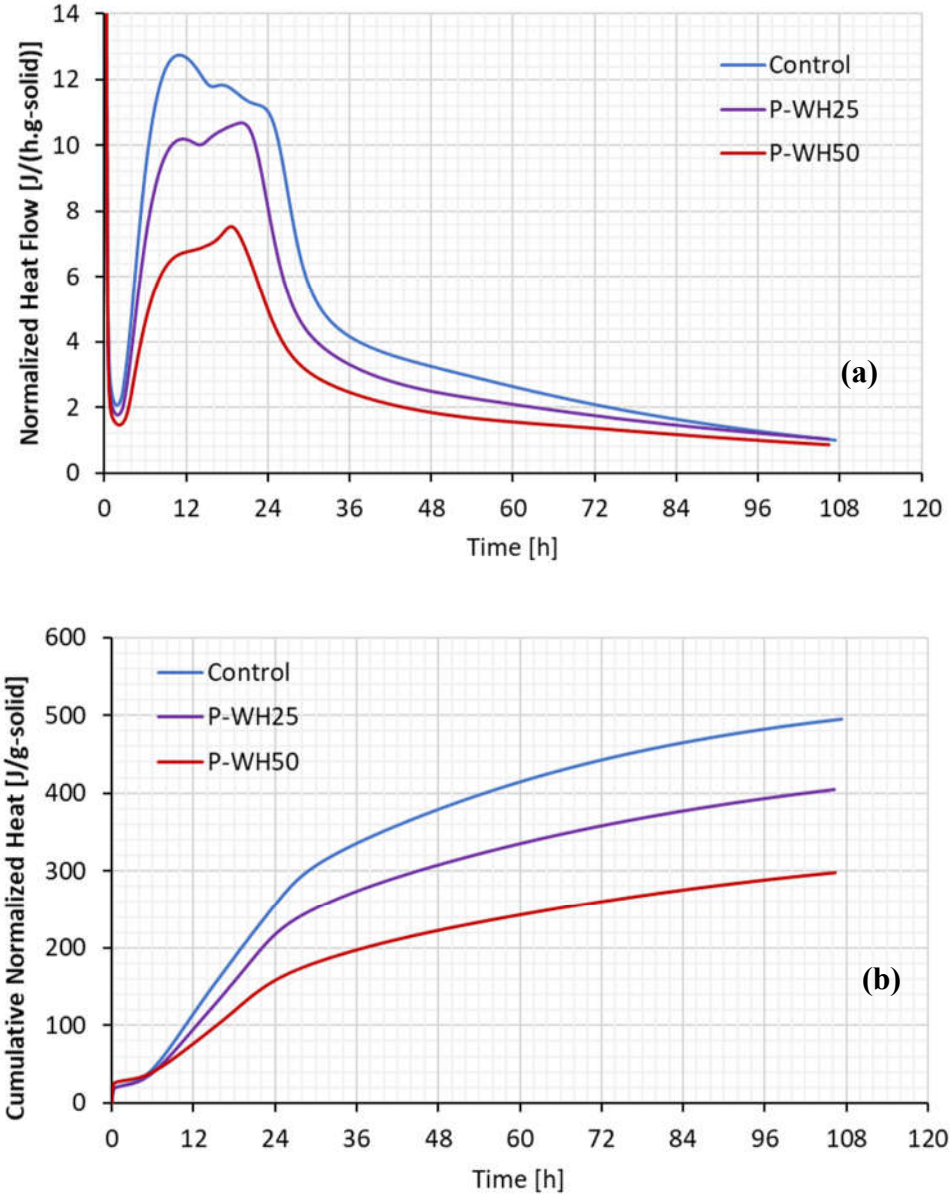

Figure 4.2 Hydration Heat of Control and P-WH25 & P-WH50 Pastes (a) Hydration Heat Evolution Rate, (b) Cumulative Hydration Heat / Solid

The second peak time of heat evolution rate was not affected by containing bottom ashes. On the other hand, bottom ashes powders' hydration heat and heat flow were influenced by the type of pozzolanic binder materials adopted, and the third peak occurred. Figure 4.1 and Figure 4.3 were showed that the third peak of the DHBA and WHBA was found greater than the second peak due to the pozzolanic reactions.

The cumulative heat of hydration for cement and bottom ash pastes over the testing period of 108 h. As expected, the cumulative heat of hydration generated for the bottom pastes was lower than that for cement paste. Increasing the bottom ash content in the pastes was caused to reducing the amount of heat evolved. The normalized heat (g-solid) of the specimen was presented in Table 4.2. As can be seen from the table, after 6 hours, the heat flow was generated and increased exponentially. At 25% of the cement with DHBA and WHBA pastes were reached the average 80% cumulative heat of the control pastes at each time interval (except the 6^{th} hour). Due to the replacement high replacement rate, the lower cumulative heat flow was reported to P-DH50, and P-WH50 pastes were reached of the control mixes cumulative heat flow's 53% and 60% on average, respectively. The reactivity of the dry-handled bottom ashes was found lower than wet-handled bottom ashes.

Table 4.2 Cumulative Normalized Heat [J/g-solid]

	Control	**P-DH25**	**P-DH50**	**P-WH25**	**P-WH50**
6 h	44.1	40.8	23.8	39.0	39.9
12 h	115.4	95.5	62.2	95.2	76.5
24 h	256.3	212.8	145	217.4	157.9
36 h	335.6	273.3	184.5	273.7	197.2
48 h	379.2	306.3	208.6	307.7	222.5
60 h	414.4	333.0	227.3	335.0	242.7
72 h	442.6	355.5	243.5	357.9	260.2
84 h	464.8	374.3	257.3	377.1	275.3
96 h	482.2	390.1	269.3	393.1	288.3

The heat of hydration per cement of the mixtures was also investigated. Normalization of the pastes according to cement paste directly showed the bottom's reactivity on pastes' hydration process. Normalized heat flow and cumulative normalized heat per cement of the mixtures were presented in Figure 4.2 and Figure 4.4. As can be seen from figures, the wet-handled bottom ashes' contribution to hydration was greater than dry-handled ashes, at 50 wt. % replacement of the bottom ashes affected the cumulative heat greater than 25wt. % as expected. The normalized (g-cement) heat of the specimens was presented in Table 4.3.

Table 4.3 Cumulative Normalized Heat [J/g-cement]

	Control	**P-DH25**	**P-DH50**	**P-WH25**	**P-WH50**
6 h	44.1	54.4	47.7	52.0	79.5
12 h	115.4	127.8	124.8	126.1	153.7
24 h	256.3	283.2	290.3	289.5	315.6
36 h	335.6	364.4	368.6	364.9	394.5
48 h	379.2	408.6	416.5	410.3	445.1
60 h	414.4	444.7	454.9	446.7	485.5
72 h	442.6	474.9	487.5	477.3	520.4
84 h	464.8	499.2	514.1	502.8	550.7
96 h	482.2	520.3	538.0	524.1	576.6

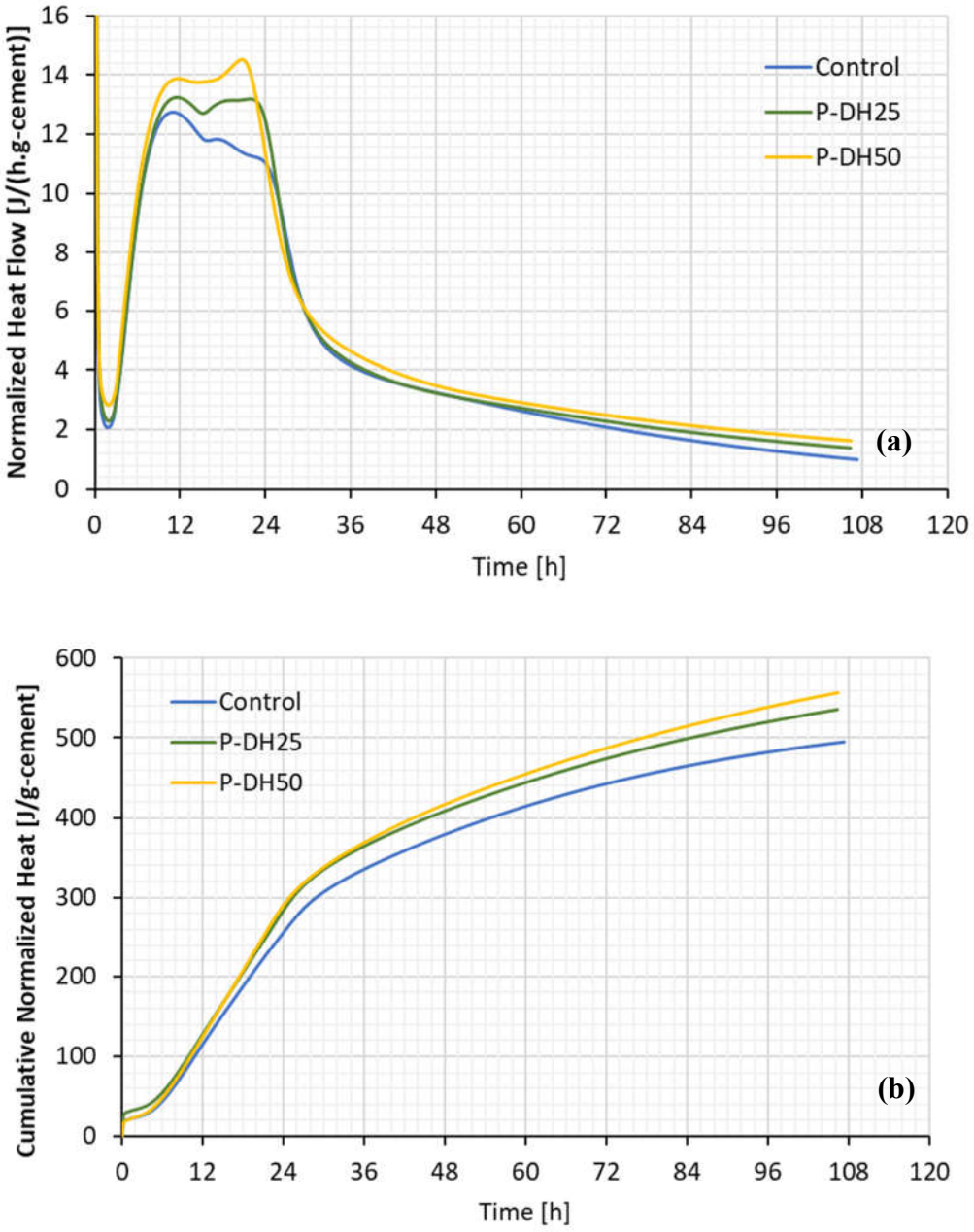

Figure 4.3 Hydration Heat of Control and P-DH25 & P-DH50 Pastes (a) Hydration Heat Evolution Rate, (b) Cumulative Hydration Heat / Cement

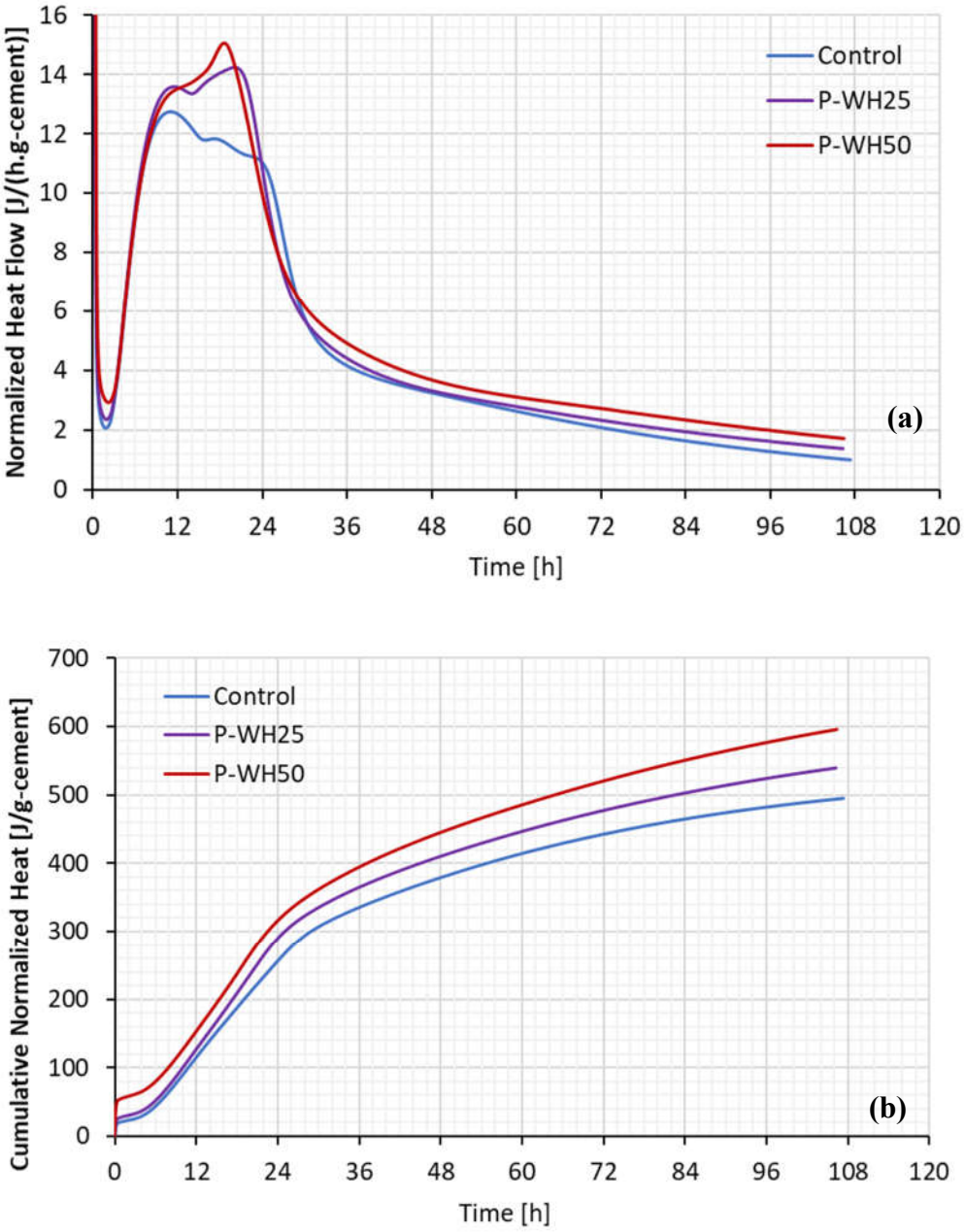

Figure 4.4 Hydration Heat of Control and P-WH25 & P-WH50 Pastes (a) Hydration Heat Evolution Rate, (b) Cumulative Hydration Heat / Cement

4.2 Consistency of the Fresh Mortars

The workability of fresh mortar includes multiple issues: diverse compatibility, stability, and mobility requirements. Using industrial by-products in mortars total or partial substitute of sand and cement paste by bottom ashes could affect the fresh concrete properties of the mix. Previous studies showed that the mortars' flow was lowered when the replacement level of the bottom ashes was higher. Besides that, the decrement of the flowability depends on different parameters like type of raw materials, water to cement ratios, and superplasticizer usage.

Consistency is one of the dominant parameters for the workability properties of the mortars and concretes. The too much wetness or dryness conditions of the mortars or concretes are caused severe problems. Therefore, the fluidity of the mortars must be optimized to get desired mechanical properties and durability of the mixes. The flow condition of the mixtures could be classified with its flow percentage as given in Table 4.4.

Table 4.4 The Consistency Stages Groups of the Mixes

Flow (%)	**0-20 %**	**20-60 %**	**60-100 %**	**100-120 %**	**120-150 %**
Consistency	Dry	Stiff	Plastic	Wet	Sloppy

In this study, the consistency of the fresh mortars was calculated with the flow table test. When identical water-cement ratios were used, the concretes containing bottom ash were fairly stiff (dry) and displayed far less workability than the control mixes. Therefore, the control and bottom ash mortars were prepared in between a flow of 100 and 110. The flow values were kept constant.

Table 4.5 The Flow Test Results of the Mortars

	Mechanical Tests		Durability Tests	
	W/B	Average Flow (mm)	W/B	Average Flow (mm)
Control	0.43	105.7	0.34	106.0
Part1: Partial replacement of fine aggregate with CBA				
DH: A25	0.49	104.0	0.43	105.3
DH: A50	0.55	102.4	0.46	104.3
WH: A25	0.55	106.4	0.46	105.7
WH: A50	0.63	105.4	0.51	105.0
Part2: Usage of CBA as an SCM				
DH: P25	0.51	108.7	0.43	106.0
DH: P50	0.50	104.4	0.47	104.0
WH: P25	0.49	106.7	0.43	105.7
WH: P50	0.62	104.9	0.47	105.3
Part 3: Combined usage				
DH: A25-P25	0.49	103.4	0.40	107.3
DH: A50-P25	0.47	101.4	0.41	104.7
DH: A25-P50	0.50	107.4	0.44	109.7
DH: A50-P50	0.54	107.4	0.48	107.3
WH: A25-P25	0.47	106.7	0.40	105.3
WH: A50-P25	0.56	101.0	0.41	107.7
WH: A25-P50	0.49	107.0	0.50	109.0
WH: A50-P50	0.65	104.7	0.56	109.3

A flow test is a measure indicating the consistency or workability of mortar. The effect of coal bottom ashes as cement replacement and replacement of sand in mortar mixtures on flow values for strength and ASR test are tabulated in Table 4.5. Flow values are given in between Figure 4.5 to Figure 4.12 with water to binder ratios for each mix. Flow values of control mixes for both mortars were 106 mm. The flow values were found between 106.4 - 102 mm, 104 - 108.7 mm, and 101-109.3 mm for Part 1, 2, and 3 mixes.

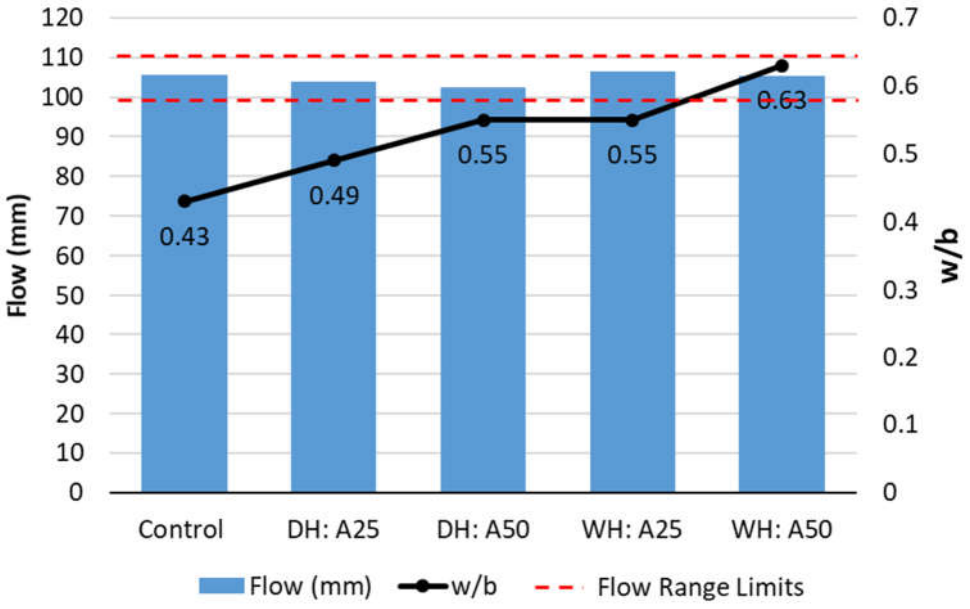

Figure 4.5 Flow and w/b for the Mechanical Test Mortars of Usage as FA

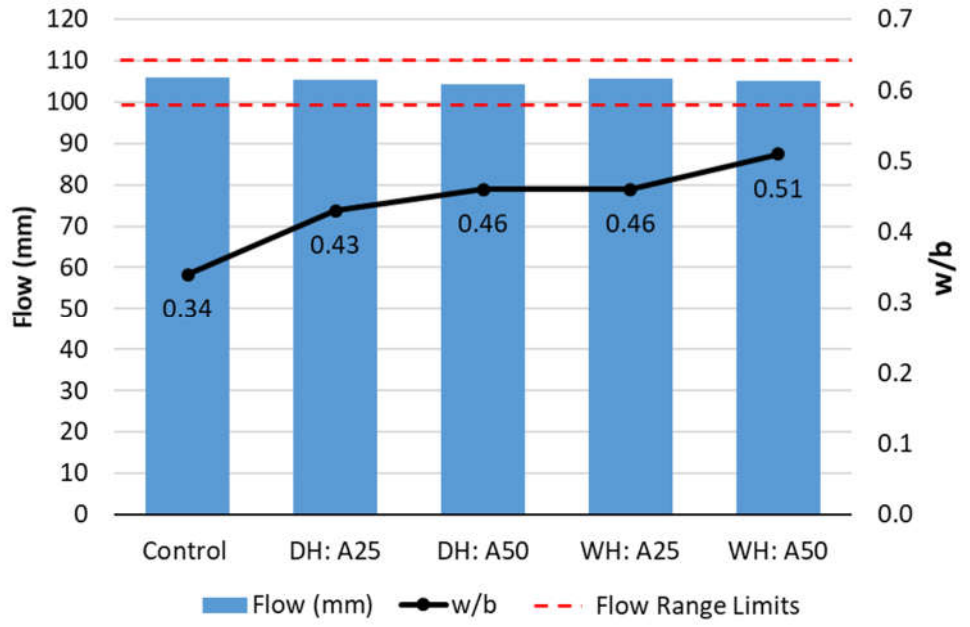

Figure 4.6 Flow and w/b for the Durability Test Mortars of Usage as FA

Highly cohesive and sticky mixes were obtained at 50% replacement for fine aggregates and binder materials with low workability. This is consistent with the literature, such as mixes with 50% and 100% bottom ash replacement required approximately 25-50% more mixing water content than standard concrete to obtain suitable workability [45].

The particle size distribution of the fine aggregates (including the bottom ashes, sand, and river sand) was kept the same; thus, the different fineness particle's water requirements would be prevented. The possible reasons for the increasing quantity of the mixing water are listed below. These results could be drawn for the first part experiments (partial replacement of fine aggregate with CBA), but they were also affected by the Part 2 and 3 experiments.

- The higher porous structure of bottom ashes compared to the sand. This led to the water absorption of coal bottom ash was higher than that of river sand. As a result, more water was required to cover the surface of bottom ash particles and increase lubrication of particles it means flowability.
- Bottom ash particles had irregular shapes and rough textures. Therefore, the interlocking and friction in between particles were increased. This means that the flow of fresh concrete was retarded.
- As shown in Figure 4.5 and Figure 4.6, additional water was used, and the water-binder ratio differences were found greater than control mixes.

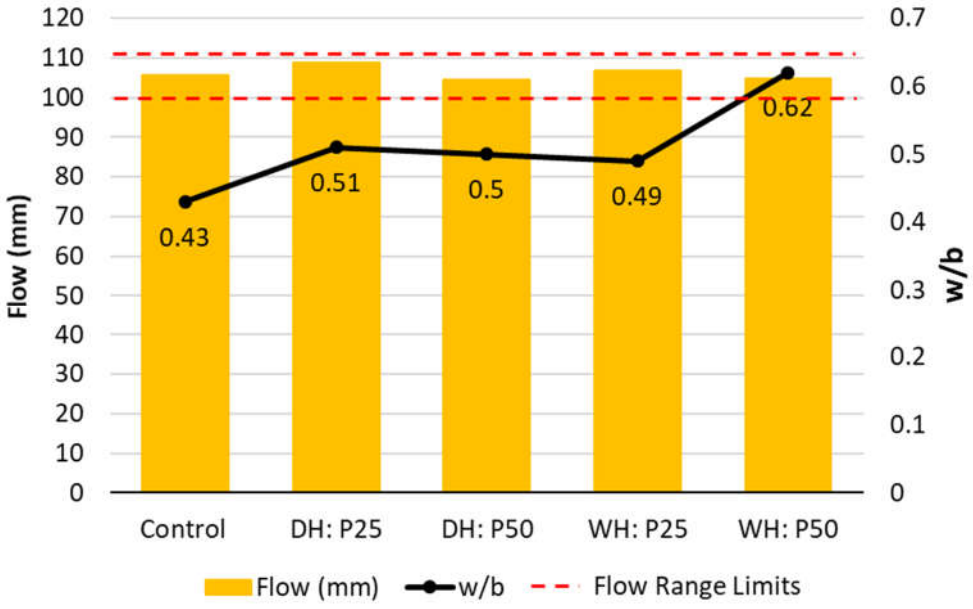

Figure 4.7 Flow and w/b of the Mechanical Test Mortars of Usage as SCM

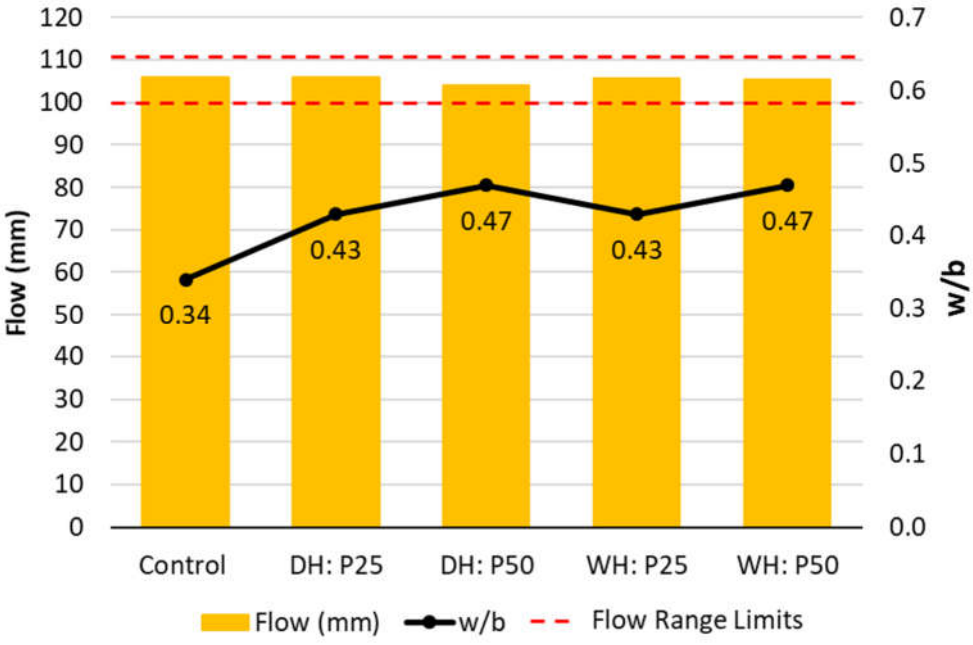

Figure 4.8 Flow and w/b for the Durability Test Mortars of Usage as SCM

Generally, the fine pozzolanic material increases the workability of the cement mortar. As shown in Figure 4.7 and Figure 4.8, the least additional water was used in this second part experiments, and the water-binder ratio differences were found smaller than the first parts. The reason could be attributed to the second part experiments results (usage of CBA as a pozzolanic material) as follows; the water in the mortar system in a fresh state was present in two ways: filling water and surface layer water. The fluidity of paste depends on the thickness of the water film. The amount of the filling water is related to the packing density of the system. Suppose the specific surface of pozzolanic material is extensive, although the filling water can be reduced. In that case, the total amount of water increases due to the significant demand for water in the surface layer [68].

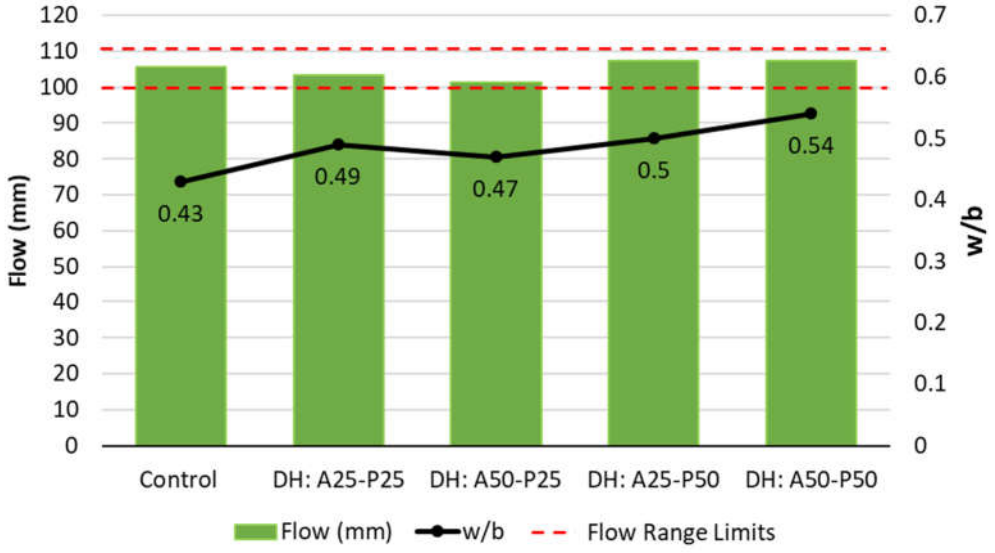

Figure 4.9 Flow and w/b for the Mechanical Test Mortars (DHBA) of Combined Usage

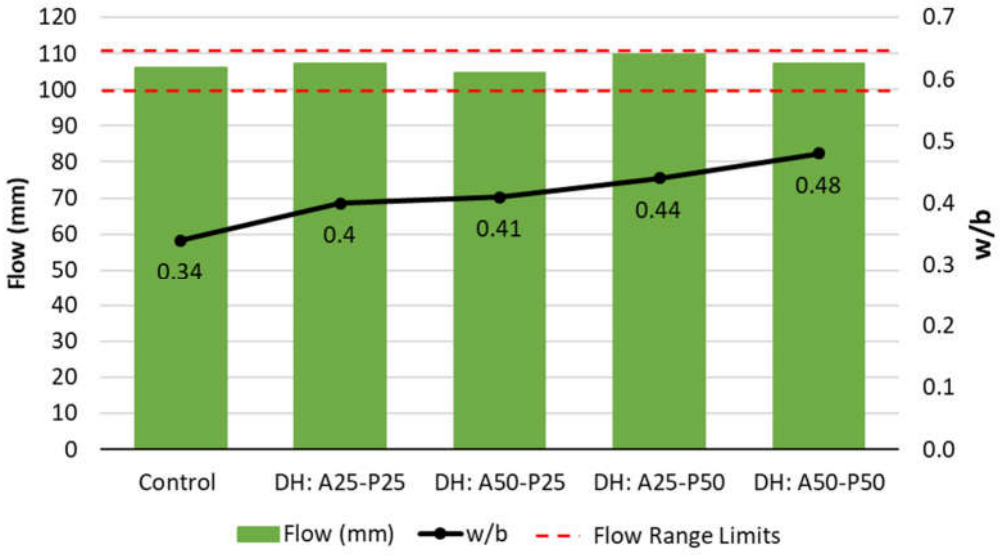

Figure 4.10 Flow and w/b of the Durability Test Mortars (DHBA) of Combined Usage

Both fine aggregate and binder materials usage of the bottom ashes was investigated, and the results were found in the third part of the experiments. The results showed that the workability was most affected.

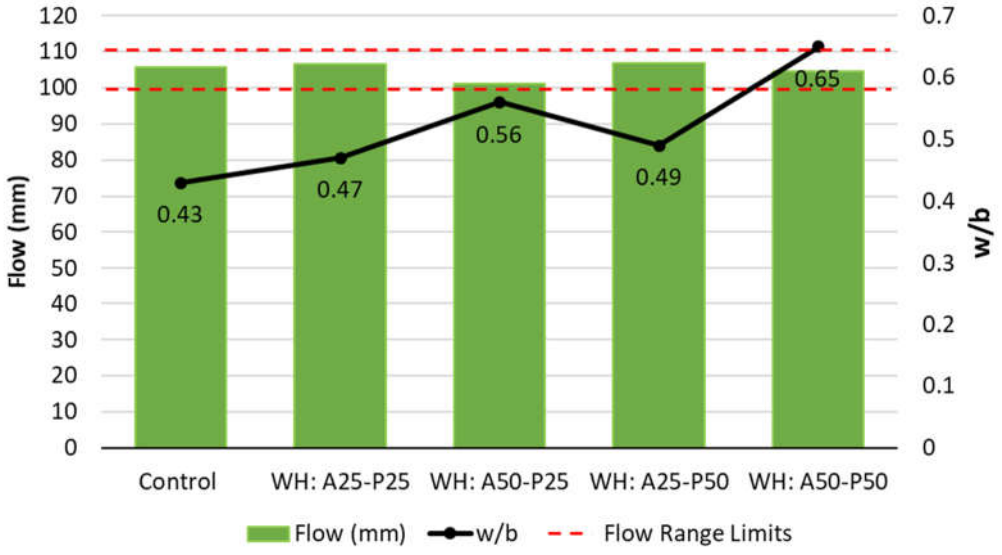

Figure 4.11 Flow and w/b for the Mechanical Test Mortars (WHBA) of Combined Usage

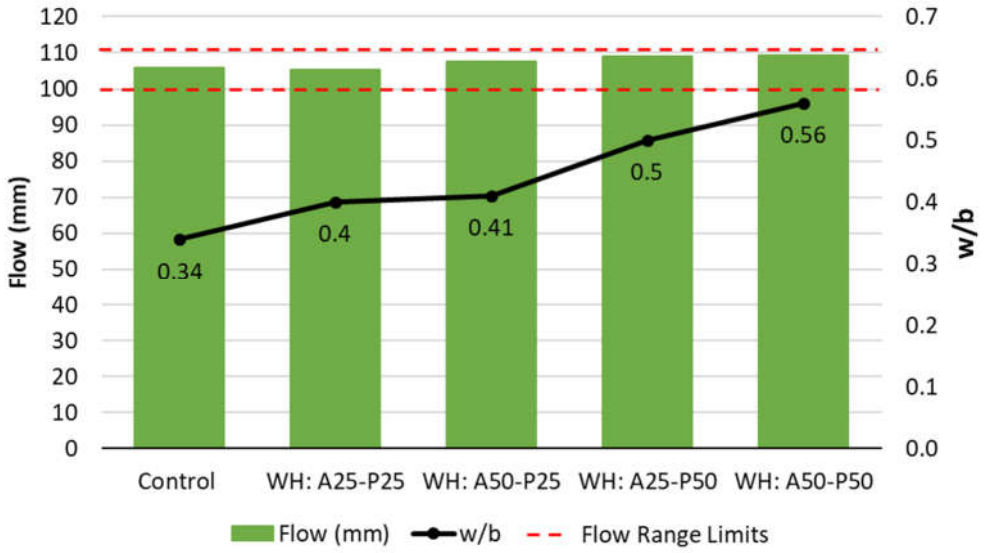

Figure 4.12 Flow and w/b for the Durability Test Mortars (WHBA) of Combined Usage

The explained effects of the usage as FA and SCM experiments were combined in the third parts' mixtures, and the water to binder ratio was found higher than the first and second parts mixes', generally. Especially when bottom ashes were replaced with fine aggregates, the w/b ratios increased more than cement replacement. The results can be seen in Figure 4.9 & Figure 4.11 and Figure 4.10 & Figure 4.12

To summarize, an increased quantity of mixing water was necessary to overcome particle angularity, rough surface texture, and excess fine specific surface area found in the bottom ash aggregates. Therefore, the workability of the mortars was decreased rather than the control mix mortars. The above factors contributed towards lowering the flow values and increasing the water to binder ratios.

4.3 Mechanical Performance

Strength and durability are the two main properties of hardened concrete. These two main parts are mortar performance and include shrinkage and creep, compressive strength, tensile strength, flexural strength, and modulus of elasticity. In this study, the compressive and flexural strength of the mortars were examined, and the results will be presented in the following sections.

4.3.1 Compressive Strength of Mortars

In general, the strength of the hardened mortar could be explained as resisting strain or rupture induced by external forces [79]. Especially, the compressive strength of mortar is the essential characteristic. It is generally assumed that an improvement in concrete compressive strength will improve its mechanical properties; however, all mechanical properties are not directly associated with compressive strength. Furthermore, strength depends on many parameters, such as the strength of the cement paste, the strength of the aggregates, and the bond between the cement paste and the aggregate particles. Additionally, many factors affect the strength of the mortars, such as the w/c ratio of the mix, used water quality, chemical and physical properties of the cement and aggregates, mixing conditions, placing and compactions into the molds, and curing conditions like humidity, temperature.

The mortars' compressive strength made with various percentages of DHBA and WHBA as a sand and cement replacement, including the control sample (entirely sand and cement), was determined according to ASTM C349 [58] 7, 28, and 90 days curing age. The mixes were evaluated in three parts, as mentioned before. The first part includes the used as a fine aggregate, and the strength results were given in Figure 4.13, and strength gaining evolution rates were given in Figure 4.14 and Table 4.6. The results were presented as an average of the three specimens.

The mortar mixes containing bottom ash showed a good strength development pattern with increasing age. The increment pattern was similar to the control mixes

of the bottom ash mixes. This proof of the increment of the compressive strength was continuous and essential. As shown in Figure 4.13, the compressive strength values were lower than the control mix at all curing ages. The usage of the bottom ashes, both dry-handled and wet-handled ones, has resulted in the strength decrement.

The 7-day strength of mixes was found as 30.87, 29.50, 21.51, 29.75, and 21.40 MPa for Control, DH: A25, DH: A50, WH: A25, and WH: A50, respectively. The 7-day strength of the 25 % replacement of sand mixes reached about 60 % of the 28-day compressive strength. However, at a 50% replacement ratio, approximately 44% compressive strength was achieved. The bottom ash mixes were found as 41.89, 30.03, 35.93, and 26,62 MPa for DH: A25, DH: A50, WH: A25, and WH: A50 with the Control mix was found 48.45 MPa.

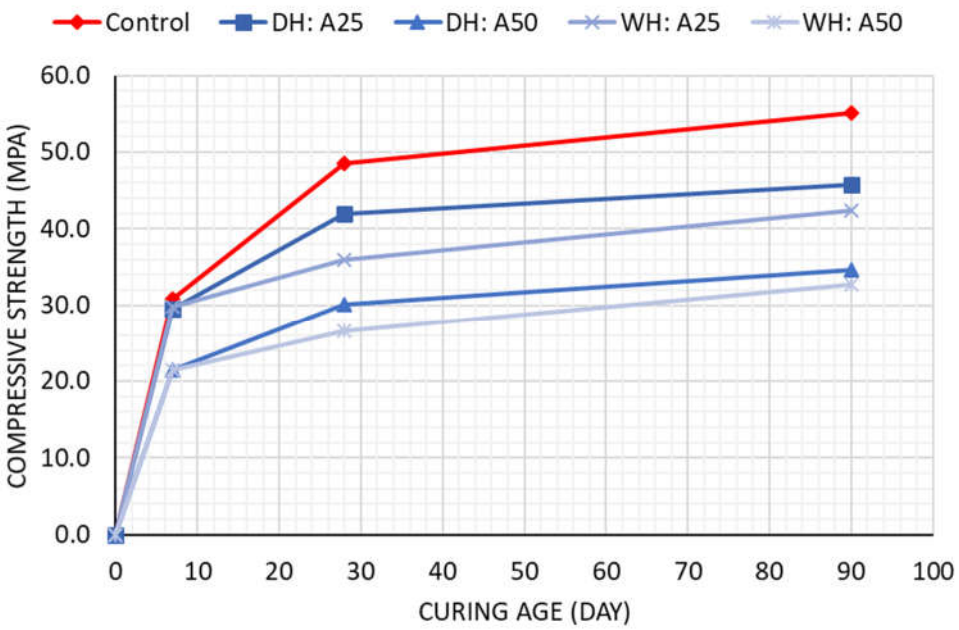

Figure 4.13 Compressive Strength vs. Age of Usage as FA Mortars

The 28-day compressive strength for DH: A25, DH: A50, WH: A25, and WH: A50 mixes were reached 86%, 62%, 74%, and 55% (Table 4.6 & Figure 4.14.) of the 28-day control compressive strength values. According to ASTM C618 [37], 75% of the

control mixes was found adequate for the compressive strength at 28-day strength. Therefore, the 25% replacement of the bottom ashes was reached sufficient compressive strength.

On the other hand, the 50% replacement was insufficient to reach 75% of strength gain, as shown in Figure 4.14. At the curing period of 90 days, the compressive strength of mixes was found as 55.07, 45.74, 34.69, 42.42, and 32,70 MPa for Control, DH: A25, DH: A50, WH: A25, and WH: A50, respectively. As a result, at the end of the 90- day curing period, DH: A25 gained 83%, A-DHBA50 gained 63%, WH: A25 gained 77%, and WH: A50 gained 59% compressive strength of the control specimen (Table 4.6 & Figure 4.14.).

Table 4.6 Strength Evolution of Usage as FA Mortars (%)

	Control	**DH: A25**	**DH: A50**	**WH: A25**	**WH: A50**
w/b	0.43	0.49	0.55	0.55	0.63
7th	100%	96%	70%	96%	69%
28th	100%	86%	62%	74%	55%
90th	100%	83%	63%	77%	59%

Usage as an only fine aggregate of the bottom ashes in the mortar caused in compressive strength decreased further. Depending on the replacement level, the acceptable strength evolution was founded. As Singh & Siddique [19] stated, the first possible reason for decreasing the strength could be replacing the stronger material with the weaker material. The other strong cause could be the physical structure of the bottom ashes. Due to the rough surface (porous) and higher water absorption capacity nature of the material, hydration of all cement particles may not have occurred, such that less paste is available for bonding. The free water in the mortar system was essential to the hydration process, and the previous studies were also reported a similar result with this study. The water absorption properties of the

different fine aggregates affected the free water required in the concrete mixes (hence W/C), which had direct bearings on the compressive strength [33].

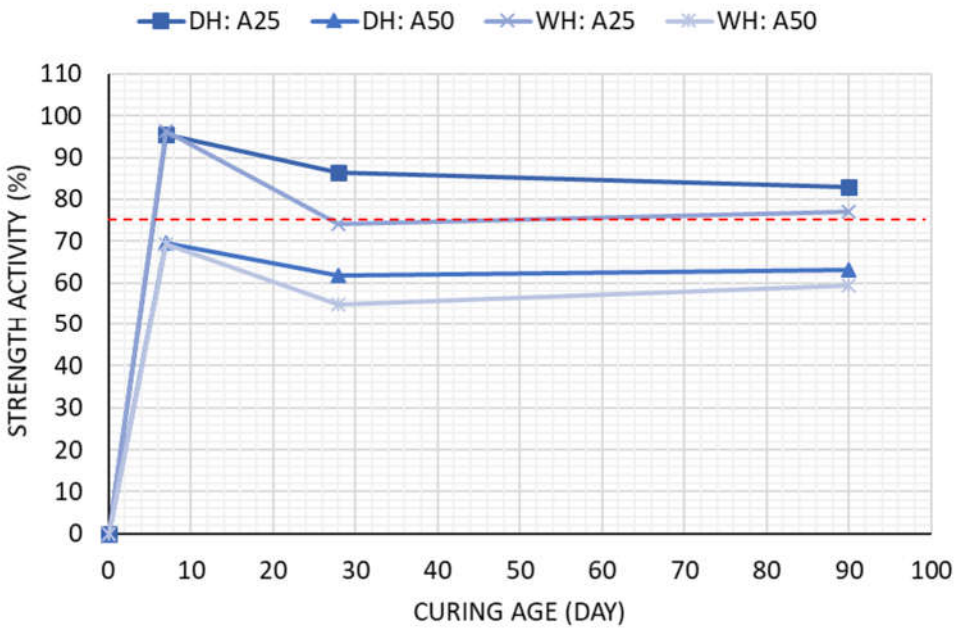

Figure 4.14 Compressive Strength Evolution vs. Age of Usage as FA Mortars

Compressive strength gaining by different types of bottom ash concrete concerning their compressive strength varies from 69-96% at seven days, 55-86% at 28 days, and varies between 59-83% at 90 days. The bottom ash mortars were gained strength at a slower rate beyond 90 days period. Since the coarser particles of the bottom ashes, pozzolanic reactions have not occurred. Jaturapitakkul and Cheerarot [69] found similar results that the bottom ash used with its non-ground size resulted in low compressive strength of the mortars at all ages.

At 25% replacement of sand replacement, the average differences in compressive strength at the age of 7 days, 28 days, and 90 days were 1.2%, 9.3%, and 11.0 %. At 50 %, average differences were higher than at 25% replacement, such as 9.4%, 20.21 %, and 21.4 %. The highest compressive strength value was found at the AC: A25 mix as 45.74 MPa at 90 days of curing age. This strength devolvement was counted as practical in mortar applications. Also, the WH: A25 mix's result was found as

42.42 MPa. Therefore, it summarized that 25% of bottom ash sand replacement as a fine aggregate in mortar could be the most efficient ratio for favorable strength, environment-saving, and cost optimization.

Replacement of the cement with bottom ashes as SCM has occurred in the second part of the experiments. The pozzolanic effect of the bottom ashes was observed, and the results were presented in the following section. As mentioned in part one, the bottom ashes for both types had porous structures. The effects of the same amount of different mineral admixtures on the mechanical properties of hardened mortar would not be the same. This difference in the effects of other minerals on the mechanical properties is the additive materials' pore size and porosity structure. It is reported in the literature that the addition of mineral admixture considerably refines the pore configuration by reducing the pore size and porosity.

The compressive strength test data observed at 7-day, 28-day, and 90-day ages are shown in Figure 4.15. As seen in the figure, compressive strength values were decreased when the replacement values were increased. At seven days, the control mixture displayed a compressive strength value of 30.87 MPa, as stated before. For this short curing age, with an increasing substitution ratio of ash, the strength of mixtures resulted in lower strength concerning this control specimen.

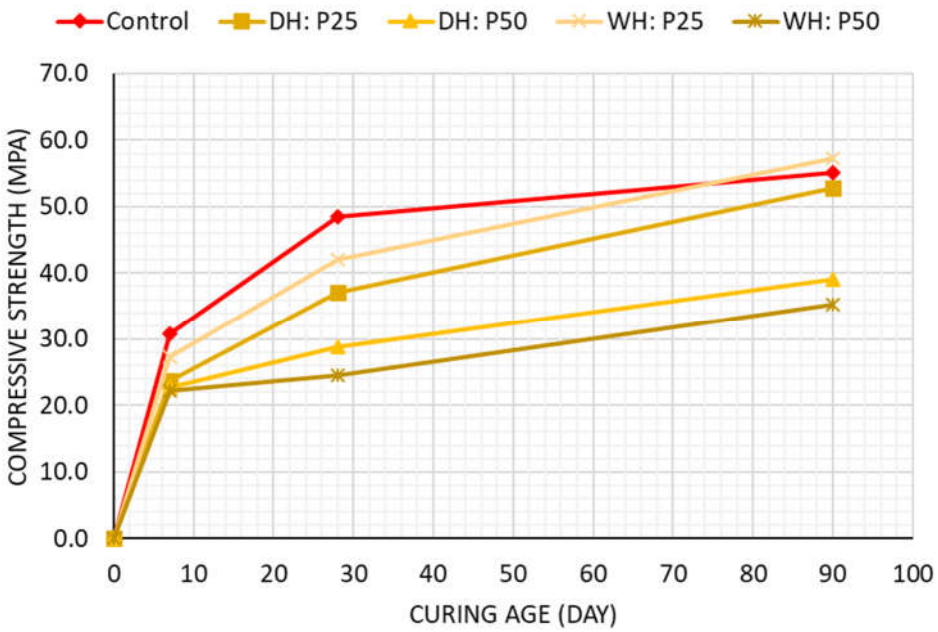

Figure 4.15 Compressive Strength vs. Age of Usage as SCM Mortars

The mixture WH: P25 had a compressive strength value of 27.32 MPa which means that 88.5% of the strength of the control sample (reference). The DH: P25 was followed as gain 76.9% of the strength as 23.73 MPa, and the DH: P50 had very close values as 22.68 MPa with 76.4% of compressive strength evolution of the control. The mixture WH: P50 has the lowest compressive strength value, 12.70 MPa, corresponding to the 41.1% strength of the reference (Table 4.7). The most inadequate performance of this mixture is probably due to the high content of bottom ash and the highest water to binder ratio (0.62) among these mixtures.

Table 4.7 Strength Evolution of Usage as SCM Mortars (%)

	Control	**DH: P25**	**DH: P50**	**WH: P25**	**WH: P50**
w/b	0.43	0.51	0.5	0.49	0.62
7th	100%	76.9%	68.0%	88.5%	73.5%
28th	100%	76.4%	51.2%	86.6%	60.7%
90th	100%	95.8%	63.9%	104.0%	71.1%

As a typical situation, the strength difference between the reference sample and mixtures was reduced with increasing curing age. When curing was extended to 28 days, compressive strength values of the mixtures DH: P25 and WH: P25 were increased to 37.07 and 42.02 MPa, which were 76.4 and 86.6 % of the strength of the 48.54 MPa reference sample, and DH: P50 and WH: P50 59.4 % (28.81 MPa) and 50.5 % (24.49 MPa) of the strength of the control, respectively. Similar to the usage as a fine aggregate, at 25% replacement of the bottom ashes as a binder, materials could be sufficient according to ASTM C618 [37]as a greater than gaining 75 percent of the control specimen 28-day strength. At the end of a 90-day curing time, the strength value of the reference sample was measured as 55.07 MPa. The strength values of mixtures of 25% were WH: P25 and AC: P25, ash containing samples measured as 57.30 MPa and 52.77 MPa 104.4 % and 95.8% of that reference's, respectively. Moreover, DH: P50 and WH: P50 39.14 MPa (71.1%) and 35.21 MPa (63.9%) of the strength of the control.

The pozzolanic reaction occurs relatively slowly but enhances strength in the long term compared to ordinary Portland cement concrete, especially using the wet-handled bottom ash in the mortar with the 25% replacement ratios. The w/b (0.49) ratio of all design mixes was the lowest rather than another two mixtures.

In the first 28 days, the bottom ash cement mortar mixes' compressive strength was found less than the control mix since the cement content was decreased compared to the control mix. However, after 28 days, the differences were gradually reduced because pozzolanic reaction started and calcium hydroxide reacts with the ground bottom ashes. In this way, the strength was increased, as can be seen in Figure 4.16. As a result, the compressive strength gained by different types of bottom ash concrete concerning their compressive strength varies from 41-88% at seven days, 50-86% at 28 days, and varies between 63-104% 90 days. In the case of wet-handled bottom ash to replace cement at the age of 90 days, it was found that cement placement by 25 % resulted in the highest compressive strength of mortar and even more enhanced the control sample.

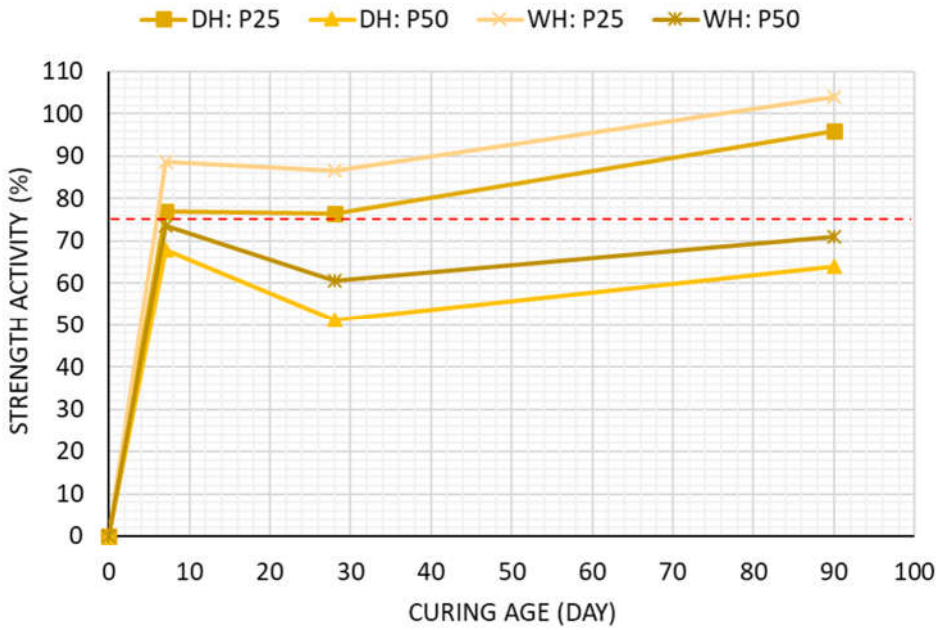

Figure 4.16 Compressive Strength Evolution vs. Age of Usage as SCM Mortars

This result could be similar to the previous studies reported by Singh & Siddique [19]; with the increasing age, reactive silica in the coal bottom ash reacts with the alkali calcium hydroxide produced by hydration of cement and forms calcium silicate and aluminate hydrates. The formation of stable calcium silicate and aluminate hydrates by chemical reactions between cement paste constituents and aggregates results in filling the voids in the interfacial transition zone and improving its compressive strength. At the curing age of 28 days, the increased pozzolanic activity of the coal bottom ash negated factors responsible for reducing the strength and played a role in improving the compressive strength. As such, the decrease in compressive strength of bottom ash concrete mixtures is not significant. After 28 days of curing age, the pozzolanic effect of coal bottom ash overcame all the adverse effects and enhanced the strength properties of bottom ash concrete mixtures.

The combined usage part of the experiments investigated combined usage, partial replacement of fine aggregate, and usage as a pozzolanic material.

As seen in Figure 4.17, compressive strength values were decreased when the replacement values were increased concerning the replacement level.

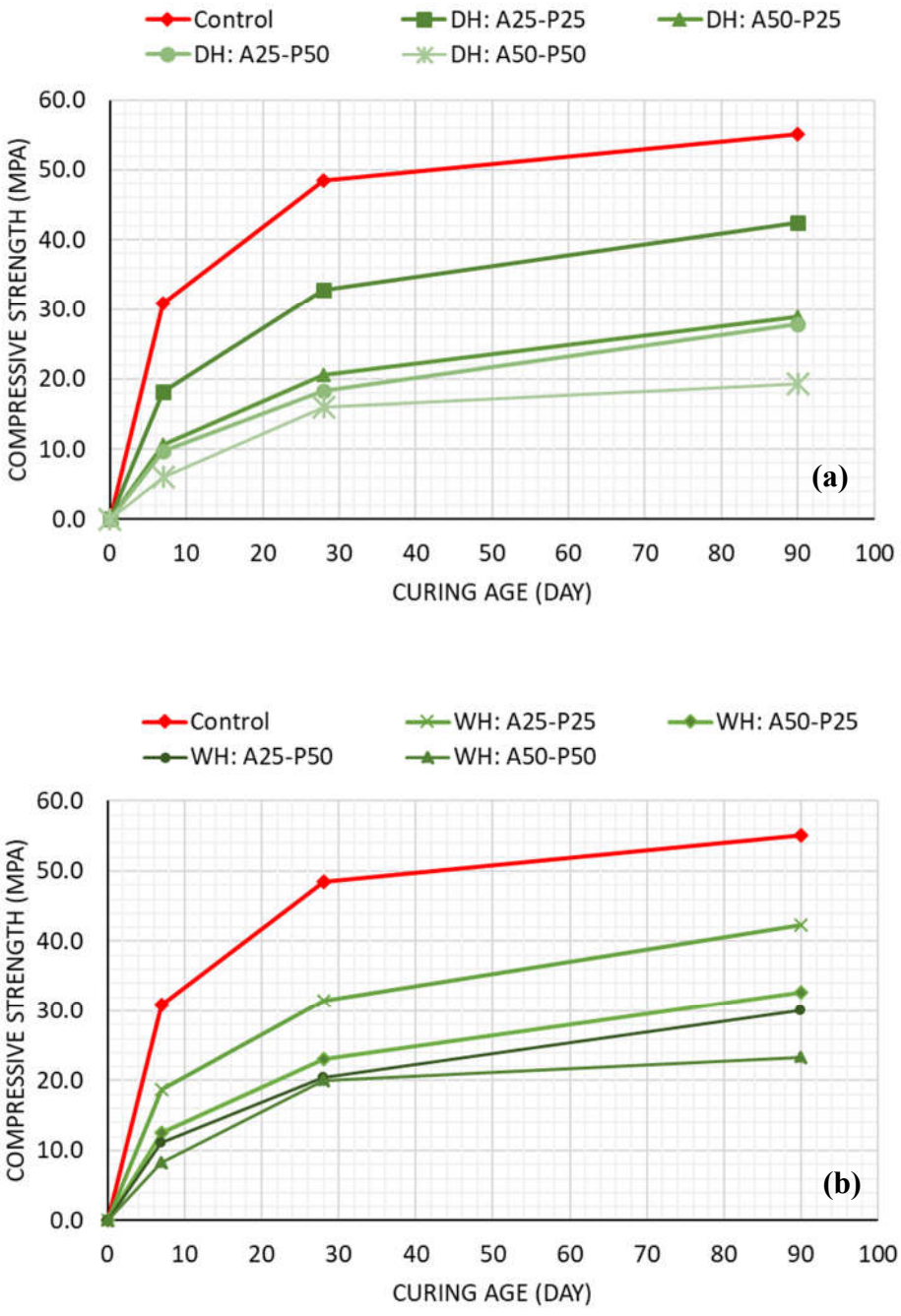

Figure 4.17 Compressive Strength vs. Age for Combined Usage Mortars with DHBA (a) and WHBA (b)

At the 25% replacement level, both fine aggregate and cement of the bottom ashes were given the best results among other mixtures. These were AC: A25-P25, and WH: A25-P25 mixtures were had 18.10 and 18.77 MPa at 7-day and 32.72 and 31.55 MPa at 28-day curing age, respectively. Although these mixtures achieved the best results, the strength evolution ratios 67.4 % and 65.0 % of the control mixture were not efficient in 28-day strength evolution, as stated in ASTM C618 [34]. However, curing due to pozzolanic reactions was dominant later, and the strength evolution exceeded the 75 % limit. The mixture DH: A25-P25 and WH: A25-P25 had a compressive strength value of 42.47 MPa and 42.26 MPa, which means that 77.51% and 76.7% of the strength of the reference.

The 25 wt. % cement replacement and 50 vol. % fine aggregate replacement mixtures (DH: A50-P25 and WH: A50-P25) were reached the average of 37.60%, 44.95%, and 55.8 % of the strength of the reference at 7-day, 28-day, and 90-day, respectively. Moreover, the 50 % cement replacement and 25 % fine aggregate replacement mixtures (DH: A25-P50 and WH: A25-P50) were reached the average 38.46%, 44.84%, and 57.0 % of the strength of the reference at 7-day, 28-day, and 90-day, respectively. Both 25 and 50 percent replacement levels were affected almost identical to bottom ashes mortar mixtures when used as fine aggregate or binder materials, separately.

However, at 50% replacement level, fine aggregate, and cement, the strength of the mixtures was decreased dramatically. The reduction of both cement and strong materials were significantly affected their compressive strength. The lowest strength values were reached at this replacement level mixtures. The DH: A50-P50 mixtures' compressive strength values were found as 6.10 MPa (19.7 % strength evolution), 16.03 MPa (33.0 % strength evolution), and 19.23MPa (34.9 % strength evolution) at 7-day, 28-day, and 90-day, respectively. The WH: A50-P50 mixtures' compressive strength values were found as 8.23 MPa (26.7 % strength evolution), 20.04 MPa (41.3 % strength evolution), and 23.31 MPa (42.3 % strength evolution) at 7-day, 28-day, and 90-day, respectively.

The mortar mixtures' strength evaluations are given in Table 4.8. The compressive strength evolution of the part three mixes was presented in Figure 4.18 according to curing age. As shown in Figure 4.18, the later age strength was increased slowly because of the pozzolanic properties of the bottom ashes. The strength gaining increment was not valid for both 50% level replacements. The strength activity of the higher percentage as aggregate and cement was caused by the prevented hydration process, and the mixtures were almost stopped their strength gained processes. The low strength values could be attributed to the aggregates condition in mixtures. The low strength values could be attributed to the aggregates condition in mixtures. Air-dry, sun-dry, and saturated surface dry conditions of the aggregates affected the strength performance of the concrete differently [70] .SSD condition of the aggregates is given better results rather than other moisture conditions of the aggregates.

Table 4.8 Strength Evolution of Combined Usage Mortars (%)

	Control	**DH: A25-P25**	**DH: A50-P25**	**DH: A25-P50**	**DH: A50-P50**
w/b	0.43	0.49	0.47	0.5	0.54
7th	100%	58.6%	34.4%	31.6%	19.7%
28th	100%	67.4%	42.3%	37.6%	33.0%
90th	100%	77.1%	52.3%	50.6%	34.9%
	Control	**WH:A25-P25**	**WH:A50-P25**	**WH:A25-P50**	**WH:A50-P50**
w/b	0.43	0.56	0.64	0.49	0.65
7th	100%	60.8%	40.8%	36.2%	26.7%
28th	100%	65.0%	47.6%	42.1%	41.3%
90th	100%	76.7%	59.3%	54.7%	42.3%

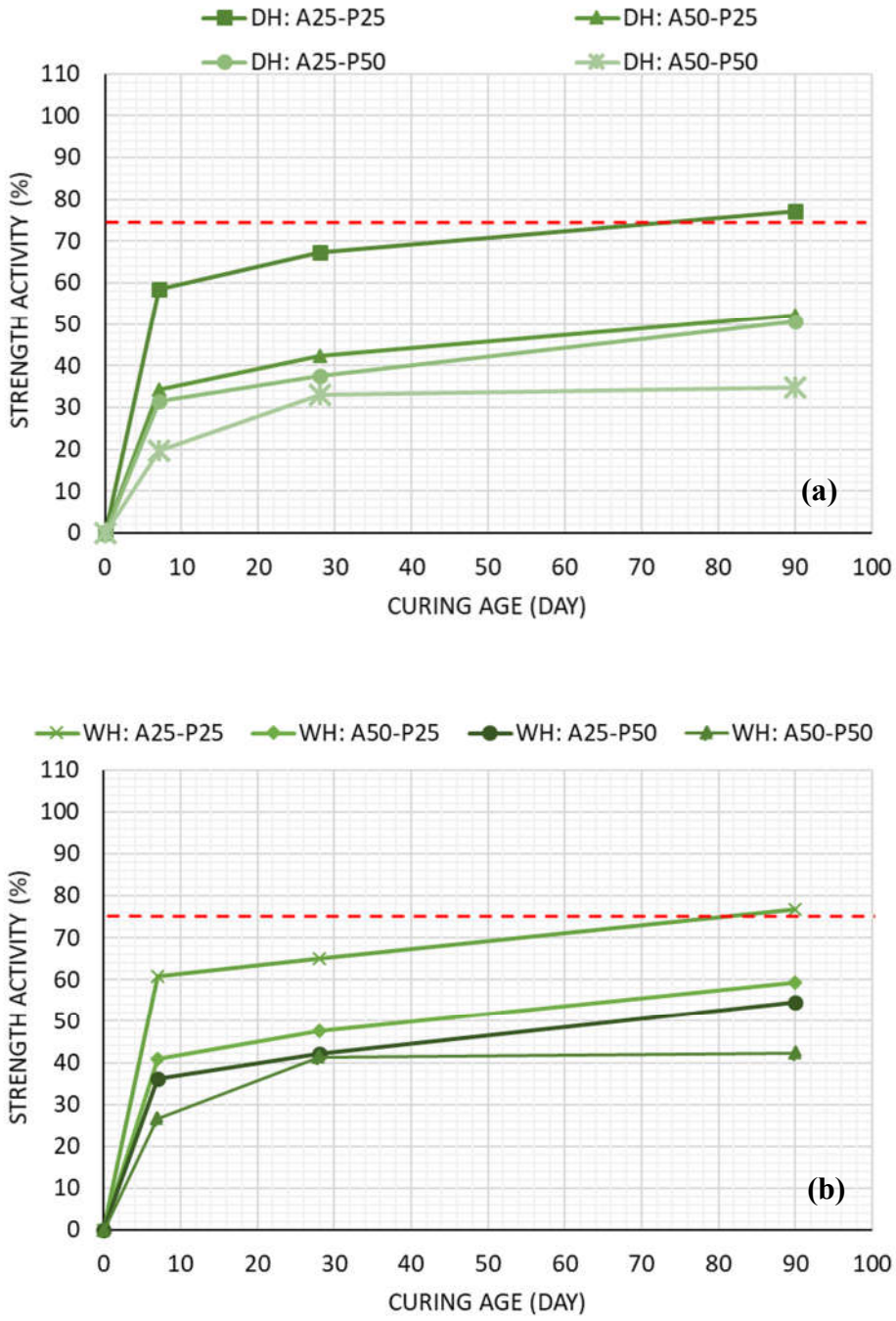

Figure 4.18 Compressive Strength Evolution vs. Age for Combined Usage Mortars with DHBA (a) and WHBA (b)

All mixture's 7-day, 28-day, and 90-day compressive strength test values were also given in Table 4.9 for DHBA and Table 4.10 for WHBA.

Table 4.9 Compressive Strength Results of the Mortars with DHBA at 7th, 28th, and 90th Day Curing Age.

CBA	wt. % of Binder	vol. % of FA	W/B	Avg. Compressive Strength (MPa)		
				7-day	28-day	90-day
Dry-Handled Bottom Ash Mortars	0	0	0.43	30.87	48.54	55.07
		25	0.49	29.50	41.89	45.74
		50	0.55	21.51	30.03	34.69
	25	0	0.51	23.73	37.07	52.77
		25	0.49	18.10	32.72	42.47
		50	0.47	10.62	20.53	28.81
	50	0	0.50	22.68	28.81	39.14
		25	0.50	9.76	18.26	27.88
		50	0.54	6.10	16.03	19.23

Table 4.10 Compressive Strength Results of the Mortars with WHBA at 7th, 28th, and 90th Day Curing Age.

CBA	wt. % of Binder	vol. % of FA	W/B	Avg. Compressive Strength (MPa)		
				7-day	28-day	90-day
Wet-Handled Bottom Ash Mortars	0	0	0.43	30.87	48.54	55.07
		25	0.55	29.75	35.93	42.42
		50	0.63	21.40	26.62	32.70
	25	0	0.49	27.32	42.02	57.30
		25	0.56	18.77	31.55	42.26
		50	0.64	12.58	23.09	32.65
	50	0	0.62	12.70	24.49	35.21
		25	0.49	11.16	20.44	30.11
		50	0.65	8.23	20.04	23.31

4.3.2 Flexural Strength of Mortars

The resistance of concrete to bending stresses is known as flexural (or bending) strength very briefly. It was also finding another way of the tensile strength of the concrete [71]. The flexural strength of mortar mixes made with various percentages of A-CBA and W-CBA as a sand and cement replacement, including the control sample (entirely sand and cement), was determined at 7, 28, and 90 days curing according to ASTM C348 [59].

The flexural strength test results with the age of only for the sand replacement bottom ashes mortar mixtures were shown in Figure 4.19. As shown, a general decrease in flexural strength with an increase in bottom ash replacement was reported. The flexural strength was affected to more extent with the increased replacement level in bottom ash mortar. If the decreasing rate was considered, the deceleration for flexural strength is similar to the compressive strength.

In other words, deceleration rates, behaviors, and the variation of flexural strengths were very identical to compressive strengths at all ages.

At seven-day curing age, bottom ash concrete mixtures DH: A25, DH: A50, WH: A25, and WH: A50 gained flexural strength 86.56%, 64.43%, 78.26%, and 56.92%, respectively of control. The 28-day flexural strength of the control mix was found as 10.37 MPa, whereas DH: A25, DH: A50, WH: A25, and WH: A50 mixes achieved in order of 84.57%, 64.958%, 76.85%, and 61.41% of control mix. At curing, a period of 91-day flexural strength of control mixture was observed very close to 28-day flexural strength of control mixture such as 10.43 MPa. Although the mix flexural strength evolution was increased to 85.62%, 69.03%, 81.50%, and 71.24% of control mix, they were slightly lower than control mortar. The flexural strength reduction was attributed similarly to that of compressive strength for the part one mortars. The previous studies were reported by Cadersa & Auckburally [45] because the bottom ash has a porous structure. Upon its use as a sand replacement, the paste

becomes weak and porous. Since the volume of pores in concrete is increased, flexural strength decreases.

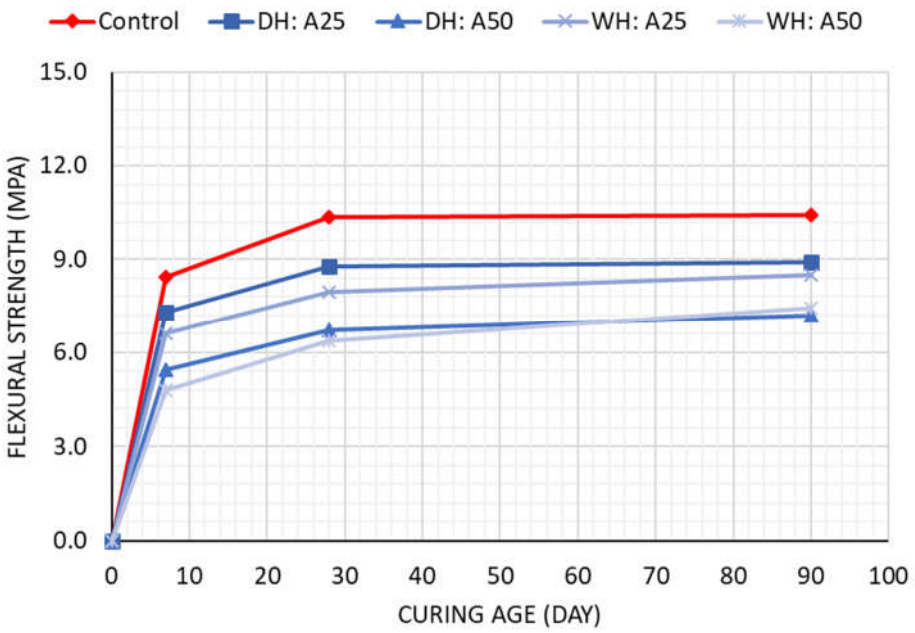

Figure 4.19 Flexural Strength Evolution vs. Age of Usage as FA Mortars

Furthermore, the high porosity of the bottom ash contributed to an increase in the interfacial transition zone and prevented the total hydration of cement particles. The interface zone increased at a higher replacement level of bottom ash, increasing the risk of micro-crack propagation and interface fractures under stress. Flexural strength was therefore reduced.

The SCM mortars' flexural strength values were shown in Figure 4.20, investigated for cement replacement. For the short curing age at 7-day, the differences between control and other mixtures' strength were relatively higher than those of different curing ages. Significantly, the DH: P50 mixture was reached even lower than half of the control mixture's strength. The DH: P25, WH: P25, and WH: P50 mixtures were reached 79.84%, 81.03%, and 76.68% of the control mix, respectively. However, the flexural strength of bottom ash mixes increased with age, and the differences were getting closed, as shown in Figure 4.20. The 28-day flexural strength values were

8.63, 6.77, 9.60, and 7.37 MPa in the order of DH: P25, DH: P50, WH: P25, and WH: P50 mixtures. This means that the strength evolution was between 65.27% to 92.60% of the control mix. At the end of a 90-day curing time, the flexural strength of mixture WH: P25 was slightly higher than that of control mortar at the same age of curing time.

Moreover, the DH: P25 mixture was almost the same with the references (gained 98.47% of control mix). The delay in hydration and slow pozzolanic activity of bottom ashes at 7-day and 28-day curing age could explain the reduction in flexural strength. At the curing period of 90 days, the fine spread of C-S-H gel and the formation of extra C-S-H gel by pozzolanic action of bottom ashes resulted in higher flexural strength.

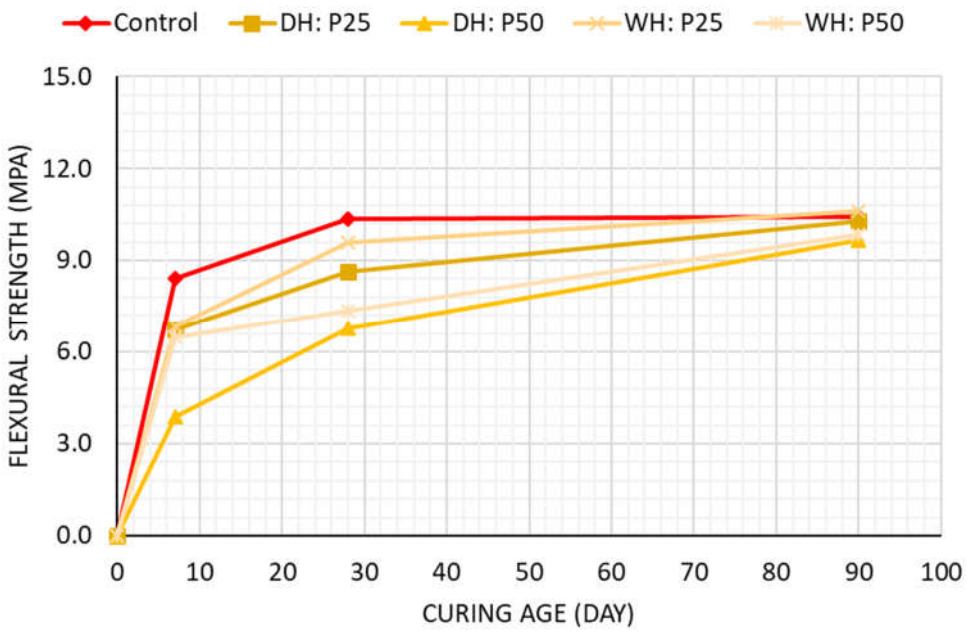

Figure 4.20 Flexural Strength Evolution vs. Age of Usage as SCM Mortars

At the combined usage mixtures, all samples' flexural strength was increased with curing age. The compressive strength evolution behavior was observed at a 25% replacement level, both as aggregate and binder materials. Opposite the compressive

strength activity, another replacement level has also given adequate results. The increment of the flexural strength was observed both at 50% replacement which can be seen in Figure 4.21, DH: A25-P25 mixtures flexural strength (10.87 MPa) exceeded the control mixtures strength (10.43 MPa) values at 90-day curing age, and the increment ratio was almost linearly increased.

The fifty percent replacement strength evolution was relatively lower, but these were also reported to grow. At 7-day curing age and the 25% cement replacement mixtures, the DH: A25-P25, DH: A50-P25, DH: A25-P25, and WH: A50-P25 mixtures were reached 61.26%, 39.13%, 58.10%, and 44.66%, of control mix, respectively. At 28-day curing age and the same cement replacement mixtures, the DH: A25-P25, DH: A50-P25, WH: A25-P25, and WH: A50-P25 mixtures were reached 74.60%, 58.20%, 63.34%, and 55.31 % of control mix, respectively. Finally, at the same twenty-five percent cement replacement and 90-day curing age, these ratios were observed as 104.22%, 68.36%, 84.37, and 72.20 in the same order. When the replacement level of the cement replacement was increased, strength evolution ratios were decreased. The average strength evolution at 7-day curing age was 30.04%, at 28-day curing age was 44.90%, and at 90-day curing, age was 65.29% of the control mix.

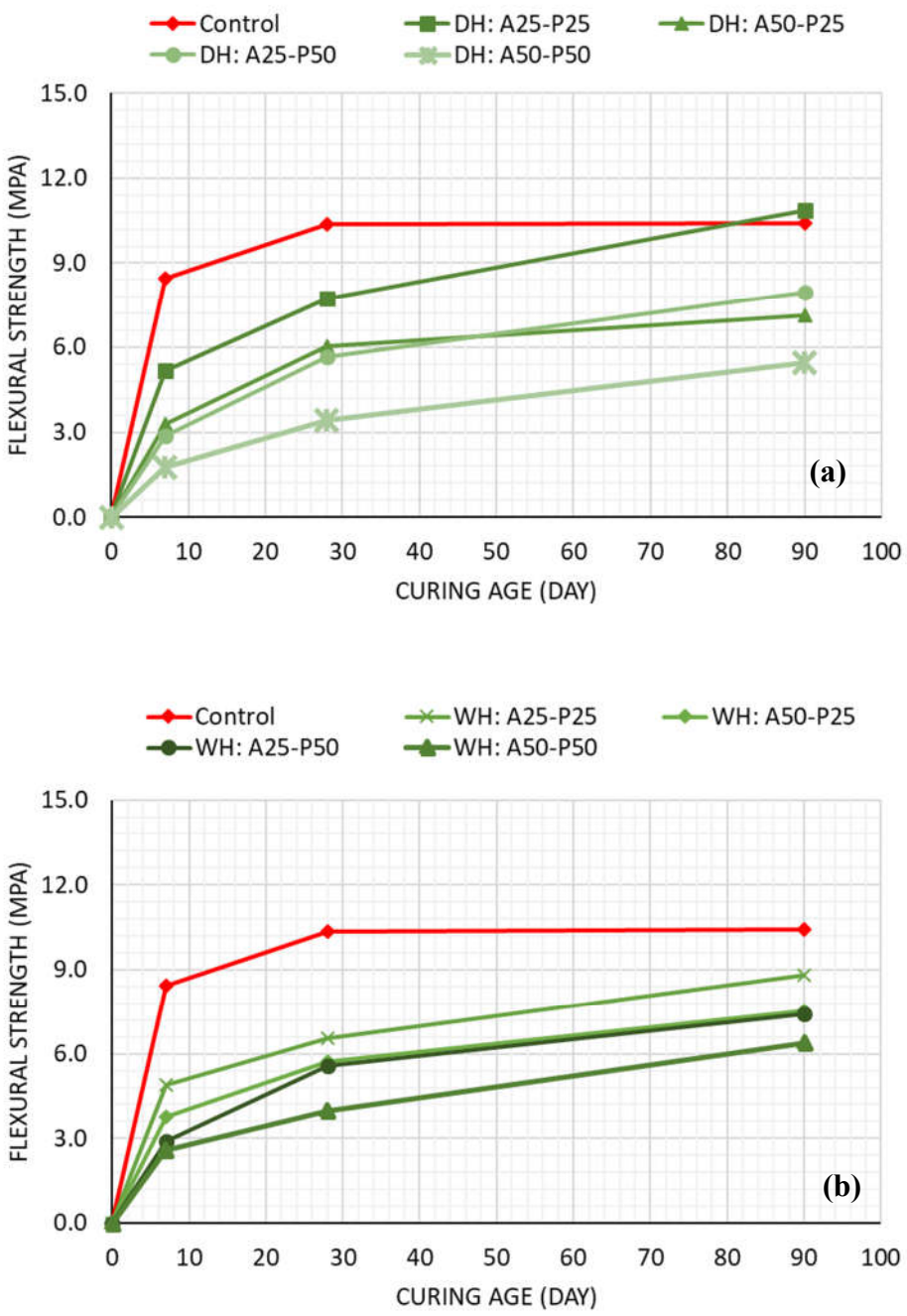

Figure 4.21 Flexural Strength Evolution vs. Age of Combined Usage Mortars with DHBA (a) and WHBA (b)

All mixtures' 7-day, 28-day, and 90-day flexural strength test values were also given in Table 4.11 for DHBA and Table 4.12 for WHBA.

Table 4.11 Flexural Strength Results of the Mortars with DHBA at 7th, 28th, and 90th Day Curing Age.

CBA	wt.% of Binder	vol. % of FA	W/B	Avg. Flexural Strength (MPa)		
				7-day	28-day	90-day
Dry-handled Bottom Ash Mortars	0	0	0.43	8.43	10.37	10.43
		25	0.49	7.30	8.77	8.93
		50	0.55	5.43	6.73	7.20
	25	0	0.51	6.73	8.63	10.27
		25	0.49	5.17	7.73	10.87
		50	0.47	3.30	6.03	7.13
	50	0	0.50	3.87	6.77	9.67
		25	0.50	4.90	6.57	8.80
		50	0.54	3.77	5.73	7.53

Table 4.12 Flexural Strength Results of the Mortars with WHBA at 7th, 28th, and 90th Day Curing Age.

CBA	wt.% of Binder	vol. % FA	W/B	Avg. Flexural Strength (MPa)		
				7-day	28-day	90-day
Wet-handled Bottom Ash Mortars	0	0	0.43	8.43	10.37	10.43
		25	0.55	6.60	7.97	8.50
		50	0.63	4.80	6.37	7.43
	25	0	0.49	6.83	9.60	10.60
		25	0.56	2.87	5.65	7.97
		50	0.64	1.77	3.43	5.47
	50	0	0.62	6.47	7.37	9.85
		25	0.49	2.90	5.57	7.43
		50	0.65	2.60	3.97	6.37

4.4 Durability Performance

4.4.1 Alkali & Silica Reactions of Mortars

One of the essential parameters of the cement system is durability. Durability is the ability to resist environmental conditions briefly. Mineral admixtures could improve the mortar durability, and generally, fly ash was given promising results as a coal combustion industrial by-product. In this study, the bottom ashes were investigated with the alkali-silica reaction test. Alkali-silica reactions were affected by many parameters such as; internal humidity of the concrete prisms, the composition of the concrete pore solution during testing, properties of hydration products formed during hydration/exposure, aggregate reactivity, type and properties of reaction products, i.e., primarily ASR-gel, formed during exposure, mainly.

As mentioned in the previous sections, the mortar mixtures and materials treatment, such as particle size distribution of the bottom ashes and river sand, w/ b ratio consideration of the ASR reaction test. The mixtures were again prepared with the three main parts: fine aggregate, cement replacement, and combined usage. According to ASTM C1260 [51], the experiments were conducted, and the results were presented in the following section.

4.4.2 Accelerated Mortar Bar Test Expansion Results

The two types of ASR tests exist in ASTM. The first one is concrete prism tests, while reasonably representative of field concrete, requiring a long testing period. The second one is the accelerated mortar bar test, and it takes a shorter time and gives results in days respectively.

The main purpose of the ASTM C1260 [51] was to identify the reactive aggregate in a short time as much as possible. It is effective in determining the ability of supplementary cementing materials to mitigate ASR-related expansion.

The accelerated expansion results for the control mortars and the 25wt% and 50wt% replacement mortars as sand, cement, and replacement (total of 17 mortar mixes) were given. ASTM C1260 [51] classifies aggregates with 16-day after casting expansions greater than 0.2% as deleterious, and those with expansions between 0.1% and 0.2% are potentially deleterious less than 0.1 % expansion as an innocuous behavior. The expansion results were obtained after testing concrete specimens modified with bottom ash additive after 3, 9, 12, 15, 30, and 45 days of curing. Although in specification indicated as 16-day observation was necessary, being sure that further day expansions were measured for the later age expansion behavior.

The results of the replacement as reactive sand with bottom ashes are given in Figure 4.22. As can be seen, the control mortar exceeded the expansion limit of 0.46 after 15-day curing, and this value increased through the curing days. The 15th-day expansions were 0.41, 0.29, and 0.28% for DH: A25, DH: A50, DH: WH50, respectively, and none of them provided the expansion limits according to specification.

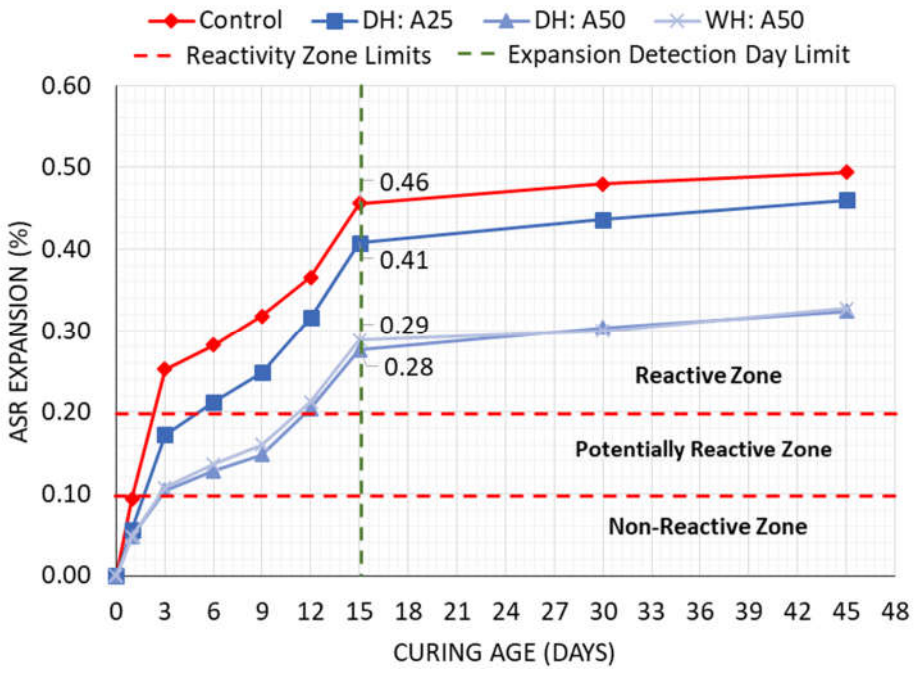

Figure 4.22. ASR Expansions of Usage as FA Mortars

Although the usage of the bottom ashes as a replacement with the river sand decreased the expansion values, all the expansion ratios were not within the prescribed limit of 0.1% based on ASTM C1260 [51], as shown in Figure 4.22. Layers of alkaline gel were around the aggregate in ASR affected mortar without mineral additives. These gel layers absorbed water and started expanding, thus causing cracks in the cement matrix. The typical ASR map was cracking on the entire surface of the CEM I 42.5 reference specimen, and also DH: A50 and WH: A50 mixes could be seen clearly with the naked eye (Figure 4.23). The cracks were radiated from the interior of the aggregate particle and in the ambient cement paste. The 25% replacement ratio with the wet-handled bottom ash specimen was broken while demolding thus, the results could not be presented.

The expansion results meant that the river sand was a very reactive aggregate. In the case of usage in the cement system, it will be concluded as a deleterious expansion.

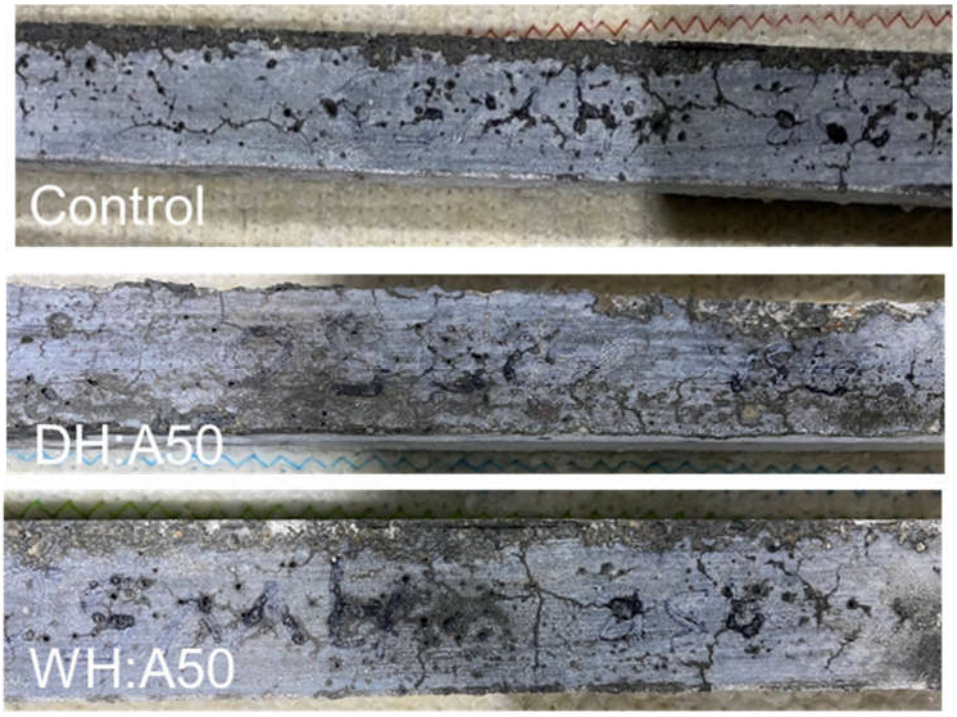

Figure 4.23 ASR Map Cracking Formation on Control, DH: A50 & WH: A50

The 25% and 50% replacement of the cement with bottom ashes expansion results are given in **Hata! Başvuru kaynağı bulunamadı.**. As seen, DH: P25 DH: P50, and WH: P50 mortars were not exceeded the expansion limit of 0.2 after 15-day curing. In general, an increase in the replacement level of cement with dry-handled and wet-handled bottom ash has a positive effect on mitigating the ASR on the mortar bars. The test results revealed that the critical expansion limit of 0.1% was exceeded only when 25% of dry-handled bottom ash was used. Same with the aggregate replacement, the 25% replacement ratio with the wet-handled bottom ash specimen was broken while demolding; thus, the results could not be presented.

Especially at a 50% replacement ratio, the mortar expansions were almost stopped. After the 15th day of curing, recorded expansion values stayed stable, as indicated in Figure 4.24. The expansion was found as 0.02% for both types of bottom ashes. Therefore, the best performance was obtained with 50% bottom ash replacement as cement with a 0.02% expansion ratio

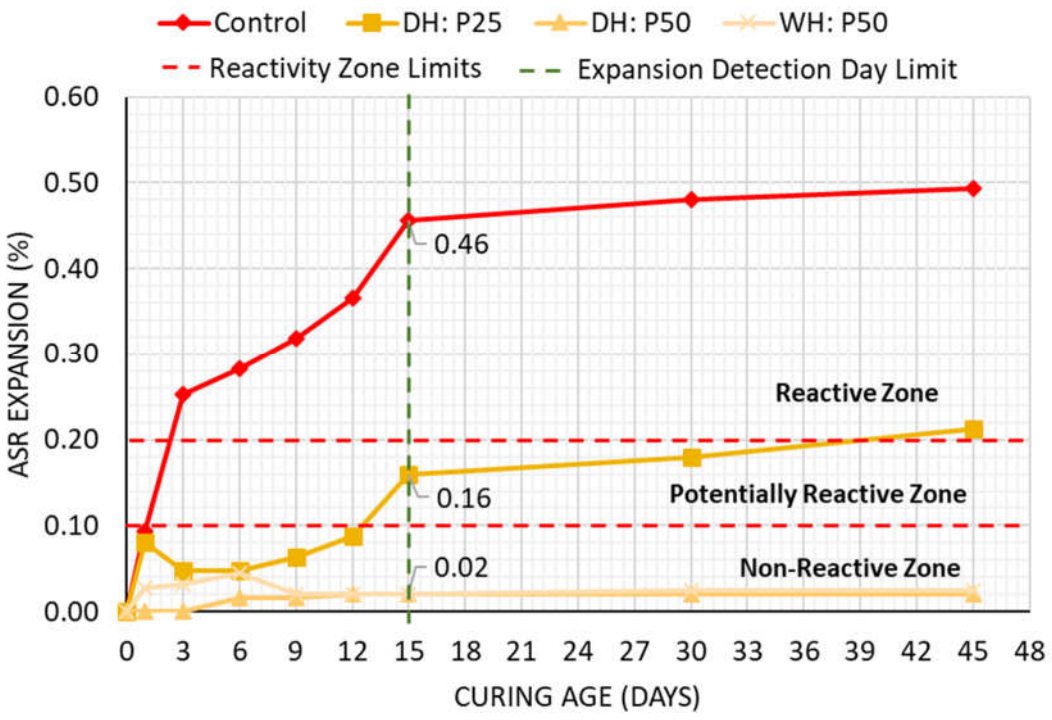

Figure 4.24 ASR Expansions of Usage as SCM Mortars.

A similar study was reported by [72] and noted that concrete prism and mortar bar test results for 70 different combinations of various pozzolans, slag, and reactive aggregates, and concludes that combinations that pass the accelerated test (i.e., < 0.10% expansion at 16 days) can be used in the field with a very low (and acceptable) risk of deleterious expansion due to ASR. The nature of the reactive aggregate will influence the level of prevention required.

As Lindgård et al. [73] stated, the role of SCMs in the prevention of ASR SCMs was known to control ASR expansion mainly by reducing the alkalinity of the pore solution by binding alkalis in the hydration products. The SCMs that were low calcium and high in silica were most effective in reducing pore solution alkalinity, thereby ASR expansions.

The alkalis in the concrete were partly consumed by the pozzolanic reaction of bottom ash or directly hydration which led to a lowering in the ASR reactivity of the glass aggregate. Therefore, the contact zone between the aggregate and the binding material looks strong in the microstructure of concrete modified with 50% of bottom ash; the cement matrix has no cracks or damages.

The pozzolanic reaction between bottom ashes and Ca $(OH)_2$ decreases the pH of the pore solution. This reduces the reactivity between the silica of aggregate and the alkalis of cement. The pozzolanic reaction occurring due to bottom ash also were reduced the permeability of mortars. Because of the decrement in permeability due to the pozzolanic reaction, water penetration was reduced. Therefore, the gel that occurred during ASR does not swell, and expansions can be stopped.

The usage of the bottom ashes as fine aggregate and SCM results were given in Figure 4.25 and Figure 4.26 for the dry-handled bottom ash and wet-handled bottom ash with various replacement ratios, respectively. At the early age, such as 1-day, 3-day, and 9-day expansion values were not found potentially deleterious expansion. As seen from Figure 4.25, DH: A25-P25 (0.09), DH: A50-P25 (0.07), DH: A25-P50 (0.06), and DH: A50-P50 (0.03) mortars were not exceeded the expansion limit of 0.1 after 15-day curing. However, after the curing age of 15 days, the expansions

occurred generally. The dry-handled bottom ash replacement as both 25% cement and sand (DH: A25-P25) was found as a 0.15 expansion at the end of the curing period. The dry-handled bottom ash replacement as 25% cement and 50% sand (DH: A50-P25) followed a 1.13 expansion at the curing period. These two mixtures exceeded the 0.1% limit of the expansion, but they were still below the 0.2 expansion limit.

On the other hand, the 25% sand and 50% cement replacement mixture (DH: A25-P50) were found to reach their maximum expansion value after the 30th-day curing period. There was no observed expansion until the end of the curing period. The lowest expansion value was found in both 50% replacement as sand and cement. It was similar to the DH: A25-P50 mixture, reached the maximum expansion value after the 15th-day curing period, and countable expansion was not observed. These DH: A25-P50 and DH: A50-P50 mixes were in the 0.1 % limit.

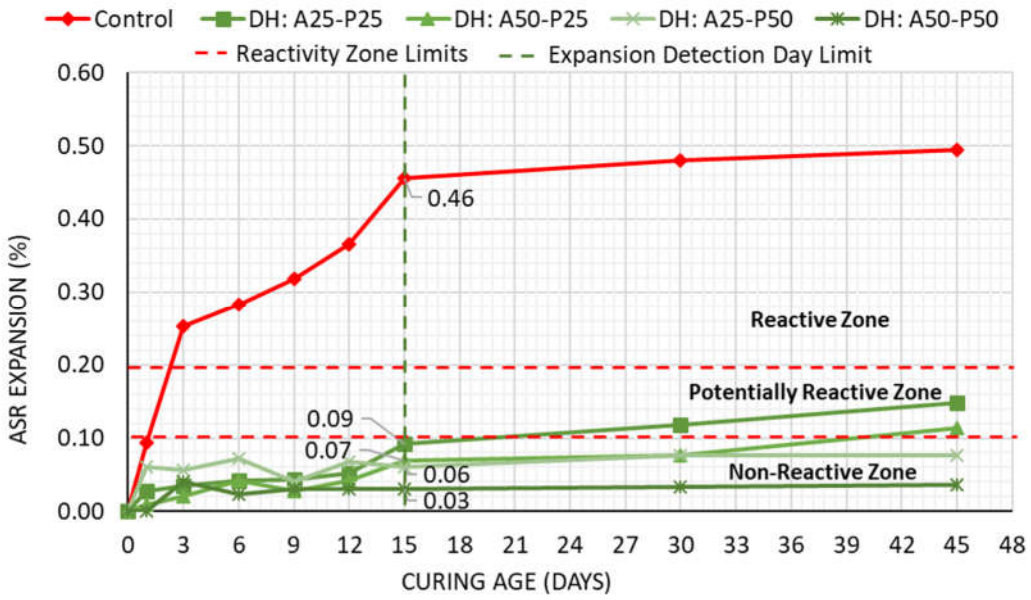

Figure 4.25 ASR Expansions of Combined Usage with DHBA Mortars

The wet-handled bottom ash mixes with various replacement levels have also behaved very well in the dry-handled bottom ash replacement, as shown in Figure 4.26. As seen, WH: A25-P25 (0.09), WH: A50-P25 (0.08), WH: A25-P50 (0.07),

and WH: A50-P50 (0.04) mortars were not exceeded the expansion limit of 0.1 after 15-day curing. The WH: A25-P25 and WH: A50-P25 mixtures' expansion rate were found as 1.49% and 1.2 % at the end of the 45th-day curing period, respectively, and these values were also in the potentially reactive range. The WH: A25-P25 mixture had expanded more than the limit allowed in the standard (0.1%) after the 15th-day curing, and the WH: A50-P25 mixtures exceeded the limit after the 30th-day curing period. The amount of reactive sand was caused by this difference probably. The WH: A25-P50 and WH: A50-P50 mixtures were in the non-reactive range, and the expansion rate was reached at 45 days curing age 0.72% 0.44%, respectively.

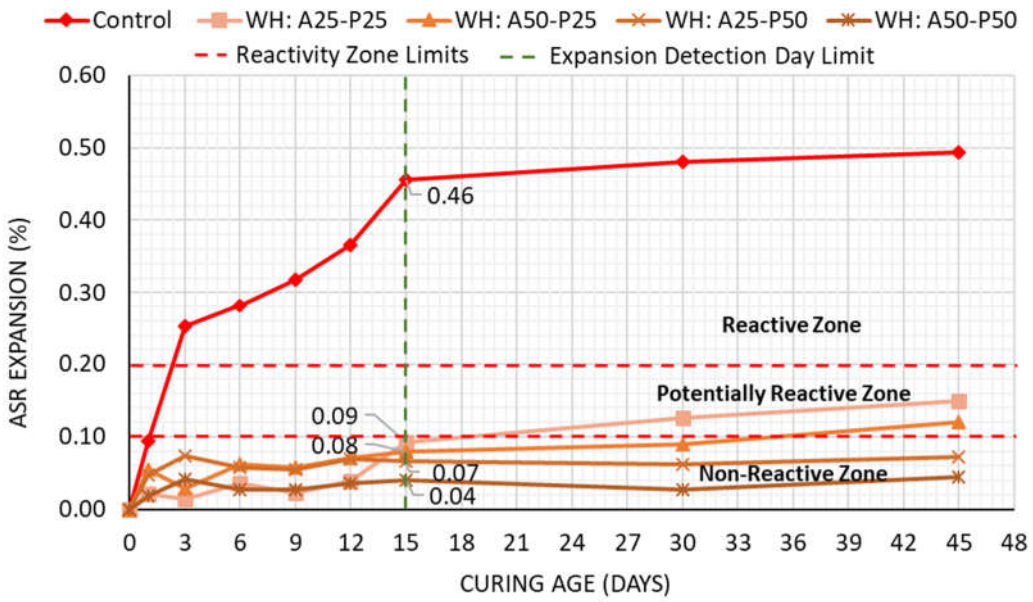

Figure 4.26 ASR Expansions of Combined Usage with WHBA Mortars

The combined usage mixes' experiment showed that the replacement of the cement was more affected the expansion of the mortars than replacement of the fine aggregate. The replacement ratio has also affected the expansion.

When bottom ash mortars were prepared with various replacement levels and usage purposes, by the contrast of the usages as an FA mortar, the expansion limit was not exceeded even after 90 days (Figure 4.25 & Figure 4.27). Also, the bottom ash

system specimens were in perfect condition even at the end of the curing period, with no surface cracks (Figure 4.28)

Figure 4.28 ASR Map Cracking Formation of Part Three Mixtures

To conclude, the role of bottom ashes could be summarized as;

- Reduction in pore solution alkalinity,
- Reduced availability of calcium, and
- Refined pore structure leading to reduced ionic mobility and water permeability.

CHAPTER 5

CONCLUSIONS AND RECOMMENDATIONS

5.1 Concluding Remarks

In this study, the utilization of two types of bottom ash was investigated in Portland cement-based mortars. The bottom ashes were provided by the same thermal power plant and originated from the same coal. However, one's ash handling system was dry, and the other was wet. Therefore, the bottom ashes were called dry-handled and wet-handled. The bottom ashes were utilized not only as supplementary cementitious material but also as fine aggregate.

The chemical and mineralogical compositions of dry-handled and wet-handled bottom ashes were similar since the coal's origin was the same. The main crystalline structures of Bas were composed of quartz and anorthite, sillimanite. The bottom ashes main oxides were found that 58.59% / 62.53% SiO_2, 22.27% / 20.04% Al_2O_3, 8.33% / 8.48% Fe_2O_3, 4.58% / 1.79% CaO, 2.17% / 2.66% K_2O for DHBA/ WHBA, respectively.

The as-is particle size distribution of the WHBA was found to be finer than DHBA. SEM micrographs and MIP results showed a more microporous structure for DHBA. WHBA's fineness modulus was found in the limits, but DHBA was higher than the upper limits. Both BAs had lower apparent, bulk (OD) and bulk (SSD) specific gravities than the sand; albeit, the specific gravities for DHBA were lower than those of WHBA. The water absorption capacities of sand, DHBA, and WHBA were 2.35%, 14.3%, and 4.04, respectively.

Both BAs were ground to a similar Blaine fineness to Portland cement for utilization as supplementary cementitious material. The time to reach 3300g/cm^2 specific surface area DHBA was ground for ~134 min; whereas, the WHBA was ground for ~236 min, possibly due to the more microporous nature of the DHBA. Although the specific gravity of the WHBA was higher than the DHBA, the grinding process has enhanced the microstructure of the bottom ashes, and ground DHBA densities were found higher than ground WHBA densities.

The heat of the hydration was investigated of the bottom ash pastes with the 25 wt. % and 50 wt. % replacement. The results showed the BAs did not delay any hydration reactions. Bottom ashes were caused a significant reduction of the heat generations such as P-DH25: -17%; P-DH50: -43%; P-WH25: -15%; P-WH50: -39%. Dry-handled bottom ashes yielded a slightly higher reduction in the heat of hydration.

The mixture designs were prepared with 25% and 50% replacement ratios as fine aggregate by volumetric and cement replacement by weight. The flow consistency remained constant with the range of 100-110 mm. The fine aggregates (bottom ashes and sands) were in oven-dry condition, and water adjustment was made according to flow range. The water addition of the mortars was done, and the w/b ratios of the mortars were found as higher than expected. The pre-soaking process was also investigated on the WH: A50-P50 mixes, but the desirable results were even could not found. The possible reason was the high porosity of the bottom ashes.

The mechanical performance and durability performance mix designs were derived from three parts. The first parts mortars were prepared as the partial replacement of fine aggregate with CBA 25% and 50% replacement ratio. The second part mortars were investigated usage as binder materials with the same percentages. The third part mortars included fine aggregate and cement replacement combinations with twenty-five and fifty percentage replacement ratios.

The compressive strength and flexural strength of the mortars were investigated as mechanical performance. Generally, the strength values were increased with the increased curing age. For the compressive strength test, 25% replacement ratios for all mixtures were passed 75% strength activity limits according to specification [37] at 28-day strength. The pozzolanic activity of the bottom ashes was contributed with the gaining strength both compressive and flexural. For P25, mixtures exceeded 75% fc-control for both at 28-d, and even 90-d strength results of WHBA were found greater than control. For both P25 and P50 mixes, flexural strengths were comparable to that of the control mix. Results support the strong pozzolanic potential of both bottom ashes. The usage as an aggregate of the bottom ashes was also given acceptable results, and they could be used for the low strength needed construction.

For A25, mixtures exceeded the strength gaining limit at 28 and 90 days. For A50 mixtures yielded comparable with fc-control A25 mixes, flexural strengths for both DHBA and WHBA were found comparable to that of the control mix, but A50 mixes were found relatively lower. The flexural strength of the mixes was found satisfactory also. The 25% replacement of the DHBA as a fine aggregate and cement mixes gave a better result at the 90th day curing period (exceeded the control mixture) among all mixes. As expected, the w/b percentages were higher at the 50 % replacement ratios than the 25 % replacement ratios. Therefore, the mechanical performance of the mixtures prepared with 50% replacement ratios was low, especially in the combined usage of mortars. Except for the A25-P25 mix, all other mixes had lower compressive and flexural strength than the control mixture. In the case of durability aspects, alkali-silica reaction results were not found in acceptable level limits for all replacement levels when the bottom ashes were used partial replacement of fine aggregate with BAs. However, P25 mixes exceeded the expansion limits after the 40th-day curing as supplementary cementitious materials, but P50 combinations for both DHBA and WHBA stayed in expansion limits in the non-reactive zone. The combined usage mixtures of all A25-P25, A50-P25, A25-

P50, and A50-P50 mixtures satisfied the acceptable expansion limits according to ASTM C1260 [51].

To conclude, the results showed that industrial by-products could be used in cement technologies at feasible amounts. Thus, this study helps the cement industry develop mortar technologies that have technical, economic, and ecological advantages for sustainable development like normal strength, durability, and environmental friendliness.

5.2 Recommendations for Future Work

Bottom ash has a high potential to develop into good pozzolanic material and fine aggregates in the cement-based industry; however, more research should be performed on other properties of concrete and mortar and the economy.

- This study focuses on similar flow performance. The usage of the bottom ashes in SSD conditions and the constant w/b could be investigated.
- Internal curing possibilities when BAs are used as FAs could be investigated.
- The performance of finer BAs as SCM could be investigated in future works.

REFERENCES

[1] International Energy Agency, "Electricity Information: Overview," *Paris*, 2020. https://www.iea.org/reports/electricity-information-overview.

[2] Türkiye Elektrik İletim A.Ş (TEİAŞ), "2018 Yılı Faaliyet Raporu," 2018, [Online]. Available: https://www.teias.gov.tr/tr-TR/faaliyet-raporlari.

[3] Z. T. Yao, M. S. Xia, P. K. Sarker, and T. Chen, "A review of the alumina recovery from coal fly ash, with a focus in China," *Fuel*, vol. 120. Elsevier Ltd, pp. 74–85, Dec. 15, 2014, doi: 10.1016/j.fuel.2013.12.003.

[4] Z. T. T. Yao *et al.*, "A comprehensive review on the applications of coal fly ash," *Earth-Science Rev.*, vol. 141, pp. 105–121, Feb. 2015, doi: 10.1016/j.earscirev.2014.11.016.

[5] R. S. Blissett and N. A. Rowson, "A review of the multi-component utilisation of coal fly ash," *Fuel*, vol. 97. Elsevier Ltd, pp. 1–23, Jul. 2012, doi: 10.1016/j.fuel.2012.03.024.

[6] European Coal Combustion Products Association, "Production and Utilisation of CCPs (EU 15)," 2016. [Online]. Available: http://www.ecoba.com/evjm,media/ccps/ECO_stat_2016_EU15_tab.pdf.

[7] American Coal Ash Association, "2019 Coal Combustion Product (CCP) Production & Use Survey Report," 2019. [Online]. Available: https://acaa-usa.org/wp-content/uploads/coal-combustion-products-use/2019-Survey-Results.pdf.

[8] C. H. Fleming, G. D. Mooney, C. Bergemann, and D. Ducon, "Bottom ash conversion options and economics," in *Electric Power Conference*, 2011, p. 18.

[9] D. K. Sarkar, "Steam Power Plant Systems," in *Thermal Power Plant*,

Elsevier, 2015, pp. 315–354.

[10] R. Siddique, “Utilization of industrial by-products in concrete,” in *Procedia Engineering*, Jan. 2014, vol. 95, pp. 335–347, doi: 10.1016/j.proeng.2014.12.192.

[11] J. Kitto and S. Stultz, *Steam: its generation and use*, 41st ed. The Babcock & Wilcox Company, Barberton, Ohio, 2005.

[12] Clarion Energy Content Directors, “Ash Handling Options for Coal-Fired Power Plants,” 2011. https://www.power-eng.com/emissions/policy-regulations/ash-handling-options-for-coal-fired-power-plants/#gref.

[13] “Submerged Chain Conveyor System (SCC System).”

[14] T. R. Naik and R. N. Kraus, “USE OF INDUSTRIAL BY-PRODUCTS IN CEMENT-BASED MATERIALS,” in *Exploiting Wastes in Concrete*, Thomas Telford Publishing, 1999, pp. 23–35.

[15] Y. Bai and P. A. M. Basheer, “Influence of furnace bottom ash on properties of concrete,” *Proc. Inst. Civ. Eng. Struct. Build.*, 2003, doi: 10.1680/stbu.2003.156.1.85.

[16] T. R. Naik, Y. M. Chun, R. N. Kraus, B. W. Ramme, and R. Siddique, “Precast concrete products using industrial by-products,” *ACI Mater. J.*, vol. 101, no. 3, pp. 199–206, 2004, doi: 10.14359/13115.

[17] S. Kizgut, D. Cuhadaroglu, and S. Samanli, “Stirred grinding of coal bottom ash to be evaluated as a cement additive,” *Energy Sources, Part A Recover. Util. Environ. Eff.*, vol. 32, no. 16, pp. 1529–1539, 2010, doi: 10.1080/15567030902780378.

[18] S. K. Kirthika, S. K. Singh, and A. Chourasia, “Alternative fine aggregates in production of sustainable concrete- A review,” *Journal of Cleaner*

Production, vol. 268. Elsevier Ltd, Sep. 20, 2020, doi: 10.1016/j.jclepro.2020.122089.

[19] M. Singh and R. Siddique, "Strength properties and micro-structural properties of concrete containing coal bottom ash as partial replacement of fine aggregate," *Constr. Build. Mater.*, vol. 50, pp. 246–256, 2014, doi: 10.1016/j.conbuildmat.2013.09.026.

[20] C. K. Nmai, "ACI Education Bulletin E1-99: Aggregates for Concrete," *ACI Education Bulletin*. pp. 1–26, 1999.

[21] I. M. Nikbin, S. Rahimi R., H. Allahyari, and M. Damadi, "A comprehensive analytical study on the mechanical properties of concrete containing waste bottom ash as natural aggregate replacement," *Construction and Building Materials*, vol. 121. Elsevier Ltd, pp. 746–759, Sep. 15, 2016, doi: 10.1016/j.conbuildmat.2016.06.078.

[22] H. K. Kim and H. K. Lee, "Effects of High Volumes of Fly Ash, Blast Furnace Slag, and Bottom Ash on Flow Characteristics, Density, and Compressive Strength of High-Strength Mortar," *J. Mater. Civ. Eng.*, 2013, doi: 10.1061/(asce)mt.1943-5533.0000624.

[23] M. Rafieizonooz, J. Mirza, M. R. Salim, M. W. Hussin, and E. Khankhaje, "Investigation of coal bottom ash and fly ash in concrete as replacement for sand and cement," *Constr. Build. Mater.*, 2016, doi: 10.1016/j.conbuildmat.2016.04.080.

[24] M. Singh and R. Siddique, "Properties of concrete containing high volumes of coal bottom ash as fine aggregate," *J. Clean. Prod.*, 2015, doi: 10.1016/j.jclepro.2014.12.026.

[25] Y. Bai, F. Darcy, and P. A. M. Basheer, "Strength and drying shrinkage properties of concrete containing furnace bottom ash as fine aggregate,"

Constr. Build. Mater., vol. 19, no. 9, pp. 691–697, 2005, doi: 10.1016/j.conbuildmat.2005.02.021.

[26] I. B. Topçu and T. Bilir, "Effect of bottom ash as fine aggregate on shrinkage cracking of mortars," *ACI Mater. J.*, 2010, doi: 10.14359/51663465.

[27] N. Ghafoori and J. Bucholc, "Properties of high-calcium dry bottom ash concrete," *ACI Mater. J.*, 1997.

[28] I. Yüksel and A. Genç, "Properties of concrete containing nonground ash and slag as fine aggregate," *ACI Mater. J.*, 2007, doi: 10.14359/18829.

[29] L. B. Andrade, J. C. Rocha, and M. Cheriaf, "Influence of coal bottom ash as fine aggregate on fresh properties of concrete," *Construction and Building Materials*. 2009, doi: 10.1016/j.conbuildmat.2008.05.003.

[30] R. Kasemchaisiri and S. Tangtermsirikul, "Properties of self-compacting concrete incorporating bottom ash as a partial replacement of fine aggregate," *ScienceAsia*, 2008, doi: 10.2306/scienceasia1513-1874.2008.34.087.

[31] M. Syahrul, M. Sani, F. Muftah, and Z. Muda, "The Properties of Special Concrete Using Washed Bottom Ash (WBA) as Partial Sand Replacement," *Int. J. Sustain. Constr. Eng. Technol.*, vol. 1, no. 2, pp. 65–76, 2010.

[32] S. Kumar and P. Vaddu, "Time dependent strength and stiffness of PCC bottom ash-bentonite mixtures," *Soil Sediment Contam.*, vol. 13, no. 4, pp. 405–413, 2004, doi: 10.1080/10588330490465996.

[33] S. C. Kou and C. S. Poon, "Properties of concrete prepared with crushed fine stone, furnace bottom ash and fine recycled aggregate as fine aggregates," *Constr. Build. Mater.*, vol. 23, no. 8, pp. 2877–2886, Aug. 2009, doi: 10.1016/j.conbuildmat.2009.02.009.

[34] ASTM C618 19, "Standard Specification for Coal Fly Ash and Raw or

Calcined Natural Pozzolan for Use," 2019.

[35] K. Yin, A. Ahamed, and G. Lisak, "Environmental perspectives of recycling various combustion ashes in cement production – A review," *Waste Management*. 2018, doi: 10.1016/j.wasman.2018.06.012.

[36] P. Aggarwal, Y. Aggarwal, and S. M. Gupta, "Effect of Bottom Ash As Replacement of Fine aggregates in concrete," *Asian J. Civ. Eng. (Building Housing) Vol.*, vol. 8, no. 1, pp. 49–62, 2007.

[37] Bureau of Indian Standards (BIS), "IS 383 : 2016-Coarse and fine aggregate for concrete," *Indian Stand.*, vol. Third edit, no. January, pp. 1–17, 2016.

[38] M. Singh and R. Siddique, "Effect of coal bottom ash as partial replacement of sand on properties of concrete," *Resour. Conserv. Recycl.*, vol. 72, pp. 20–32, 2013, doi: 10.1016/j.resconrec.2012.12.006.

[39] R. V. Ranganath, B. Bhattacharjee, and S. Krishnamoorthy, "Influence of size fraction of ponded ash on its pozzolanic activity," *Cem. Concr. Res.*, vol. 28, no. 5, pp. 749–761, 1998, doi: 10.1016/S0008-8846(98)00036-2.

[40] G. Singh, S. Kumar, S. K. Mohapatra, and K. Kumar, "Comprehensive Characterization of Grounded Bottom Ash from Indian Thermal Power Plant," *J. Residuals Sci. Technol.*, vol. 14, no. 1, pp. 1–10, 2017, doi: 10.12783/issn.1544-8053/14/1/1.

[41] R. A. Khan and A. Ganesh, "The effect of coal bottom ash (CBA) on mechanical and durability characteristics of concrete," *J. Build. Mater. Struct*, vol. 3, pp. 31–42, 2016, doi: https://doi.org/10.5281/zenodo.242470.

[42] H. K. Kim and H. K. Lee, "Coal bottom ash in field of civil engineering: A review of advanced applications and environmental considerations," *KSCE J. Civ. Eng.*, 2015, doi: 10.1007/s12205-015-0282-7.

[43] S. S. G. Hashemi, H. Bin Mahmud, J. N. Y. Djobo, C. G. Tan, B. C. Ang, and N. Ranjbar, "Microstructural characterization and mechanical properties of bottom ash mortar," *J. Clean. Prod.*, 2018, doi: 10.1016/j.jclepro.2017.09.191.

[44] H. K. Kim and H. K. Lee, "Use of power plant bottom ash as fine and coarse aggregates in high-strength concrete," *Constr. Build. Mater.*, 2011, doi: 10.1016/j.conbuildmat.2010.06.065.

[45] A. S. Cadersa and I. Auckburally, "Use of Unprocessed Coal Bottom Ash as Partial Fine Aggregate Replacement in Concrete," *Univ. Mauritius Res. J.*, 2014.

[46] M. Golias, J. Castro, and J. Weiss, "The influence of the initial moisture content of lightweight aggregate on internal curing," *Constr. Build. Mater.*, 2012, doi: 10.1016/j.conbuildmat.2012.02.074.

[47] I. B. Topçu, A. R. Boğa, and T. Bilir, "Alkali-silica reactions of mortars produced by using waste glass as fine aggregate and admixtures such as fly ash and Li2CO3," *Waste Manag.*, 2008, doi: 10.1016/j.wasman.2007.04.005.

[48] C. Comi, B. Kirchmayr, and R. Pignatelli, "Two-phase damage modeling of concrete affected by alkali-silica reaction under variable temperature and humidity conditions," *Int. J. Solids Struct.*, vol. 49, no. 23–24, pp. 3367–3380, Nov. 2012, doi: 10.1016/j.ijsolstr.2012.07.015.

[49] C. Karakurt and I. B. Topçu, "Effect of blended cements produced with natural zeolite and industrial by-products on alkali-silica reaction and sulfate resistance of concrete," *Constr. Build. Mater.*, vol. 25, no. 4, pp. 1789–1795, 2011, doi: 10.1016/j.conbuildmat.2010.11.087.

[50] S. Abbas, U. Arshad, W. Abbass, M. L. Nehdi, and A. Ahmed, "Recycling untreated coal bottom ash with added value for mitigating alkali–silica

reaction in concrete: A sustainable approach," *Sustain.*, vol. 12, no. 24, pp. 1–24, 2020, doi: 10.3390/su122410631.

[51] ASTM C 1260 – 14, "Standard Test Method for Potential Alkali Reactivity of Aggregates (Mortar-Bar Method)," *West Conshohocken, PA ASTM*, vol. 04, no. October 2001, 2014.

[52] ASTM C128 - 15, "Standard Test Method for Relative Density (Specific Gravity) and Absorption of Fine Aggregates, ASTM International, West Conshohocken, PA, 2015," *ASTM Internasional*, vol. i. pp. 15–20, 2015, [Online]. Available: www.astm.org.

[53] Q. Zeng, K. Li, T. Fen-Chong, and P. Dangla, "Pore structure of cement pastes through NAD and MIP analysis," *Adv. Cem. Res.*, vol. 28, no. 1, pp. 23–32, 2016, doi: 10.1680/adcr.14.00109.

[54] ASTM C136/C136M - 14, *ASTM C 136-06: Standard Test Method for Sieve Analysis of Fine and Coarse Aggregates*. 2014.

[55] ASTM:C33/C33M - 18, "Standard Specification for Concrete Aggregates," *ASTM Int.*, pp. 1–8, 2018.

[56] ASTM C1702 - 17, "ASTM C1702 Standard test method for measurement of heat of hydration of hydraulic cementitious materials using isothermal conduction calorimetry," *ASTM Int.*, pp. 1–9, 2017.

[57] ASTM C1437 - 15, "C1437 - Standard test method for flow of hydraulic cement mortar," 2015. [Online]. Available: https://www.astm.org/Standards/C1437.

[58] ASTM C349 -18, "Standard test method for compressive strength of hydraulic-cement mortars (using portions of prisms broken in flexure)," *ASTM lnternational*. pp. 1–4, 2018.

[59] ASTM C348 - 19, “Standard Test Method for Flexural Strength of Hydraulic-Cement Mortars,” *Annu. B. ASTM Stand.*, vol. 03, no. Reapproved, pp. 98–100, 2018.

[60] TS EN 196-1, *Methods of testing cement—part 1: determination of strength*, vol. 1, no. 1994. Ankara: Turkish Standard Institute, 2002.

[61] ASTM C188 - 17, “Standard Test Method for Density of Hydraulic Cement,” *ASTM Int.*, vol. 95, no. C, pp. 1–3, 2017.

[62] M. Cheriaf, J. C. Rocha, and J. Péra, “Pozzolanic properties of pulverized coal combustion bottom ash,” *Cem. Concr. Res.*, 1999, doi: 10.1016/S0008-8846(99)00098-8.

[63] ASTM C204, “Standard Test Methods for Fineness of Hydraulic Cement by Air-Permeability,” *ASTM Int. West Conshohocken, PA*, pp. 1–10, 2011.

[64] F. Moghaddam, V. Sirivivatnanon, and K. Vessalas, “The effect of fly ash fineness on heat of hydration, microstructure, flow and compressive strength of blended cement pastes,” *Case Stud. Constr. Mater.*, vol. 10, 2019, doi: 10.1016/j.cscm.2019.e00218.

[65] P. Kosmatka SH, Voight GF, Taylor, *Integrated Materials and Construction Practices for Concrete Pavement: A State-of-the-Practice Manual*, no. 2. 2006.

[66] ASTM C230/C230M - 14, “Standard Specification for Flow Table for Use in Tests of Hydraulic Cement 1,” *Annu. B. ASTM Stand.*, pp. 1–6, 2014.

[67] ASTM C490/C490M - 17, “ASTM C490 / C490M-11e1, Standard Practice for Use of Apparatus for the Determination of Length Change of Hardened Cement Paste, Mortar, and Concrete,” 2017.

[68] C. Zhang, A. Wang, M. Tang, and X. Liu, “The filling role of pozzolanic

material," *Cem. Concr. Res.*, 1996, doi: 10.1016/0008-8846(96)00064-6.

[69] C. Jaturapitakkul and R. Cheerarot, "Development of Bottom Ash as Pozzolanic Material," *J. Mater. Civ. Eng.*, 2003, doi: 10.1061/(asce)0899-1561(2003)15:1(48).

[70] D. T. C. Lee and T. S. Lee, "The effect of aggregate condition during mixing on the mechanical properties of oil palm shell (OPS) concrete," in *MATEC Web of Conferences*, 2016, vol. 87, doi: 10.1051/matecconf/20178701019.

[71] T. Y. Erdoğan, *Materials of Construction*. Metu Press, 2002.

[72] M. D. A. Thomas and F. A. Innis, "Effect of slag on expansion due to alkali-aggregate reaction in concrete," *ACI Mater. J.*, vol. 95, no. 6, pp. 716–724, 1998, doi: 10.14359/416.

[73] J. Lindgård, Ö. Andiç-Çakir, I. Fernandes, T. F. Rønning, and M. D. A. Thomas, "Alkali-silica reactions (ASR): Literature review on parameters influencing laboratory performance testing," *Cement and Concrete Research*, vol. 42, no. 2. Pergamon, pp. 223–243, Feb. 01, 2012, doi: 10.1016/j.cemconres.2011.10.004.

APPENDICES

A. Appendix – Blaine Test Results

Reference		**DBA/15**	
Time duration (s)	74	Time duration (s)	3.165
Density (g/cm^3)	3.15	Density (g/cm^3)	2.56
Temperature (^{o}C)	25	Temperature (^{o}C)	25
Porosity	0.486	Porosity	0.5
b	0.9	b	0.9
Specific surface (cm^2/g)	3420	Specific surface (cm^2/g)	939.96
Viscosity (µPa.s)	18.32	Viscosity (µPa.s)	18.32
W=	2.34		

Reference		**DBA/30**	
Time duration (s)	74	Time duration (s)	7.595
Density (g/cm^3)	3.15	Density (g/cm^3)	2.60
Temperature (^{o}C)	25	Temperature (^{o}C)	25
Porosity	0.486	Porosity	0.5
b	0.9	b	0.9
Specific surface (cm^2/g)	3420	Specific surface (cm^2/g)	1431.39
Viscosity (µPa.s)	18.32	Viscosity (µPa.s)	18.32
W=	2.38		

Reference		**DBA/60**	
Time duration (s)	74	Time duration (s)	16.355
Density (g/cm^3)	3.15	Density (g/cm^3)	2.63
Temperature (^{o}C)	25	Temperature (^{o}C)	25
Porosity	0.486	Porosity	0.5
b	0.9	b	0.9
Specific surface (cm^2/g)	3420	Specific surface (cm^2/g)	2078.60
Viscosity (µPa.s)	18.32	Viscosity (µPa.s)	18.32
W=	2.41		

Reference		**DBA/120**	
Time duration (s)	74	Time duration (s)	37.130
Density (g/cm^3)	3.15	Density (g/cm^3)	2.70
Temperature (^{o}C)	25	Temperature (^{o}C)	25
Porosity	0.486	Porosity	0.5
b	0.9	b	0.9
Specific surface (cm^2/g)	3420	Specific surface (cm^2/g)	3052.53
Viscosity (µPa.s)	18.32	Viscosity (µPa.s)	18.32
W=	2.47 g		

Reference		**DBA/180**	
Time duration (s)	74	Time duration (s)	75.530
Density (g/cm^3)	3.15	Density (g/cm^3)	2.78
Temperature (^{o}C)	25	Temperature (^{o}C)	25
Porosity	0.486	Porosity	0.5
b	0.9	b	0.9
Specific surface (cm^2/g)	3420	Specific surface (cm^2/g)	4228.406179
Viscosity (µPa.s)	18.32	Viscosity (µPa.s)	18.32
W=	2.54 g		

Reference		**WBA/15**	
Time duration (s)	74	Time duration (s)	2.335
Density (g/cm^3)	3.15	Density (g/cm^3)	2.22
Temperature (^{o}C)	25	Temperature (^{o}C)	25
Porosity	0.486	Porosity	0.5
b	0.9	b	0.9
Specific surface (cm^2/g)	3420	Specific surface (cm^2/g)	932.37
Viscosity (µPa.s)	18.32	Viscosity (µPa.s)	18.32
W=	2.03 g		

Reference		**WBA/30**	
Time duration (s)	74	Time duration (s)	2.745
Density (g/cm^3)	3.15	Density (g/cm^3)	2.31
Temperature (ºC)	25	Temperature (ºC)	25
Porosity	0.486	Porosity	0.5
b	0.9	b	0.9
Specific surface (cm^2/g)	3420	Specific surface (cm^2/g)	971.08
Viscosity (µPa.s)	18.32	Viscosity (µPa.s)	18.32
W=	2.11 g		

Reference		**WBA/60**	
Time duration (s)	74	Time duration (s)	3.045
Density (g/cm^3)	3.15	Density (g/cm^3)	2.42
Temperature (ºC)	25	Temperature (ºC)	25
Porosity	0.486	Porosity	0.5
b	0.9	b	0.9
Specific surface (cm^2/g)	3420	Specific surface (cm^2/g)	975.56
Viscosity (µPa.s)	18.32	Viscosity (µPa.s)	18.32
W=	2.21 g		

Reference		**WBA/120**	
Time duration (s)	74	Time duration (s)	6.220
Density (g/cm^3)	3.15	Density (g/cm^3)	2.51
Temperature (ºC)	25	Temperature (ºC)	25
Porosity	0.486	Porosity	0.5
b	0.9	b	0.9
Specific surface (cm^2/g)	3420	Specific surface (cm^2/g)	1341.83
Viscosity (µPa.s)	18.32	Viscosity (µPa.s)	18.32
W=	2.30 g		

Reference		**WBA/180**	
Time duration (s)	74	Time duration (s)	18.870
Density (g/cm^3)	3.15	Density (g/cm^3)	2.53
Temperature (ºC)	25	Temperature (ºC)	25
Porosity	0.486	Porosity	0.5
b	0.9	b	0.9
Specific surface (cm^2/g)	3420	Specific surface (cm^2/g)	2324.102035
Viscosity (µPa.s)	18.32	Viscosity (µPa.s)	18.32
W=	2.31 g		

Reference		**WBA/210**	
Time duration (s)	74	Time duration (s)	25.685
Density (g/cm^3)	3.15	Density (g/cm^3)	2.60
Temperature (ºC)	25	Temperature (ºC)	25
Porosity	0.486	Porosity	0.5
b	0.9	b	0.9
Specific surface (cm^2/g)	3420	Specific surface (cm^2/g)	2635.330733
Viscosity (µPa.s)	18.32	Viscosity (µPa.s)	18.32
W=	2.38 g		

Reference		**WBA/240**	
Time duration (s)	74	Time duration (s)	44.710
Density (g/cm^3)	3.15	Density (g/cm^3)	2.65
Temperature (ºC)	25	Temperature (ºC)	25
Porosity	0.486	Porosity	0.5
b	0.9	b	0.9
Specific surface (cm^2/g)	3420	Specific surface (cm^2/g)	3418.659816
Viscosity (µPa.s)	18.32	Viscosity (µPa.s)	18.32
W=	2.42 g		

B. Appendix- Mix proportions of Specimens

Table B.1 Mixture Proportions of Usage as FA Mortars with w/b=0.5

Materials (g)	Control	DH: A25	DH: A50	WH: A25	WH: A50
PC	450.0	450.0	450.0	450.0	450.0
Sand	1350.0	1012.5	675.0	1012.5	675.0
S-DH	-	185.9	371.8	-	-
S-WH	-	-	-	226.8	453.5
Water	225	225	225	225	225
Add. Water	-	50.4	103.6	60.0	100.5
Total water	225	275.4	328.6	285.0	325.5
w/b_{od}	0.5	0.61	0.73	0.63	0.72
w/b_{ssd}	0.43	0.49	0.55	0.55	0.63

Table B.2 Mixture Proportions of Usage as SCM Mortars with w/b=0.5

Materials (g)	Control	DH: P25	DH: P50	WH: P25	WH: P50
PC	450.0	337.5	225.0	337.5	225.0
Sand	1350.0	1350.0	1350.0	1350.0	1350.0
G-DH	-	112.5	225.0	-	-
G-WH	-	-	-	112.5	225.0
Water	225	225	225	225	225
Add. Water	-	37.8	31.7	25.0	85.7
Total water	225	262.8	256.7	250.0	310.7
w/b_{od}	0.5	0.58	0.57	0.56	0.69
w/b_{ssd}	0.43	0.51	0.50	0.49	0.62

Table B.3 Mixture Proportions of Combined Usage (DHBA) with w/b=0.5

Materials (g)	Control	DH: A25 - P25	DH: A50- P25	DH: A25 - P50	DH: A50- P50
PC	450.0	337.5	337.5	225.0	225.0
Sand	1350.0	1012.5	675.0	1012.5	675.0
S-DH	-	185.9	371.8	185.9	371.8
G-DH	-	112.5	112.5	225.0	225.0
Water	225	225	225	225	225
Add. Water	-	50.4	69.1	57.4	99.0
Total water	225	275.4	294.1	282.4	324.0
w/b_{od}	0.5	0.61	0.65	0.63	0.72
w/b_{ssd}	0.43	0.49	0.47	0.50	0.54

Table B.4 Mixture Proportions of Combined Usage (WHBA) with w/b=0.5

Materials (g)	Control	WH: A25 - P25	WH: A50- P25	WH: A25 - P50	WH: A50- P50
PC	450.0	337.5	337.5	225.0	225.0
Sand	1350.0	1012.5	675.0	1012.5	675.0
S-WH	-	226.8	453.5	226.8	453.5
G-WH	-	112.5	112.5	225.0	225.0
Water	225	225	225	225	225
Add. Water	-	63.0	103.0	33.0	109.0
Total water	225	288.0	328.0	258.0	334.0
w/b_{od}	0.5	0.64	0.73	0.57	0.74
w/b_{ssd}	0.43	0.56	0.64	0.49	0.65

Table B.5 Mixture Proportions of Usage as FA Mortars with w/b=0.47

Materials (g)	Control	DH: A25	DH: A50	WH: A25	WH: A50
PC	440.0	440.0	440.0	440.0	440.0
Reactive Sand	990.0	742.5	495.0	742.5	495.0
S-DH	-	149.7	299.4	-	-
S-WH	-	-	-	182.6	365.2
Water	206.8	206.8	206.8	206.8	206.8
Add. Water	-	48.4	74.8	48.4	66.0
Total water	206.80	255.2	281.6	255.2	272.8
w/b_{od}	0.47	0.58	0.64	0.58	0.62
w/b_{ssd}	0.34	0.43	0.46	0.46	0.51

Table B.6 Mixture Proportions of Usage as SCM Mortars with w/b=0.47

Materials (g)	Control	DH: P25	DH: P50	WH: P25	WH: P50
PC	440.0	330.0	220.0	330.0	220.0
Reactive Sand	990.0	990.0	990.0	990.0	990.0
G-DH	-	110.0	220.0	-	-
G-WH	-	-	-	110.0	220.0
Water	206.8	206.8	206.8	206.8	206.8
Add. Water	-	37.1	54.7	37.1	54.7
Total water	206.8	243.9	261.5	243.9	261.5
w/b_{od}	0.47	0.55	0.59	0.55	0.59
w/b_{ssd}	0.34	0.43	0.47	0.43	0.47

Table B.7 Mixture Proportions of Combined Usage (DHBA) with w/b=0.47

Materials (g)	Control	DH: A25 - P25	DH: A50- P25	DH: A25 - P50	DH: A50- P50
PC	440.0	330.0	330.0	220.0	220.0
Reactive Sand	990.0	742.5	495.0	742.5	495.0
S-DH	-	149.7	299.4	149.7	299.4
G-DH	-	110.0	110.0	220.0	220.0
Water	206.8	206.8	206.8	206.8	206.8
Add. Water	-	37.1	54.7	37.1	54.7
Total water	206.80	243.9	261.5	243.9	261.5
w/b_{od}	0.47	0.55	0.59	0.55	0.59
w/b_{ssd}	0.34	0.40	0.41	0.40	0.41

Table B.8 Mixture Proportions of Combined Usage (WHBA) with w/b=0.47

Materials (g)	Control	WH: A25 - P25	WH: A50- P25	WH: A25 - P50	WH: A50- P50
PC	440.0	330.0	330.0	220.0	220.0
Reactive Sand	990.0	742.5	495.0	742.5	495.0
S-WH	-	182.6	365.2	182.6	365.2
G-WH	-	110.0	110.0	220.0	220.0
Water	206.8	206.8	206.8	206.8	206.8
Add. Water	-	37.1	54.7	63.7	89.1
Total water	206.80	243.9	261.5	270.5	295.9
w/b_{od}	0.47	0.55	0.59	0.61	0.67
w/b_{ssd}	0.34	0.44	0.48	0.50	0.56